Comparative Study of Electro-Optical Properties of Liquid Crystal Molecules

THESIS SUBMITTED FOR THE AWARD OF THE DEGREE OF
Doctor of Philosophy

in

Applied Physics

By
Narinder Kumar
Enrolment No.: 730/15

Under the Supervision of

Prof. Devesh Kumar

BABASAHEB
BHIMRAO
AMBEDKAR
UNIVERSITY
LUCKNOW
प्रज्ञा शील करुणा
ESTABLISHED 1996

Department of Applied Physics
School for Physical Science
Babasaheb Bhimrao Ambedkar University, Lucknow,
U.P. (India)-226025

October, 2020

Dedicated

To

My Respected

Teachers

And

My Loving Family

DECLARATION

I declare that the thesis entitled "**Comparative study of electro-optical properties of liquid crystal molecules**" has been prepared by me under the supervision of **Prof. Devesh Kumar,** Department of Applied Physics, School for Physical Sciences, Babasaheb Bhimrao Ambedkar University, Lucknow. No part of this thesis has formed the basis for the award of any degree, diploma or fellowship previously. I declare that the material embodied in the present work is based on original research work, and the indebtedness to others has been duly acknowledged at relevant places. It has also declared that the thesis is essentially free from any kind of plagiarism.

Narinder Kumar

Date: 09-10-2020
Place: Lucknow

Narinder Kumar

Department of Applied Physics,
School for Physical Science,
Babasaheb Bhimrao Ambedkar Univerisity,
Vidya Vihar, Raebareli Road, Lucknow,
226025, U. P. India

CERTIFICATE

This is to certify that the thesis titled "**Comparative study of electro-optical properties of liquid crystal molecules**" submitted by **Mr. Narinder Kumar** is an original research work and has not been previously submitted in part or full for the award of any other degree or diploma to this or any other university or institutions.

The thesis submitted to the Babasaheb Bhimrao Ambedkar University, Lucknow, satisfies all the requirements as stipulated in the *Doctor of Philosophy (Ph.D.) regulations-1999 as amended in 2008/2010/2013* and it is fit for the submission and evaluation for the award of Doctor of Philosophy of the University.

Date: 09-10-2020
Place: Lucknow

Prof. Devesh Kumar
(Supervisor)

Prof. B. C. Yadav
(Head of Department)

ACKNOWLEDGMENT

It gives me immense pleasure that I have an opportunity to place on record the contributions of several people who have been influential in forming this thesis. I want to thank the almighty for the blessings. I have benefited from numerous people during this work and I attempt to list these people here, and I fervently hope I have not missed anyone. First and foremost, I would like to express my sincere gratitude to my supervisor **Prof. Devesh Kumar**, Department of Physics, BBAU, Lucknow, for his continuous support in my Ph.D. work and related research, for his patience, motivation, and immense knowledge. I feel extremely privileged to get an opportunity to work with him, who has been my inspiration and has provided me with constant support, encouragement, and strong guidance. His guidance helped me in all the time of research and writing of this thesis. Apart from this, I have learned from him how to remain calm in adverse situations, which is very necessary for a research career.

I am very thankful to the Head of department (HOD) **Prof. B. C. Yadav**, for provided me all kind of departmental facility.

I would like to express my heartfelt reverences towards **Dr. Anoop Ayyappan** from the Indian Institute of Technology (IIT), Kharagpur (WB), for the scientific discussion on various topics. During my Ph.D. duration, I visited many times to his laboratory and given me an opportunity for lab work.

I would also like to thank faculties of Department of Physics **Dr. A. K. Yadav, Dr. Devendra Singh, Dr. Ramesh Chandra and Dr. K. B. Thapa** for their encouragement, insightful comments, and hard questions during the DRC meetings. Their critical review and valuable comments on my presentations always helped me to convey

the main message easily to the audiences during the oral presentations. I am extremely grateful to my colleague **Mr. Pawan Singh** (Research Scholar) for his help to begin the research work and constant, affectionate support. I have learned a lot from him, through both personal and scholarly interactions. I extend my thanks to our research group (Dr. Pranav Upadhaya, Dr. Suresh Kumar, Dr. Asheesh Kumar, Dr. Jeevitesh K. Rajput, Dr. Yash Kaur Singh, Dr. Ratindra Gautam, Dr. Vivek Kumar Nautiyal, Dr. Dharmveer Singh, Dr. Rajkamal, Dr. Surya Pratap Gautam, and Dr. Monika) and to my lab mate (Miss. Shivani Chaudhary, Miss. Rolly Yadav, Miss. Nidhi Awasthi, Miss. Anamika Shukla, Miss. Bhavna Pal, and Mr. Mirtunjai Mishra) who provided a friendly and cooperative environment in the lab during my Ph. D. period. I also thank my friends Mr. Diptarka Roy (Research Scholar) and Mr. Krishan Pal (Research Scholar) for their cooperative company and help during my stay in BBAU. Now I want to thank one and all who directly or indirectly helped me during my Ph. D.

Finally, I would like to appreciate the support and facilities by Staff at the Library and Computer Center of the Physics Department as well as the university for the necessary literature survey and other requirements.

Nobody has been more important to me in the pursuit of this thesis than my family members. I would like to thank my parents, whose love, guidance and blessings were always with me. Whatever I have achieved to date is due to their sacrifice in their life to fulfill my demands. A warm thanks to my wife, **Mrs. Rajni Bala**, for making my hectic and stressful Ph. D. time cheerful with all their love, care, and sense of humor.

Narinder Kumar

(Narinder Kumar)

LIST OF PUBLICATIONS

1. **Narinder Kumar**, Pawan Singh, Pranav Upadhyay, Shivani Chaudhary, Khem B. Thapa, A. K. Dwivedi, Devesh Kumar "Odd–even effect of 7O.m liquid crystal compound series studied under the effect of the electric field by density functional theory (DFT) methods, ***European Physical Journal- Plus***, 135, 388, 2020.

2. **Narinder Kumar,** Pawan Singh, Khem B Thapa and Devesh Kumar, "Molecular spectroscopy and adverse optical properties of N-(p-hexyloxy-benzylidene)–p-toluidine (HBT) liquid crystal molecule studied by DFT methodology" **IOP SciNotes**, 1, 015202, 2020.

3. **Narinder Kumar,** Bhavna Pal, Shivani Chaudhary, Devendra Singh, Devesh Kumar, "Reduced graphene oxide contains a minimum of six oxygen atoms for higher dipolar strength: A DFT study", **French-ukrainian Journal Of Chemistry**, 08(01), 167-173, 2020.

4. **Narinder Kumar,** P. Singha, S. Chaudharya, K. B. Thapaa, P. Upadhyayb, A. K. Dwivedi and D. Kumara, "Spectroscopy Existing behind the Electro-Optical Properties with an Even-Odd Effect of nCB Liquid Crystal Molecules: A Theoretical Approach", ***Acta Physica Polonica A***, 137,1135, 2020.

5. **Narinder Kumar,** Shivani Chaudhary, Pranav Upadhyay, A. K. Dwivedi, and Devesh Kumar, "Even–odd effect of the homologous series of nCHBT liquid crystal molecules under the influence of an electric field: A theoretical approach", ***Pramana – Journal of Phyics,*** 94, 106, *2020.*

6. **Narinder Kumar,** Pawan Singh, Khem B. Thapa, Devesh Kumar, "Electro-optical effect of the nCOOCB liquid crystal molecules under the terahertz (THz) frequency range: A theoretical approach" ***Journal of Physical Science***, 31(3) (2020).

7. **Narinder Kumar,** Bhavna Pal, Pawan Singh, Khem B. Thapa, Devendra Singh, Devesh Kumar, "Electro-optical effect of E7 liquid crystal molecule studied under

the impact of an external electric field (THz): A theoretical approach", ***Jordan Journal of chemistry***, (2020) (Accepted).

8. **Narinder Kumar** , Shivani Chaudhary, Pawan Singh, Khem B. Thapa, Devesh Kumar, Electro-optical odd-even effect of APAPA liquid crystal molecules studied under the influence of an extraneous electric field (THz): A theoretical approach, ***Journal of Molecular Liquid***, 318 (2020) 114254.

9. Pawan Singh, Khem B. Thapa, **Narinder Kumar** & Devesh Kumar, Tunable transmission of a nematic liquid crystal as defect in a 1D periodic structure of dielectric materials by orientation and re-orientation of liquid crystal molecules" ***European Physical Journal E,*** 41, 100, 2018.

10. Pawan Singh, Krishan Pal, Khem B. Thapa, **Narinder Kumar**, Devesh Kumar, Embedded Liquid Crystal Defect with Graphene Layers in Asymmetric One-Dimensional Photonic Crystal as Sensor Application, ***1st Edition, Chapter 8, CRC Press***, 2019.

11. Pawan Singh, Khem B Thapa, **Narinder Kumar** and Devesh Kumar "Omnidirectional reflection band of one-dimensional periodic structure (1DPS) of Si/SiO2 with defect mode of nematic liquid crystal (5CB)" ***Journal of Physical Science,*** 30(3), 117–129, 2019.

12. Pawan Singh, Khem B. Thapa, **Narinder Kumar**, Devendra Singh, DeveshKumar, "Study of transmission property of periodic layer consisting of SiO 2 and TiO 2 layers with anisotropic liquid crystal (LC) and LiNbO 3 as defect layers for optical switching" ***Results in Physics***, 13, 102346, 2019.

13. Pawan Singh, Khem B. Thapa, **Narinder Kumar**, Anil K. Yadav and Devesh Kumar, Tunable optical filter based on one-dimensional periodic structure composed of SiO2 and anisotropic metamaterial (AMM) with a liquid crystal defect layer sandwiched by two SiO2" ***International Journal of Modern Physics B,*** 33(18), 1950194, 2019.

14. Pawan Singh, Krishan Pal, **Narinder Kumar**, Sudesh K.Singh, Khem B. Thapa, Devesh Kumar, "Tunable Sensing Property of 1D Periodic Structure with Defect of Liquid Crystal Sandwiched by Metallic Layers" ***Sensor Letters,*** 17(10):800-803, 2019.

15. Gulam Abbas, **Narinder Kumar**, Devesh Kumar, and Gajanan Pandey "Effect of Reaction Temperature on Shape Evolution of Palladium Nanoparticles and Their Cytotoxicity against A-549 Lung Cancer Cells" ***ACS Omega***, 4, 26, 21839–21847, 2019.

16. Dharmendra Pratap Singh, Abhishek Kumar Misra Kamal KumarPandey Bhavna Pal, **Narinder Kumar** Devendra Singh, Kirill Kondratenko, Benoit Duponchel, Paul Genevray, Redouane Douali "Spectroscopic, dielectric and nonlinear current–voltage characterization of a hydrogen-bonded liquid crystalline compound influenced via graphitic nanoflakes: An equilibrium between the experimental and theoretical studies" ***Journal of Molecular Liquid,*** 302, 112537, 2020.

17. Pawan Singh, Khem B Thapa, **Narinder Kumar**, Devendra Singh & Devesh Kumar "Effective optical properties of the one-dimensional periodic structure of TiO_2 and SiO_2 layers with a defect layer of nanocomposite consisting of silver nanoparticle and E7 liquid crystal" ***Pramana - Journal of Physics,*** 93, 50, 2019.

18. Pawan Singh, Khem B Thapa, **Narinder Kumar**, Krishan Pal and Devesh Kumar "Graphene layers on semi-finite 1D asymmetric periodic structure of Si/Glass materials with defect of nematic liquid crystal for a sensor device" ***Material Research Express,*** 6, 066209, 2019.

19. Shivani Chaudhary, **Narinder Kumar,** Pawan Singh, Khem B. Thapa, Devesh Kumar, " Electro-optical parameters with adverse order of 10CB liquid crystal molecule under the influence of an external high electric field: A theoretical approach", ***Jordan journal of Physics*****, 14(1), 2021.**

LIST OF COMMUNICATED MANUSCRIPT

1. **Narinder Kumar,** Pawan Singh, Khem B. Thapa, Devesh Kumar, "Molecular spectroscopy and electro-optical effect of I52 liquid crystal molecules studied under the influence of an external electric field (THz): A theoretical approach", **Journal of Molecular Modeling.**

2. **Narinder Kumar,** Pawan Singh, Khem B. Thapa, Devesh Kumar, "Electro-optical even-odd effect of liquid crystal molecules studied under the influence of an electric field (THz): A theoretical approach", **Condensed Matter Physics.**

3. **Narinder Kumar,** Pawan Singh, Khem B. Thapa, Devesh Kumar, "Quantum mechanical study to investigate the π-π interaction between Graphene and liquid crystal molecules for the solar cell applications", **Structural Chemistry.**

4. **Narinder Kumar,** Pawan Singh, Khem B. Thapa, Devesh Kumar, "A binary mixture of MBBA and PAA liquid crystal most suitable for the THz application devices: A theoretical approach"**, Brazillian journal of Physics.**

5. **Narinder Kumar,** Pawan Singh, Khem B. Thapa, Devesh Kumar, "Odd-Even effect observed in the electro-optical properties of the homologous series of HnCBP liquid crystal studied under the impact of the electric field: A theoretical approach", **Iranian Journal of Mathematical Chemistry.**

6. **Narinder Kumar,** Pawan Singh, Khem B. Thapa, Devesh Kumar, "A Quantum mechanical study of the re-entrant nematic phase of the homologous series of MBC liquid crystal molecules studied under the influence of an electric field", **Bulletin of Material Science.**

LIST OF CONFERENCES AND SEMINARS

1. Attended the National Conference held on "Science for society: An interdisciplinary approach" during 31 Oct-02 Nov, 2015, organized by B. B. A University, (UP).

2. Poster presentation in the International Conference held on "Structure and Dynamics of Biomolecules" during January 27-28, 2017, organized by D. D. U Gorakhpur (UP).

3. Oral presentation in the National Seminar held on "Nano Science and Nano Biotechnology" during February 25-26, 2017, organized by D. A. V College Kanpur (UP). **(Best Poster award)**

4. Attended the one-week TEQIP-II, short term course held on "Laser and its Applications- LAP-2017" during 27-31st March 2017, organized by M. N. N. I. T., Allahabad (U.P).

5. Poster presentation in the National Conference held on "National conference on Liquid Crystal" on October 11-13, 2017, organized by I. I. S. E. R. Mohali (Chandigarh).

6. Poster presentation in the National Symposium held on "Multidimensional Aspect of Spectroscopy" during November 17-18, 2017, in D. D. U Gorakhpur (UP).

7. Attended the National Seminar held on "CSIR-National botanical research institute, Lucknow" during November 20, 2017, organized by S. J. N. P. G. College Lucknow (UP).

8. Oral presentation in the International Conference held on "Science and Tech. for sustainable future (NISC-2018)" during January 10-11, 2018, organized by B. B. A. U. Lucknow (U.P).

9. Poster presentation held on National Science Day during February 27-28, 2018, organized by B. B. A. U. Lucknow (UP).

10. Poster presentation in the National Conference held on “Soft Matter” organized by D. D. U Gorakhpur (UP), during March 27-28, 2018.

11. Attended Council of Science & Tech. in April 26, 2018 at Lucknow (U.P).

12. Oral presentation in the International Conference held on “Chemical Science: National and global perspective” during October 29-31, 2018, organized by Lucknow Christian college (U.P).

13. Poster presentation in the National Symposium held on "Advanced material Science" during December 7-8, organized by D. D. U., G. K. P, 2018 (U.P).

14. Poster presentation in the National Conference held on “Liquid crystal” organized by Allahabad University during December 19-21, 2018 (U.P).

15. Oral presentation in the National Conference held on “Advances in materials science (NCAMS-2019)” organized by Marwar Business School during February 21-22, 2019 (UP).

16. Oral presentation in the National Conference held on “Smart Materials, Devices, and sustainable tech. (SMDST-2019)” organized by M. M. M. University of tech. during March 15-16, 2018 (UP).

17. Poster presentation in National Conference held on “Innovation in applied science and engg. (NCIASE-2019)” organized by N.I.T Jalandhar during April 27-28, 2019 (P.B).

18. Attended workshop held on the "Application of Gaussian & gauss view software", during 18-19 July 2019 organized by Lucknow University, Lucknow (U.P).

19. Attended the International Conference held on “Ultrasonic and Material science for advanced technology” during November 16-18, 2019, organized by V. B. S. P. U, Jaunpur-222003 (U.P).

20. Attended a one day webinar on "Virtual Lab" conducted by F.E.T, M.J.P Rohilkhand University, Bareilly, held on 6th June 2020.

21. Poster presentation in the International e-Conference on Advanced Functional Materials and Optoelectronic Devices (ICAFMOD-2020) held during June 13-15, 2020, organized by Veer Bahadur Singh Purvanchal University, Jaunpur-222003, U. P., India.

22. Attended National Webinar on “Smart Materials for Future Applications” during 16th & 17th June, 2020, organized by Department of Physics, Faculty of Engineering & Computing Sciences, Teerthanker Mahaveer University Moradabad, Moradabad-244001, Uttar Pradesh, India.

23. Attended 1st International e-Conference on "Recent Advances in Physics & Materials Science-2020 (IC-RAPMS-2020)" held during 9-10 July, 2020, organized by Kurseong College, Darjeeling, West Bengal, India-734203.

ABSTRACT

Under the impact of an external electric field, the birefringence and order parameter, dipole moment, and refractive index express an even-odd effect. The molecular polarizability is responsible for an even-odd effect of the optical parameters. The electric field is an alternative of temperature to determine the liquid crystal (LC) series's optical parameters. The birefringence and transition temperature enhance for the odd member and reduce for the even alkyl chain members. The LC has nematic to smectic phase stability under an external electric field with adverse birefringence and order parameter. The refractive index reveals stability in the smectic, nematic, and isotropic phases. The director angle maintains stability for the nematic phase in the adverse order and smectic phase stable in positive order. The density functional theory (DFT) methods (B3LYP and M062X) reveals the same nature of optical characteristics for all the series, however, with different values. The odd carbon atom numbers present higher value as a comparison with the even carbon atom numbers of the alkyl chain length for the phase transition temperature.

Chapter 1 contains a brief introduction to the liquid crystals. Chapter 1 also has a historical background with the latest applications of liquid crystal. This chapter also explores the different types of liquid crystals with different phases.

Chapter 2 represents a brief description of the methodology which has been used in the present work. The description of DFT and *Ab initio* methods are also given in chapter 2.

Chapter 3 represents the studied of the effect of an external electric field on the nCB liquid crystal series with an extension of the liquid crystal molecules' alkyl chain. The C-C and C-H atom's stretching contributes to the anisotropy of polarizability for the new molecular compound of the nCB series. The molecular polarizability is responsible for an even-odd effect of the optical parameters. The electric field is an alternative of temperature to determine the optical parameters of the LC series. Under the effect of an external electric field, the birefringence and order parameter express an even-odd effect.

The birefringence and transition temperature enhance for the odd member and reduce for the even alkyl chain members.

Chapter 4 represent an investigates of the *N-(p-hexyloxy-benzylidene)–p-toluidine* (HBT) liquid crystal molecule having maximum absorbance due to the O-C stretching during the intermolecular interaction. Under an external electric field extension, the HBT LC has nematic to smectic phase stability with adverse birefringence and order parameter. The refractive index reveals stability in the smectic, nematic, and isotropic phases. The director angle maintains stability for the nematic phase in the adverse order and smectic phase stable in positive order.

Chapter 5 represents the homologous series of the organic compound *N(p-n-Heptyloxy-Benzylidene) p-Toluidine* (7O.m) reveals the odd-even effect under the impact of an external applied electric field by density functional theory (DFT) methods. The order parameter, dipole moment, and birefringence exhibit an odd-even effect. Simultaneously, the Isotropic polarizability and HOMO-LUMO gap do not exhibit any odd-even effect under the impact of an external applied electric field. The HOMO-LUMO gap remains constant for the homologous series of 7O.m (m=1-10). The refractive index and isotropic polarizability continuously increase with an extension of alkyl chain length. The density functional theory (DFT) methods (B3LYP and M062X) reveals the same nature of optical characteristics for all the series but with different values.

Chapter 6 represents the electric field effect on 4-(trans-4’-n-alkyl-cyclohexyl) isothiocyanate-benzene (nCHBT) liquid crystal molecules. Under the impact of an electric field, the order parameter, magic angle, HOMO-LUMO gap, range of director angle, isotropic polarizability, and the refractive index does not express any even-odd effect while the birefringence reveals the even-odd effect. The extension of the nCHBT LC molecule's alkyl chain length represents the even-odd effect of the temperature variation from nematic to isotropic phase transition and dipole moment HOMO-LUMO gap remains constant. Still, isotropic polarizability, order parameters, and refractive index have continuously increased. The odd carbon atom numbers present higher value as a comparison with the even carbon atom numbers of the alkyl chain length for the phase transition temperature. The nCHBT liquid crystal molecule reveals the birefringence and

order parameter are reciprocal to each other. For the whole, series the order parameter has continuously increased, and the birefringence decreased. The external electric field's influence is an alternative to the temperature for the optical parameter of nCHBT LC.

Chapter 7 contains a summary and conclusion of the entire work. This work also includes future prospects of unknown optical properties of liquid crystal molecules.

LIST OF ABBREVIATIONS

S. No.	Abbreviation	Full-Form
1	1D	one Dimensional
2	2D	two Dimensional
3	3D	three Dimensional
4	7O.m	*N(p-n-Heptyloxy-Benzylidene) p-Toluidine*
5	APAPA	Anisylidene-Para-Amino-Phenyl-Acetate
6	BDE	Bond Dissociation Energy
7	BE	Binding Energy
8	CB	Cyanobiphenyl
9	CHBT	4-(trans-4_-n-alkyl-cyclohexyl) isothiocyanatebenzene
10	Cr	Crystalline phase
11	DFT	Density Functional Theory
12	DSC	Differential Scanning Calorimetry
13	Eq.	Equation
14	FF	Force Field
15	HBT	N-(p-hexyloxy-benzylidene)–p-toluidine
16	HF	Hartree-Fock
17	HOMO	Highest Occupied Molecular Orbital
18	Hz	Hertz
19	IE	Interaction Energy
20	Iso	Isotropic Phase
21	LC	Liquid Crystal
22	LCAO	Linear Combination of Atomic Orbital
23	LDA	Local Density Approximation
24	LUMO	Lowest Unoccupied Molecular Orbitals
25	MM	Molecular Mechanics
26	MO	Molecular Orbital
27	Mol	Mole

28	N	Nematic phase
29	POM	Polarized Optical Microscopy
30	QM	Quantum Mechanics
31	QTAIM	Quantum Theory of Atoms in Molecules
32	RGO	Reduced Graphene Oxide
33	Sm	Smectic phase
34	SmA	Smectic phase A
35	SmB	Smectic phase B
36	SmC	Smectic phase C
37	SmX, SmY	Smectic phase of unknown identity
38	SCF	Self Consistent Field
39	STO	Slater Type Orbital
40	UV	Ultraviolet

LIST OF TABLES

LIST OF FIGURES

	Eq. 3 under the impact of the electric field. The difference of director angle ($\Delta\theta^o$) continually increases, but the minimum director angle (θ^o_{min}) continuously decreases; however, the maximum director angle (θ^o_{max}) remains constant.)	
Figure 6.9	Isotropic polarizability has been calculated under the extension of the alkyl chain (The Isotropic Polarizability was studied by DFT methodology (B3LYP & M062X) under the extension of alkyl chain length of CHBT liquid crystal. The Isotropic Polarizability is not calculated under the electric field; it is estimated only under the extension of alkyl chain length. The nature of both methods is similar.)	129

CONTENTS

CHAPTER 1

Introduction

The states of matter are mainly classified into three categories: solid, liquid and gas. Different properties are exhibited by these states of matter like solids have a definite shape, liquids are able to flow, and gases do not have fixed shape or volume [1]. The concept of liquid crystal lies between a crystalline solid and an isotropic liquid. The interconversion between different states can be achieved by increasing or decreasing temperature [2]. But a peculiar phenomenon happened with Austrian botanist Reinitzer when he was studying the properties of some esters of cholesterol. In 1888, an intermediate state of matter between the solid and liquid state was discovered by the Friedrich Reinitzer which is known as liquid crystal state [3]. After reviewing the sample under the polarizing microscope, the conclusion came as a new state of matter, which has properties totally different from the isotropic liquid [4]. This new state is perfectly ordered like the arrangement of molecules in a solid but has a tendency to flow like an isotropic liquid, so these are named as liquid crystals [5]. The ordering in a liquid crystal is of two types: positional and orientational, depending upon the lattice position acquired by molecules and alignment of molecules in a specific direction, respectively [6]. In the isotropic liquid, both types of order are present. In a plastic crystal, only positional ordering is present [7]. In liquid crystals, orientational ordering is present while positional ordering disappears either fully or partially, as shown in Fig. 1.1. These liquid crystals show some characteristics of a crystalline solid, which can be seen through X-ray diffraction, and some flow properties similar to liquids [8]. The general structure of liquid crystal contains two aromatic benzene rings connected by a linkage group, and the aromatic ring also connected with the X and Y terminal group because they provide

stability to the liquid crystal. The lateral substitute enhances the anisotropy of the liquid crystals due to the polarity, as shown in Fig. 1.2.

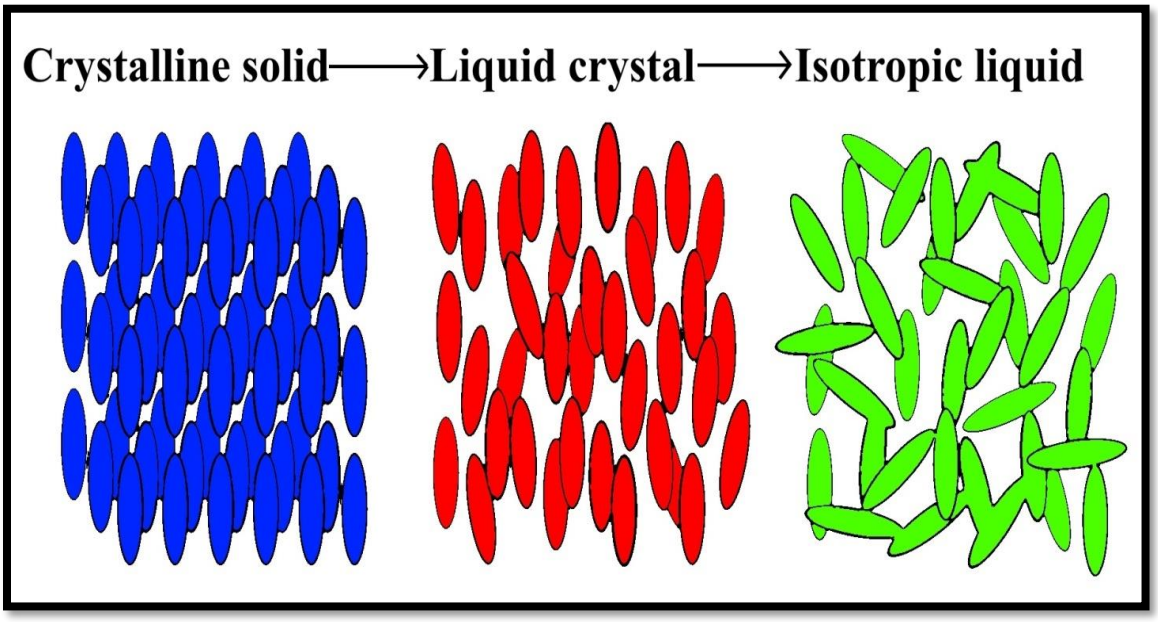

Figure 1.1 The phase transformation from crystalline to Isotropic phase

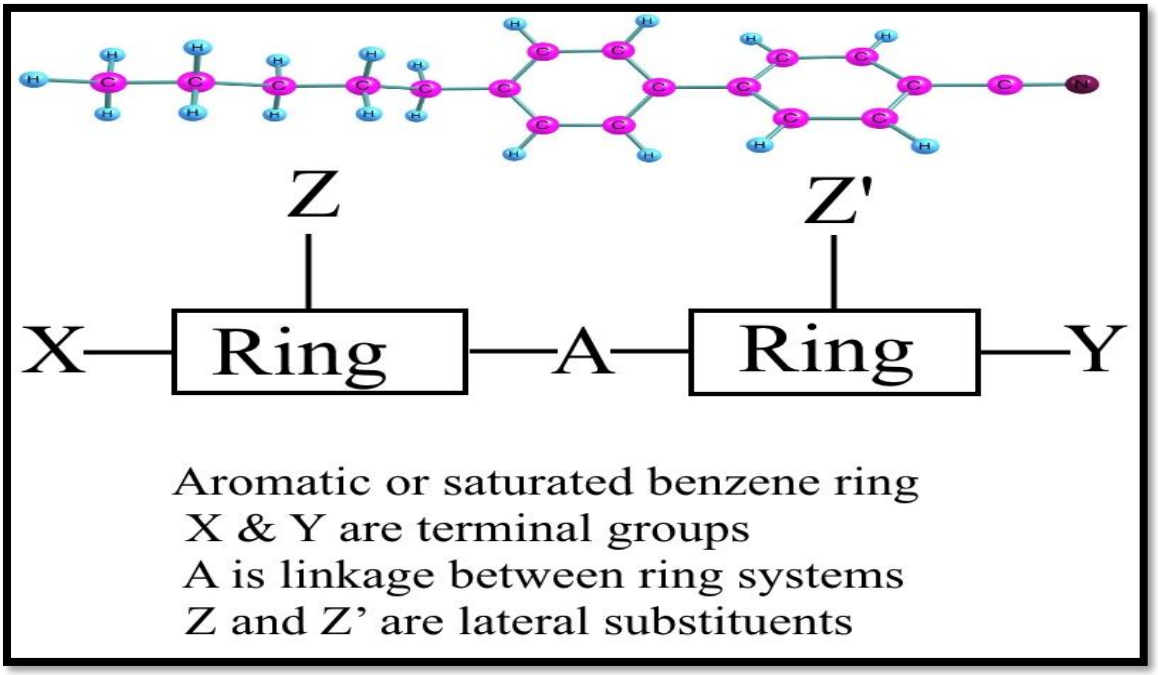

Figure 1.2 General Skelton of liquid crystal

Table 1.1 Description of rigid core, linking group flexible chain and lateral substituents of liquid crystal

Rigid Core or Ring	Linking Group	Flexible chain	Lateral Substituents
2,5-Pyrimidinyl	-C≡C-	Alkyl chain	CN
1,4-Phenyl	$-CH_2-CH_2-$	Alkoxy chains	F/Cl/Br/I
2,6-Naphtyl	-COO-	NCS	CH3
1,4-Biphenyl	-CH=CH-	F/Cl/Br/I	CN
1,4-Cyclopentyl	$-(CH=CH)_n-$	CN	NO_2
1,4-Cyclohexyl	-COS-	CF_3	
	-N=N-	CH_3	
	-CH=N-	NO_2	
	$-O-CH_2-CH_2-O$		
	-CH=CH-COO-		

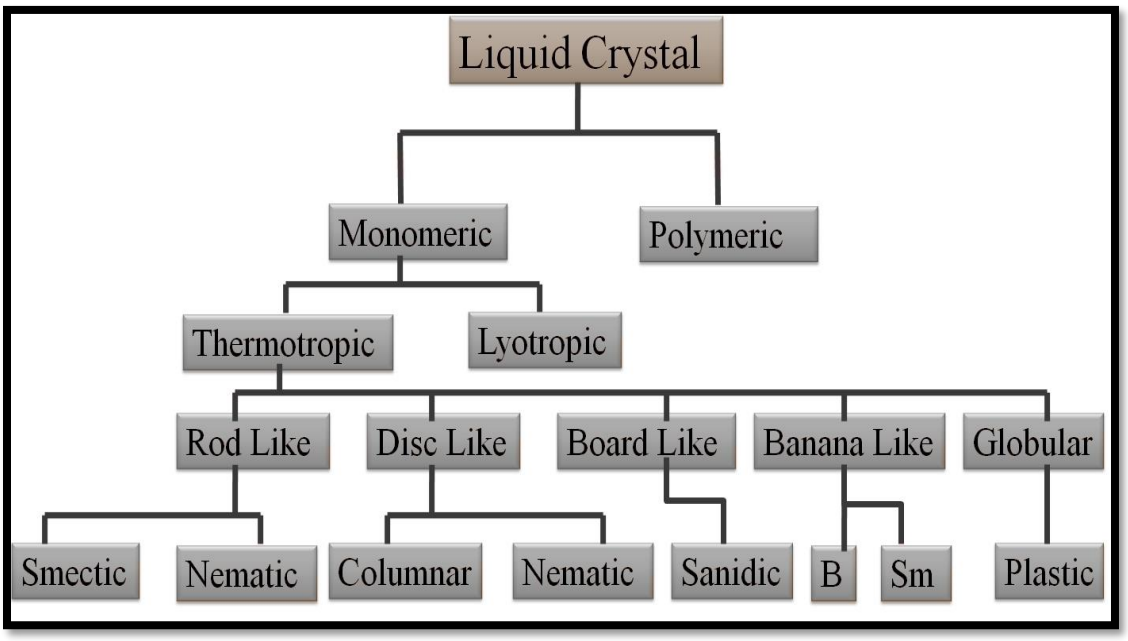

Figure 1.3 Classification of liquid crystal

Based on the structure, two types of liquid crystals are:

1.1.1 Calamitics: In this, the liquid crystals are shaped in the form of a rod having one axis longer than the other [9].

1.1.2 Discotics: In this, the liquid crystals are shaped in the form of a disc having one axis shorter than the other [10]. In between these two above, there exist lathlike species.

Another class is a thermotropic liquid crystal, where a change in temperature exhibits the change. The calamitic thermotropic liquid crystals are classified into nematic and smectic liquid crystals [11]. The subsequent class is discotic nematic and columnar. By the influence of solvents, the liquid crystals are named as Lyotropic liquid crystals. The role of a surfactant is very crucial in this case [12]. The liquid crystals in the nematic phase do not change their direction of propagation while going through the sample. But positional order is absent [13]. If we take the case of isotropic liquid–nematic transition, the translational symmetry is maintained while the rotational symmetry is lost [14].

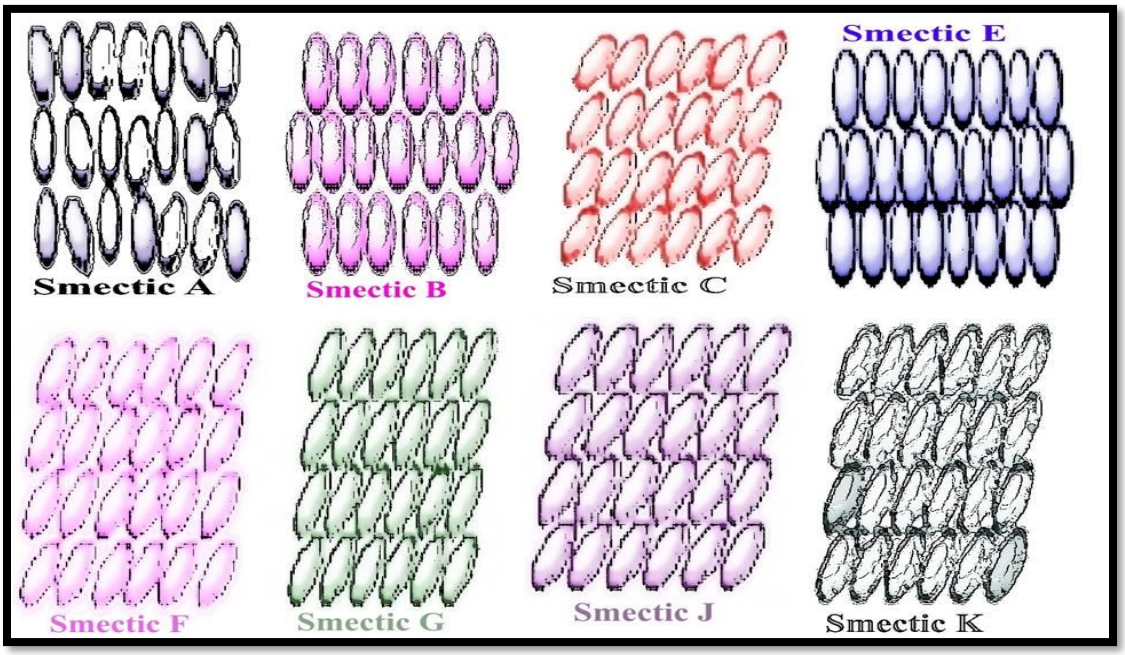

Figure 1.4 Types of Smectic liquid crystals

The liquid crystals in the smectic phase are obtained when the crystalline order is absent in two dimensions. By this, we get a stack of two-dimensional liquid. These have well-defined structures with well-defined interlayer spacing [15]. The Classification of liquid crystal as shown in Fig 1.3. In smectics, the positional and orientational ordering remains intact. This helps in translation in two directions and rotation in one direction [16]. The strength of interlayer attractions was weak in comparison to lateral forces, so the layers of the molecules can slide over one another [17]. This enhances the fluidity of smectics over the nematics as smectics have higher viscosity. Another key feature of the smectic phase is it has periodicity along one direction [18]. One can find a large number of smectic phase as no point group is forbidden [19]. From layer formation, one smectic phase is different from the other one another. Smectic A phase is considered to be the simplest phase in which the average molecular axis is perpendicular to the smectic layers [20]. There is a random arrangement of different layers of the smectic phase, and they are capable of translating and rotating along their axes [21]. One can observe optical patterns arising due to the distortion caused by the flexibility of layers [22]. For getting a phase having a bit lower symmetry, the temperature must be decreased up to a certain level. These phases produce a crystalline structure when the long-axes of the molecule are orthogonal to the plane of the layers [23]. One of the exceptions is the smectic D phase, which is a cubic phase but does not contain layers. Some smectic phases possess 2D character like smectic B, smectic I, and smectic F as shown in Fig. 1.4. The higher-order smectic phase possesses 3D character smectic L and smectic J [24].

The subsequent classification is given in following sections as;

1.1.3 Chiral Calamitic Mesophase

Some chiral compounds have a structure similar to non-chiral compounds, and these are capable of forming liquid crystals [25]. But the chiral and non-chiral compounds have totally different properties. An optically active material whose long molecular axis is varying continuously throughout the medium at a steady rate forms a helical structure known as twisted nematic or chiral nematic [26]. This is first observed in derivatives of cholesterols, so the name cholesteric was given to this category. Being helical in nature,

these phases have special optical properties and are useful in many practical applications [27]. Due to symmetrical properties, these are non-ferroelectric in nature. When the temperature of these phases was lowered to the clearing point, an anomalous phase called the blue phase appeared [28]. The temperature range was practically very narrow, and these are in between cholesteric and isotropic phase [29].

The tilting in the chiral smectic phase leads to the ferroelectric properties. They have lower symmetry; therefore show spontaneous polarization and piezoelectric behavior, so these are ferroelectric liquid crystals [30]. The types of interaction between molecules or with any applied electric field changes due to permanent dipoles present in the phase. As the ferroelectric smectic C phase forms the helical structure, it is optically active in nature [31]. The chiral nature of liquid crystal molecules shown in Fig. 1.5.

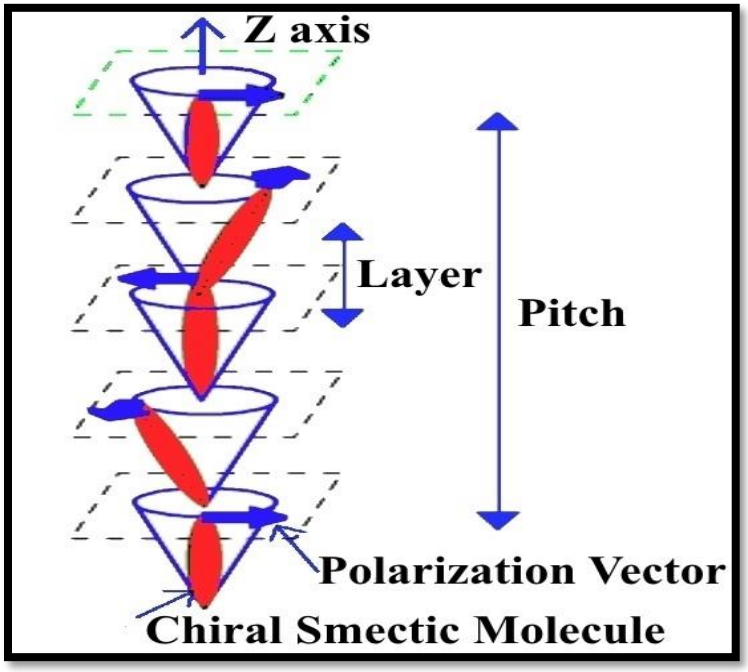

Figure 1.5 Chiral Calamitic Mesophase director orientation

1.1.4 Cubic Mesophases

These phases usually occur in Lyotropic systems and are very less frequent in thermotropic liquid crystals. The cubic structures are formed due to the formation of the

micelle, a kind of structure having hydrophilic ionic end and hydrophobic alkyl chain in the Lyotropic systems [32]. One of the examples of cubic structure in thermotropic liquid crystals is substituted alkoxy biphenyl carboxylic acids [33].

1.2 Liquid Crystal Polymers

The liquid crystals having low molecular mass are taken as a monomer to form liquid crystal polymers. One of the types of liquid crystals form due to the presence of a rigid macromolecule, and another is due to the presence of a large number of monomer forming a rigid chain segment [34]. For the formation of a rigid main-chain liquid crystal polymer, the low molar mass molecules must be joined together in the form of a chain. To get a semi-flexible polymer, the linking units must be long and flexible [35]. The molecular arrangement of liquid crystal polymers shown in Fig. 1.6.

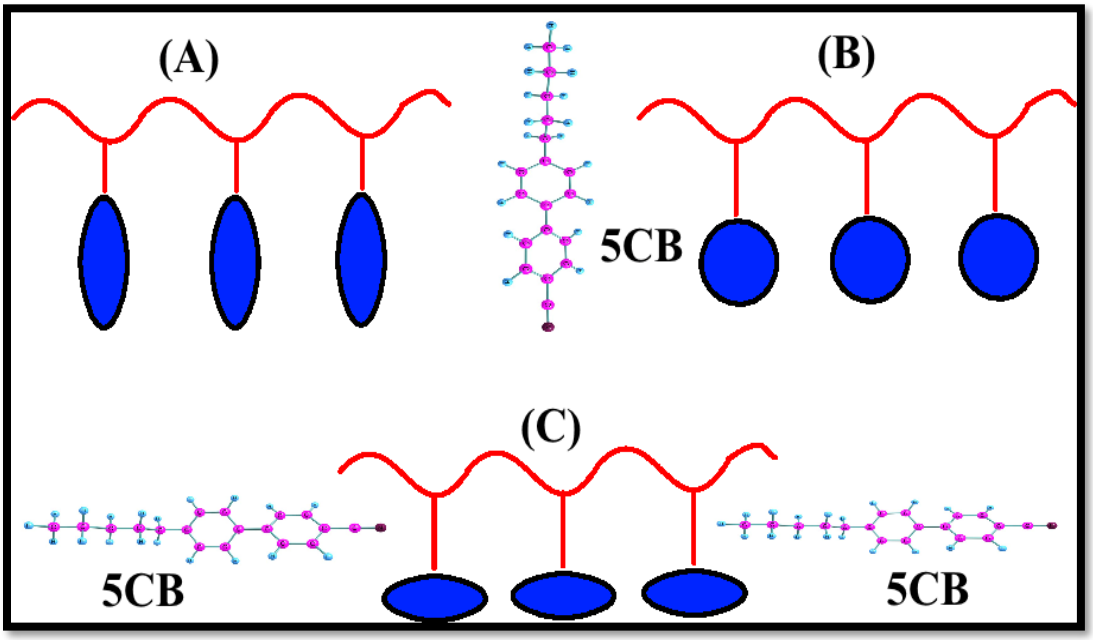

Figure 1.6 Different molecular arrangement of Liquid Crystal Polymers

1.3 Lyotropic liquid crystals

This consists of different molecules having a non-mesogenic liquid; it is always present in the solution form. Usually, the mixture is formed by amphiphilic molecule and water

for e.g., soap and water [36]. The concentration of water shows different mesophases like lamellar, hexagonal, and cubic phase. When the amphiphilic molecules are arranged in the form of a layer, then the lamellar phase arises [37]. The polar heads of subsequent layers contain water in between, whereas the alkyl chain is in the non-polar region. The hexagonal phase composed of micelle arranged in the form of a cylinder, giving rise to the hexagonal pattern. In the cubic phase, the micelle forms an emulsion in water shaped in a sphere having an alkyl chain in the interior and polar head groups on the exterior [38].

1.4 Phase Identification

To identify a liquid crystalline phase, the textures of the phase must be analyzed with a polarized optical microscope. If the texture of the phase changes even in a narrow temperature range, then this indicates that the phase transition has occurred [39]. This is a reversible phenomenon as one can get previously observed phase by altering the heating or cooling rates. The phase identification under the impact of temperature as shown in Fig. 1.7.

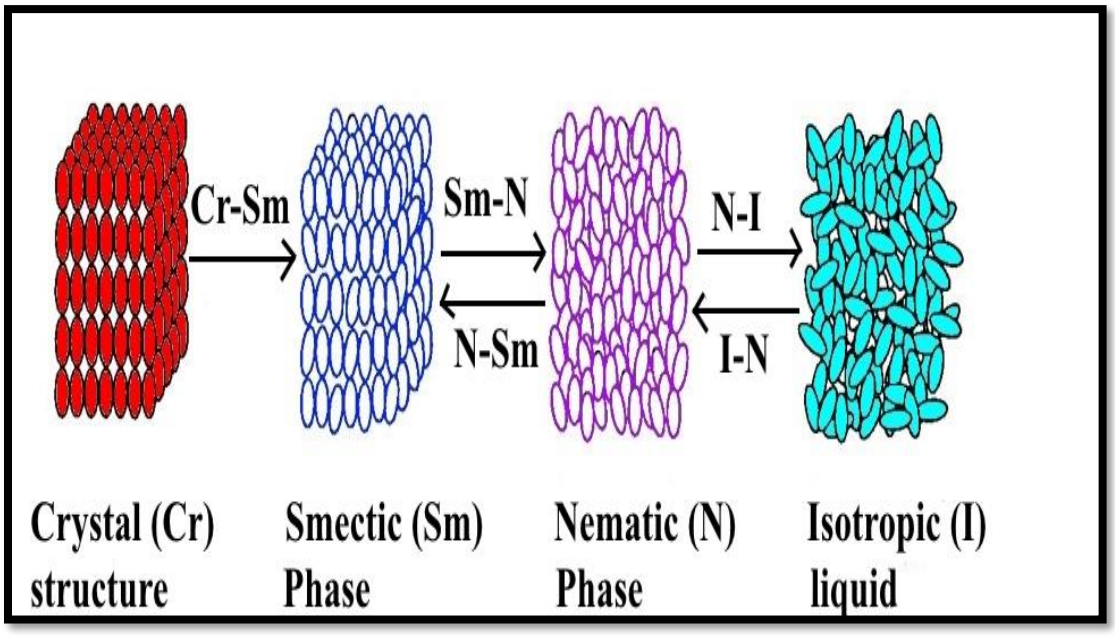

Figure 1.7 Phase Identification under the impact of temperature

1.5 Physical Properties due to Anisotropic Behaviour

Most of the physical properties of the liquid crystals are not direction-dependent, i.e., anisotropic. Due to anisotropic behavior and interaction of liquid crystal with environment results in many spectacular phenomena [40]. One of the examples is the properties of liquid crystal are affected due to changes in the value of the electric field. With the help of this, liquid crystals are being used in optical display devices. Some of the important phenomena are field-induced domain patterns, flexoelectric distortion, ferroelectric switching, etc. One of the essential physical properties by which the liquid crystal mixture is optimized is optical anisotropy [41]. The material can be birefringent due to optical anisotropy. In-display devices, liquid crystals are aligned in such a way that it can control the amount of polarized light [42].

1.6 Dielectric Anisotropy

The interaction of matter with the electric field results in the dielectric properties of the material. Dielectric permittivity is the measure of this phenomenon. For a material having non-polar molecules, induced polarization is of two types:

(a). Electronic polarization

(b). Ionic polarization

Materials consisting of polar molecules also have orientational polarization in addition to the above polarization [43]. A theoretical study of liquid crystal having anisotropic behavior reveals that the anisotropy arises due to individual molecular entities.

A dipole-dipole correlation in smectic phases is different from the nematic phases. It arises due to the different types of interaction with the surrounding dipoles of molecules. This leads to a change in the value of dielectric anisotropy [44]. The Dielectric permittivity (ε) of liquid crystal under the impact of temperature (°C) is represented by the Fig. 1.8.

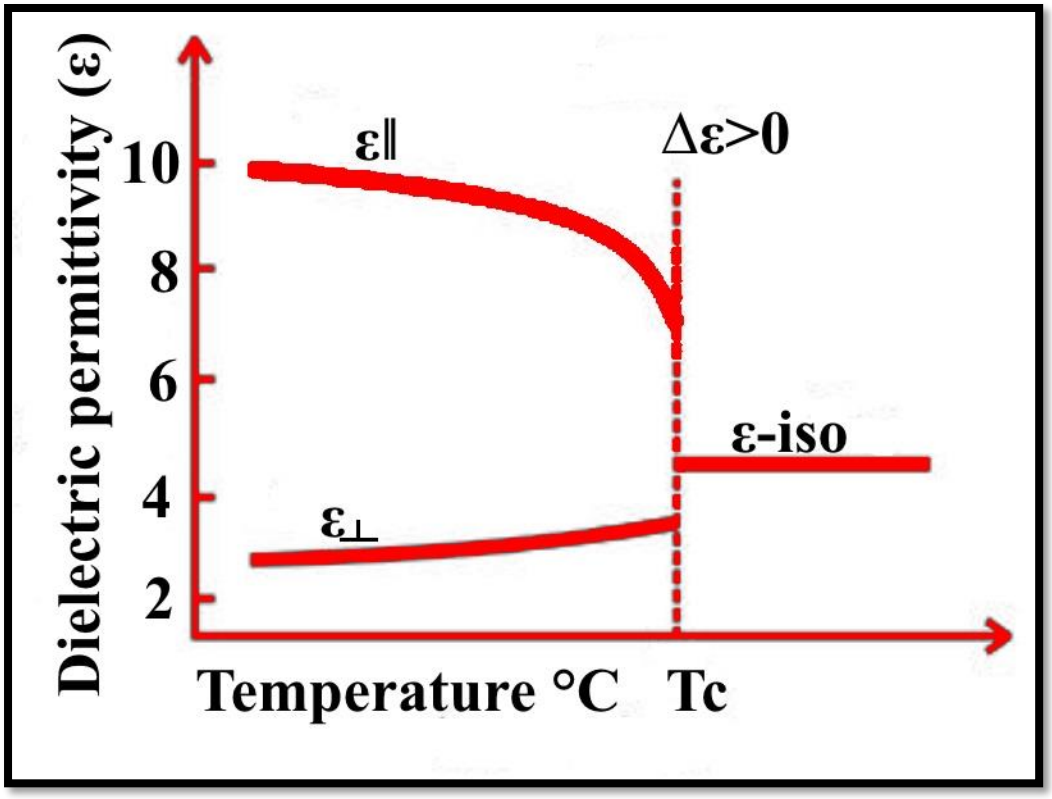

Figure 1.8 Dielectric permittivity (ε) of LC under the impact of temperature (°C)

1.7 Diamagnetic Anisotropy

A property most widely used in the study of liquid crystals is magnetic susceptibility as liquid crystals gave a quick response to change in the magnetic field. Like, many of the organic substances, liquid crystals are diamagnetic in nature [45]. The magnetic properties of individual molecular components result in diamagnetic behavior. Magnetic susceptibility is the measure of response occurred when external magnetic field changes in a liquid crystal. The nature of the response is linear when the value of the magnetic field is small [46]. Magnetic susceptibility has a negative value for diamagnetic material and does not depend on field strength and temperature. Liquid crystals containing aromatic ring have positive dielectric anisotropy; with the substitution of every cyclohexane ring with a benzene ring, the value decreases. A negative value is observed in cycloaliphatic LC [47].

1.8 Transportation in Liquid Crystal

1. Coefficient of Viscosity: The obstruction of a fluid to flow when shear stress is applied is known as viscosity. The different layers of a fluid offer internal friction due to their velocity gradients. The viscous force is directly proportional to the area and velocity of the fluid layer and inversely proportional to the separation between the layers [48]. A proper distinction between dynamic viscosities and kinematic viscosities is not possible in the case of the nematic liquid crystal [49]. The anisotropic behavior of viscosity is observed in liquid crystals. It is a collective property that results due to the interaction of different molecules with one another [50]. The rotation of a molecule around a particular axis gives rise to rotational viscosity. In the presence of an electric or magnetic field, the reorientation of the director axis changes the value of rotational viscosity.
2. Mass Diffusion: In liquid crystalline phase, the mass diffusion is anisotropic in nature.
3. Electrical Conductivity: The conduction of electricity in a liquid crystal is due to residual impurities [51].

1.9 Elastic Constants

The liquid crystals show elastic behavior if the uniform alignment of the director and layer are tried to be deformed. A uniform strain can cause a change in distance between adjacent layers, and this is opposed by restoring forces. But in nematic liquid crystals, permanent opposing forces are absent [52].

1.10 Nematic Liquid Crystals

The molecules of a uniaxial nematic phase have their long axes parallel to each other, and they have complete rotational symmetry. The aromatic and alicyclic core units combined to form a nematic phase, but there is no specific rule to decide the core unit [53]. The short terminal chain leads to the formation of the nematic phase. Normally the core consists of two or more 1, 4 di-substituted rings having six members. But an exception of

acyclic and one ring structures forms nematic phase on dimerization exists [54]. Hydrogen bonding is the main key factor in the formation of the nematic phase. The intermolecular hydrogen bonding generates a central core structure with an elongated chain. The core structure having a phenyl ring is replaced by the alicyclic ring; this increases the stabilization of the nematic phase as they arrange themselves in a better space-filling manner [55]. This leads to anisotropic polarizability as the liquid crystalline order is still maintained. In the selection of a material for a particular application, the physical properties play an important role [56]. For fast switching applications, the material should have a low value of viscosity. The linking groups in a nematic liquid crystal are very important, one of which is the ester group. This group is versatile and is used more commonly because of its stability, easy synthesizing methods [57]. By using ester as a linking group, the liquid crystals have a lower value of the melting point. The cyano group and alkyl group are used as a terminal group, and this eases the generation of a liquid crystal. These groups provide flexibility and anisotropy in the physical properties of a mesogen [58]. Proper molecular orientation is very necessary for the generation of mesophases, and this is made easy by a proper terminal unit. The physical properties of a mesogen are also dependent on this terminal group [59]. The molecular length of a mesogen is increased by the alkyl chain, and this helps in the interaction of a mesogen with one another. But this decreases the melting point of the molecule, so to overcome this van der Waal interaction plays an important role. Also, a peculiar phenomenon is observed, the namely odd-even effect [60]. The chain length odd in number facilitates the transition in the nematic phase as compared to the even length of the molecular chain. The branching of the molecular chain causes chirality [61]. The molecular arrangement of liquid crystal as shown in Fig. 1.9.

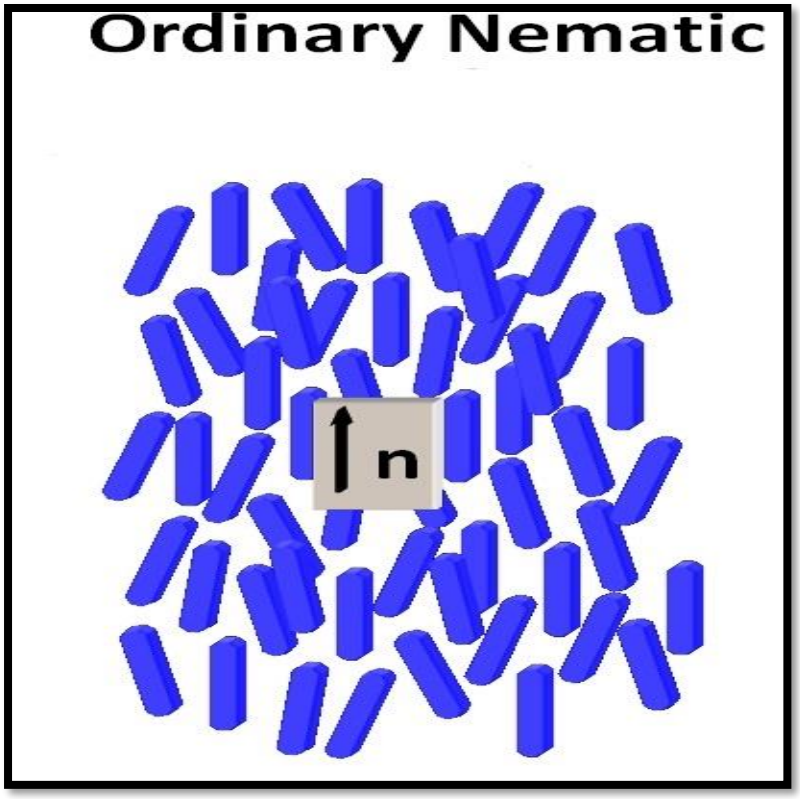

Figure 1.9 Molecular arrangement of ordinary Nematic LC

1.11 Smectic Liquid Crystals

In this phase, long molecular axes are ordered orientational and positional order is reduced. Two types of phases arise due to different orientations. One is orthogonal, and the other is the tilted phase as shown in Fig 1.10. With the help of optical instruments, one can distinguish one phase from the other [62]. Smectic liquid crystals are characterized by their periodicity in the space in one direction. A very large number of smectic phases are present due to group symmetry. One of the simplest is smectic A formed by the disordered liquid stacking in two dimensions [63]. For the smectic C phase, the molecules must be aligned in a tilted direction as compared to the stacked layers of liquid crystal. Another point of differentiation between smectic A and smectic C is optical alignment, the former is uniaxial, and the latter is biaxial [64]. From the uniaxiality of smectic liquid crystal, the focal-conic texture arises. They sometimes aligned to form a polygon-shaped structure and sometimes homeotropic textures. But it is

difficult to differentiate between homeotropic smectic A and homeotropic nematic texture [65].

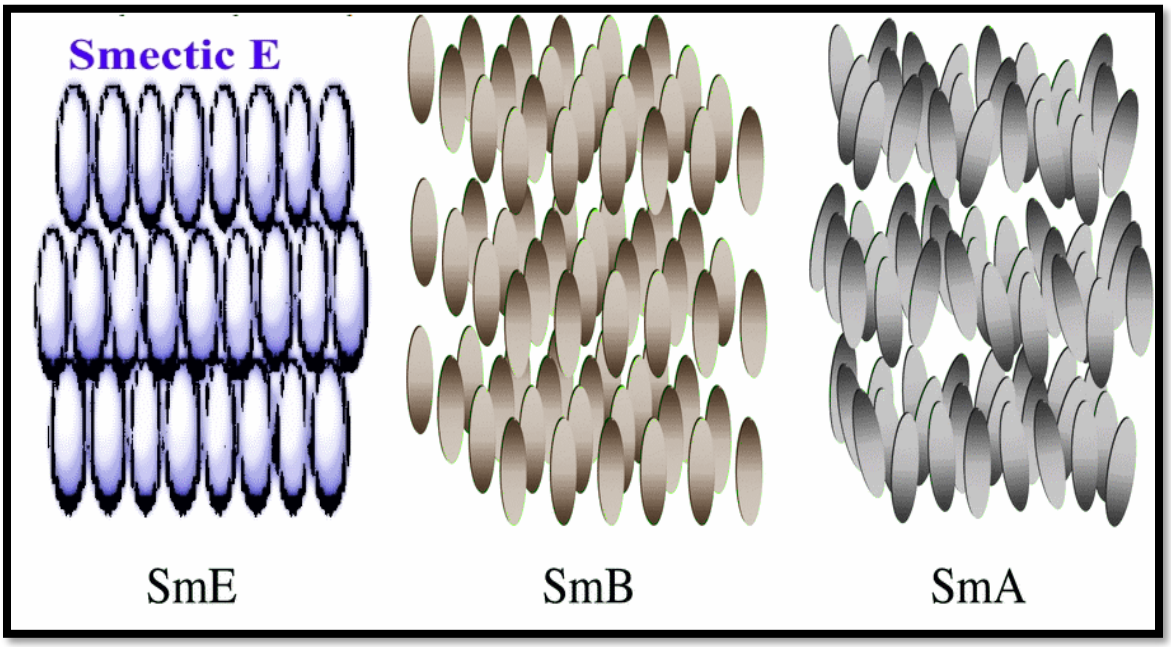

Figure1.10 Molecular arrangement of Smectic LC

1.12 Smectic With Ordered Layers

X-ray diffraction reveals that the three-dimensional positional order exists in smectics, and these are different from crystals as they have the ability to realign themselves. In the smectic G and smectic J phase, the molecules are free to rotate about their long molecular axis. But, this type of rotation is not allowed in the case of the smectic E phase [66]. In all these cases, there is no focal conic texture, but some mosaic textures are observed in some regions. Due to the lamellar structure of the smectic phases, the molecules of this phase must be capable of attracting laterally with each other [67]. The cores of the molecules are straight, narrow, and have a similar type of units tend to form smectic phase more easily. Biphenyl core is the best-suited example for this phase as it helps in lateral attractions [68]. The ordered layers of Smectic liquid crystal as shown in Fig. 1.11.

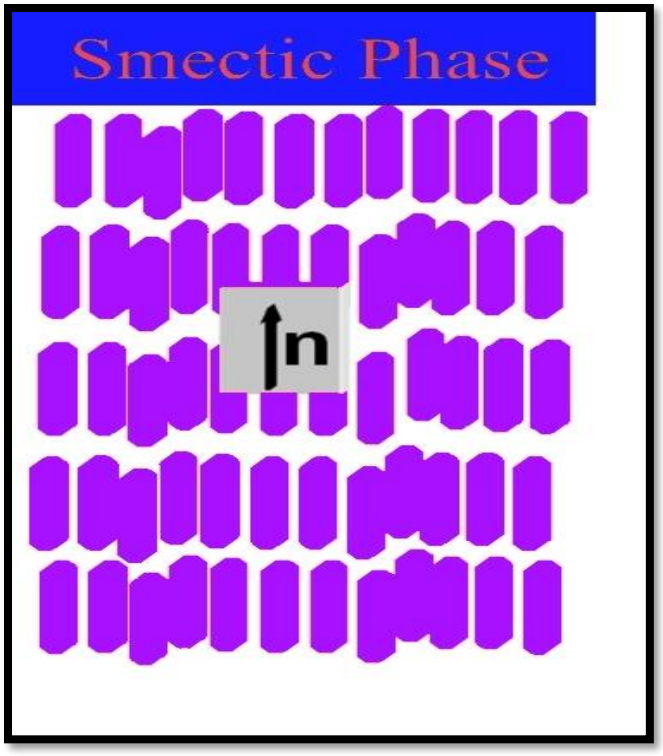

Figure 1.11 Smectic LC With Ordered Layers

1.13 Discotic Liquid Crystal

The first disc-like molecule showing liquid crystalline behavior is benzene-hexa-n-alkanoates; it consists of translational periodicity. Two types of discotic phases exist, and they are discotic nematic and discotic columnar. The side chain of a molecule hinders the formation of a discotic phase [69]. The Discotic liquid crystal with molecular arrangement of the molecules as shown in Fig. 1.12.

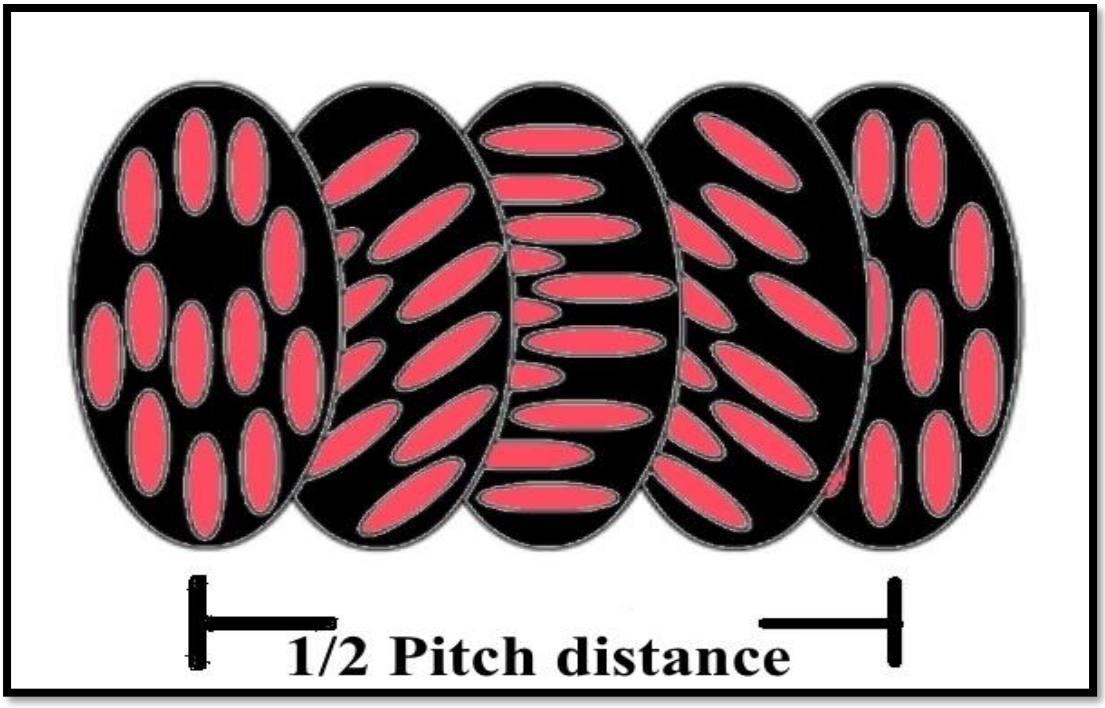

Figure 1.12 Discotic Liquid Crystal with molecular arrangement

1.13.1 Discotic Nematic Phase

The simplest discotic phase is a discotic nematic phase as it has a low value of viscosity, and it is least ordered. The anisotropic nature of discs helps them to align along the director axis with their short axes. There are a limited number of physical properties that can be measured in a discotic phase, but the values of elastic constant showed a similar order for discotic as well as calamitic [70]. The The molecular arrangement of discotic Nematic liquid crystal as shown in Fig. 1.13.

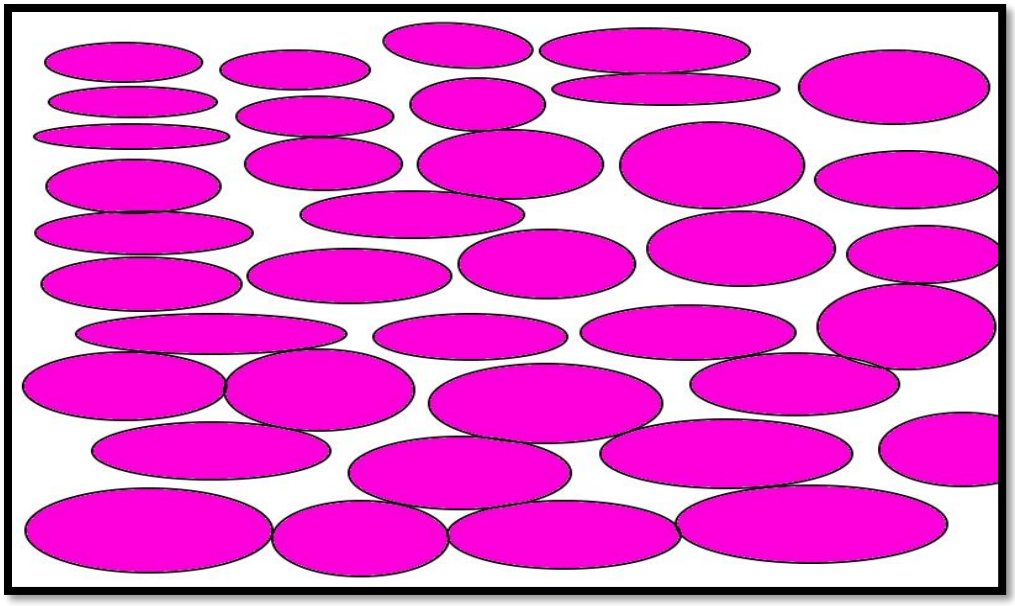

Figure 1.13 The molecular arrangement of discotic Nematic liquid crystal

1.13.2 Discotic Columnar Phase

This phase consists of discs placed one over the other forming columns of a liquid crystal, and this constitutes two-dimensional lattices. The distance between the two nearest neighboring species of this phase is equal and is independent of direction [71]. The central core of a discotic phase is generally a benzene ring or polyaromatic, but for columnar phases, alicyclic cores are required. The homologous series of discotic phases showed that the lower members of the series are discotic nematic; the transition members are both discotic and discotic nematic, lastly the higher homologous transit from discotic to isotropic phase [72]. The molecular arrangement of Discotic columnar Phase as shown in Fig. 1.14.

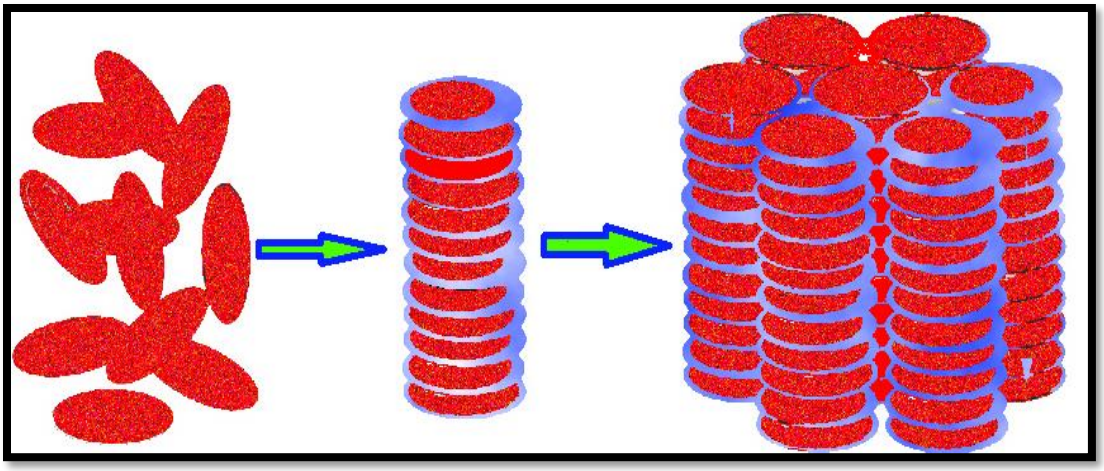

Figure 1.14 Molecular Arrangement of Discotic Columnar Phase

1.14 Polymer Liquid Crystal

A basic unit repeats on itself, forming a macromolecule, results in the formation of polymer liquid crystal. The Polymer liquid crystal with different arrangement of molecules as shown in Fig.1.15. There are two types of polymer liquid crystal:

1. Homopolymer liquid crystal: These consist of similar repeating units.
2. Copolymer liquid crystal: These consist of one or more different repeating units.

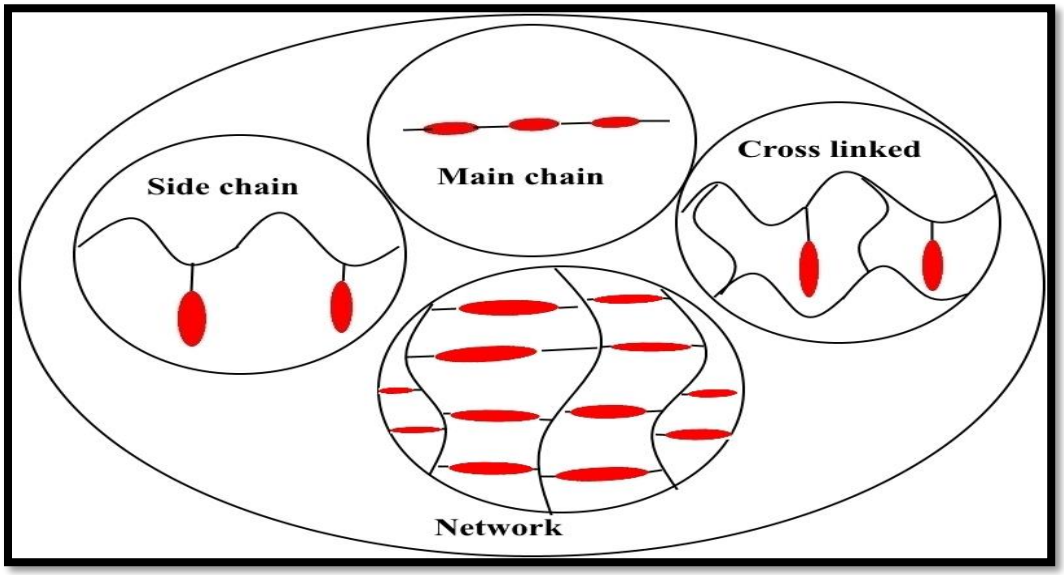

Figure 1.15 Polymer Liquid Crystals with different arrangement

The chain length can vary in a polymer liquid crystal, and it is independent of the basic units from which it is constituted [73]. The degree of polymerization is known as the average size of the individual chain. The property of a particular polymer liquid crystal depends on the type of synthesis by which they are obtained. For the synthesis of a polymer liquid crystal, a mesogen having a low value of molar mass can be utilized as a monomer [74]. To synthesize a macromolecule, a monomer is generated first by the conventional methods, and then polymerization of that monomeric unit forms liquid crystal polymer. The properties of a polymer, in combination with the properties of a liquid crystal, make it usable in a very wide variety of applications [75].

1.15 Chiral Liquid Crystal

A molecule and its mirror image do not superimpose each other; they are known as chiral molecules. It tends to the asymmetric property of the molecule, and this leads to either right-handed chirality or left-handed chirality [76]. One of the important consequences of chirality is spontaneous polarization, which leads to ferroelectric properties and makes liquid crystal to be used in electro-optical applications. In the case of achiral liquid crystals, there is no spontaneous polarization just as in the nematic phase [77].

1.15.1 Chiral Nematic Phase

This is also known as a cholesteric phase because cholesterol derivatives are the first thermotropic liquid crystals showing this phase. The texture of a chiral nematic is in resemblance with the nematic phase as shown in Figure 16. To introduce chirality in a liquid crystal material, one has to add chiral dopant molecule, and it is not necessary that they are mesogens [78]. The Chiral Nematic phase with different director orientation of the molecules shown in Fig. 1.16.

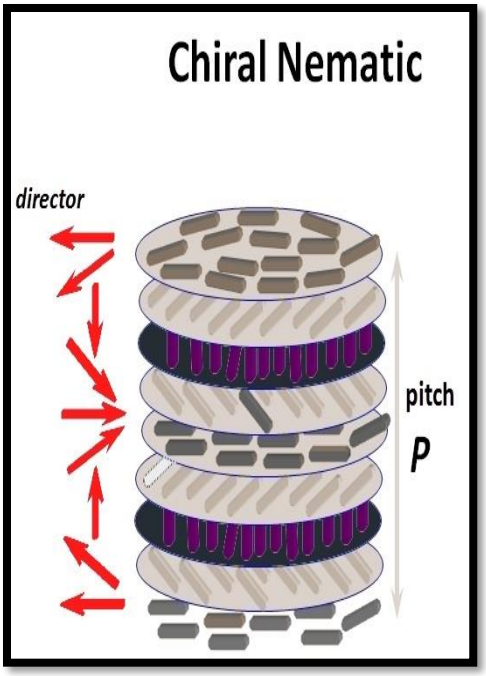

Figure 1.16 Chiral Nematic Phase with different director orientation

1.16 Physical as well as Optical Properties of Liquid Crystal

The physical properties of a liquid crystal are classified in two fields; scalar and non-scalar physical properties [79]. The scalar physical properties are transition temperature, transition enthalpy, entropy changes [80]. The non- scalar properties are dielectric, diamagnetic, optical, elastic, and viscous coefficients [81].

1.16.1 Transition Temperature: The temperature difference of melting and clearing points of a phase of a liquid crystal decides the stability of that liquid crystal. As in polymorphic substances, the higher-ordered phase has a lower transition temperature [82]. Due to the increase in the alkyl chain, the clearing point of a mesogen decreases. The mesogen containing an odd number of the alkyl chain, show a decrement in clearing point, this leads to odd-even effect [83]. If clearing is taking place in a very narrow range of temperature, the compound is more likely to be a pure one. The presence of an impurity in a compound increases the range of temperature of clearing [84].

1.16.2 Transition Enthalpy: In the process of melting, the enthalpy (energy) is supplied from outside, and in the process of crystallization, the enthalpy is released to the surroundings [85]. This causes a structural change in the compound, but only change in enthalpy cannot determine the type of phase in a liquid crystal. An approximate range of change in enthalpy from 30 to 50kJ/mol is required to change a crystalline phase into an isotropic phase [86]. Some smaller enthalpy changes also arise in the transition from the nematic to isotropic phase. In some cases, it is very difficult to detect the smaller enthalpy changes as they are nearly equal to 300kJ/mol [87].

1.17 Anisotropic Physical Properties

1.17.1 Refractive Index: This arises due to optical anisotropy in the mesogen, and it is helpful in the optimization of the mesogen so makes it better to be used in display devices [88]. The liquid crystals having two refractive indices are called birefringent, and this birefringence is dependent on two factors; the wavelength of the incident light and temperature of the surrounding. An instrument Abbe's refractometer is helpful in the determination of refractive indices of a mesogen [89]. The refractive index of general liquid crystal as shown in Fig. 1.17.

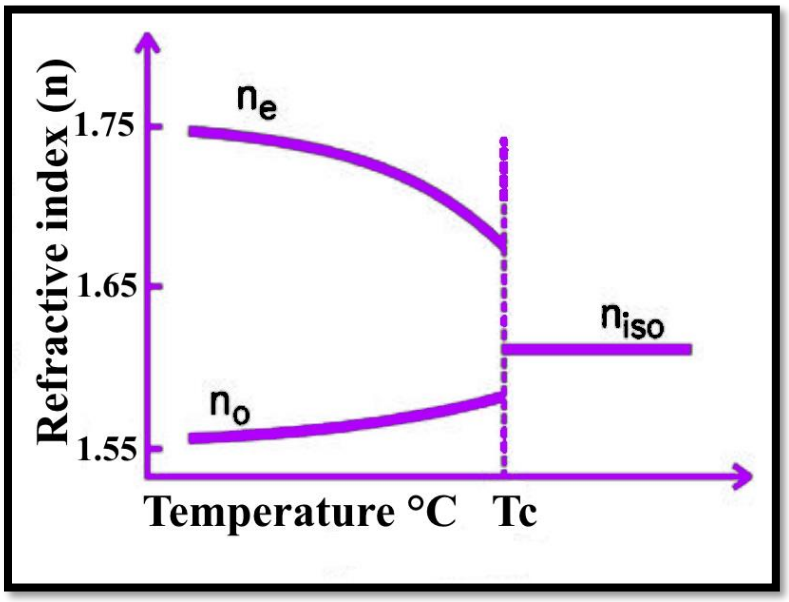

Figure 1.17 Refractive index of general liquid crystal

1.17.2 Dielectric Permittivity: The dielectric property of a mesogen is dependent on the application of the electric field. The electric field polarizes the mesogen, and hence the capacitance increases [90]. In the case of nonpolar molecules, two types of polarization exist electronic and ionic polarization. In the case of polar molecules, other than these two polarizations, one additional type of polarization exists, i.e., orientational polarization [21].

1.17.3 Diamagnetic Anisotropy: To study the behavior and properties of liquid crystals, the sensitivity of liquid crystals towards the magnetic field have been exploited from the earlier times [19]. Like most of the organic materials, liquid crystals are also diamagnetic in nature. When a cyclohexane derivative ring substitutes a benzene ring, the value of diamagnetic anisotropy decreases [91]. In a pure cycloaliphatic liquid crystal, diamagnetic anisotropy has a negative value. To define the orientational order of a mesophase, this can be used as an order parameter [92].

1.18 Order Parameter

This differentiates the mesogen from one another on the basis of the configuration of molecules, as they are more ordered or less ordered [93]. For different causes, this order parameter behaves differently. It sometimes considered as a scalar quantity as in liquid-vapor transition and sometimes as a vector quantity as in ferromagnetic transitions. For the measurement of the order parameter, infrared and Raman spectroscopies play an important role [94]. Also, birefringence is directly related to the order parameter. In the case of rod-like molecules, the mean directions of long axes are parallel to one another [95]. Due to the orientational order present in the liquid crystal, the anisotropic properties are found in liquid crystal. These direction-dependent properties are affected due to the presence of the electric field, magnetic field, and shear strain [96]. We can calculate the orientational order parameter by taking the orientation of long molecular axis as a unit vector **a**; then the orientational distribution function is represented as

$$f(\theta,\Phi).f(\theta,\Phi)d\Omega$$

Where $d\Omega = \sin\theta d\theta d\Phi$ and $d\Omega$ is the solid angle.

For isotropic phase f (θ, Φ) is constant and in uniaxial crystals f = f(θ), which shows it only depends on polar angle θ [97]. The order parameter is zero for an unordered phase at high temperature and is non zero for an ordered phase at low temperature. Also, it can be positive or negative. If two order parameters shows similar absolute value, but they are opposite in signs, then they belong to different states [98]. In the case of the second-order phase transition, the order parameter increases from zero as the temperature is being lowered up to a value of transition temperature. Around transition temperature, the order is very low in value. For a magnetic system, magnetization is considered as an order parameter. The highest value of the order parameter is 1 [82]. The order parameter of general liquid crystal as shown in Fig. 1.18.

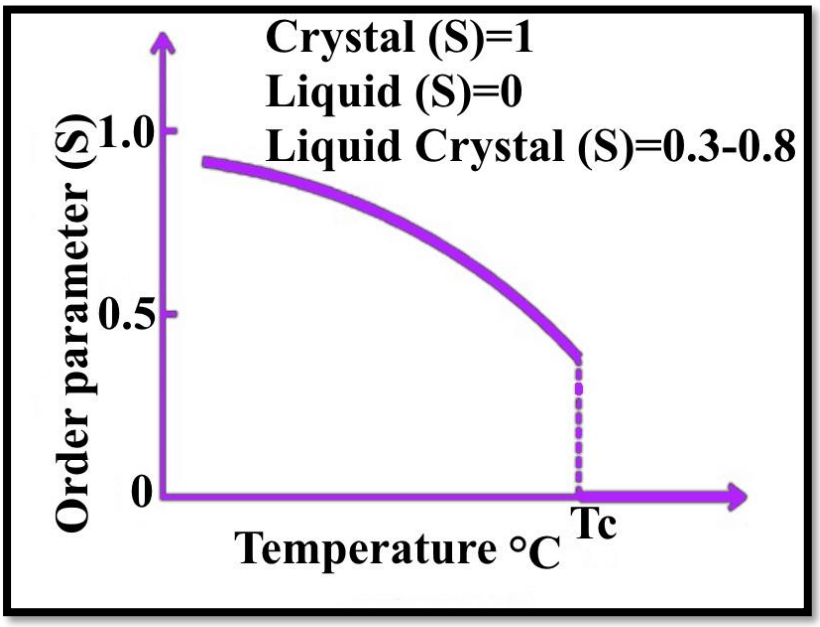

Figure 1.18 Order parameter of general liquid crystal

1.19 Elastic Properties of Liquid Crystals

The liquid crystal director **n** can vary with space due to the presence of an external electric field. This variation of the director is directly linked to the energy, and it is called the deformation of the director. It is concluded that elastic energy is proportional to the square of the spatial rate of variation [22]. In the case of nematic liquid crystals, the possible deformations are splay, twist, and bend. When an observable change in director is observed across the length L, then the angle between the average directions of long molecular axes is changed through a/L as 'a' is molecular size [19]. In the case of cholesteric liquid crystal, the director twists in space, and the axis around which it twists is known as the helical axis. These cholesteric liquid crystals are also known as chiral nematic liquid crystals. By mixing nematic hosts with a chiral dopant, the cholesteric liquid crystal can be obtained [99].

The smectic liquid crystals have partial positional order along with orientational order, as in the above two cases. The compression in the smectic layer is directly proportional to the elastic energy [100]. The twist and bend deformations of the director are not allowed in case of smectic liquid crystals as it changes the thickness of the layer and requires a lot of energy [101]. If the temperature is lowered, some of the chiral liquid crystals change their phases from isotropic-cholesteric-smectic A. One observable phenomenon occurs when the temperature is changed that is the color of liquid crystal changes [102]. This leads to a new type of liquid crystal known as thermochromic liquid crystal, and this phenomenon is used in the manufacturing of thermometers. The resistivity of the liquid crystal is very high, and dipole moments are induced in them with the help of an external electric field [103].

1.20 Magnetic Susceptibility

The magnetic interaction between the molecules is weak, and the localized magnetic field of all the molecules is nearly similar to the applied external magnetic field [104].

In the case of uniaxial liquid crystal, the shape of the molecule is considered to be cylindrical. The angle between the long molecular axis and the applied external field decides the response of liquid crystal [105]. The decomposition of the magnetic field into parallel and perpendicular components occurs. The liquid crystal rotates due to the thermal motion [106].

1.21 Anchoring Energy

When there is no externally applied field, the anchoring condition decides the orientation of the liquid crystal. The LC's anchoring energy is considered on the molecular level. The interaction energy between LC layers to explain the experimental values of anchoring energy. The polar terminal and azimuthal anchoring energy depends upon the order parameter [107].

1.22 Structural Properties of Liquid Crystals

The molecules containing a certain degree of rigidity have well defined molecular structure. Like n-alkanoic acids are present in the form of extended conformers, but due to flexibility, they cannot form thermotropic liquid crystals [108]. The molecular electronic structure is responsible for the molecular shape and hence rigidity. The carbon bond having sp^2 hybridization when it comes in contact with the double bondhinders the internal rotation of the molecule and provides rigidity, and hence the formation of the nematic phase becomes easier [109]. The linearity is provided by the linkage groups, and some chemical changes alter the electronic structure [110].

1.23 Birefringence

The difference between the refractive indices of a given liquid crystal leads to the birefringent nature. The orthogonal polarization in the optical radiation is responsible for the birefringence [111]. Like nematic liquid crystals have birefringence in the range of 0.1 to 0.2. The electronic structure and energy levels affect the optical properties of the liquid crystal [112]. The ring units of a liquid crystal and their electronic structure are responsible for the polarisability, refractive indices, and light

absorption [80]. Most likely, the ring units are cyclohexane and phenyl rings having σ bonded carbon atoms. The polarized absorption spectra are found in the liquid crystal having biphenyl units. Also, the changes in the alkyl chain are also responsible for the change in birefringence [113]. The birefringence of general liquid crystal as shown in Fig. 1.19.

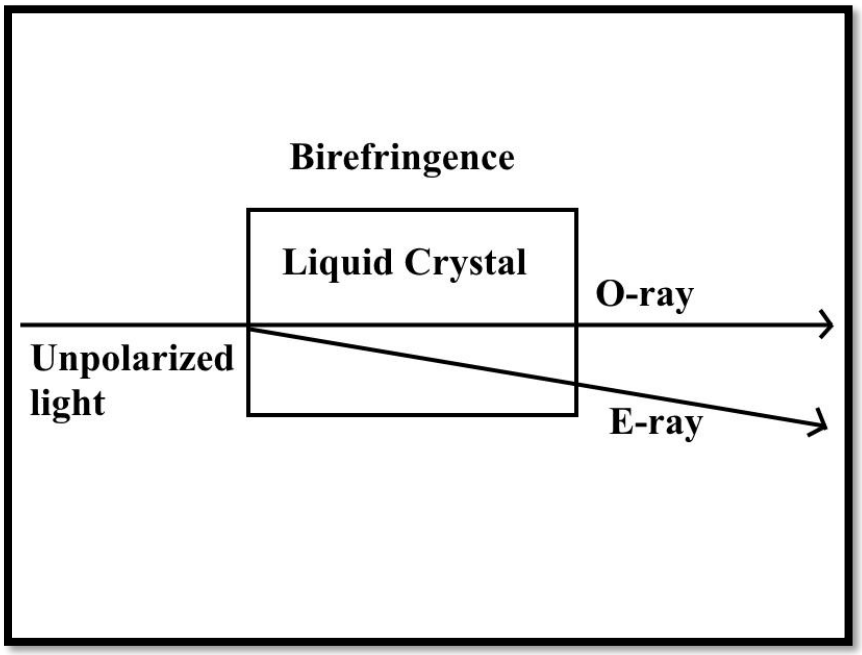

Figure 1.19 Birefringence of general liquid crystal

1.24 Elasticity

The deformations of a solid are different from the liquid crystal in the way as there is an absence of translational displacement of molecules [114]. This arises due to the slipping of the liquid layers of the liquid crystal. The conservation of elastic energy holds during the shear deformation of the liquid crystal [115]. The change in density is directly proportional to the elasticity of the liquid crystal. One can determine the change in density with the help of a particular modulus, but elasticity is dependent on the orientational order [116]. The order parameter remains constant while the director field changes with the externally applied electric field direction. The deformation

corresponding to the splay, bend, and twist affects the elastic energy, and the rest are forbidden [117].

1.25 Tensor Properties of Liquid Crystal

Like non-cubic crystals, the properties of a liquid crystal depend on the direction along which they are measured. This is known as tensor properties, and it changes with the change in orientation of the defined axis. A scalar rank tensor property does not depend on the direction for e.g. density [118].

1.26 Applications of Liquid Crystal

(a) Temperature sensors

(b) Medical use (cancer medicine)

(c) Electrical devices

(d) Solar Cell

(e) Liquid Crystal Display (LCD)

(f) Chromatographic separations

(g) LC thermometer

(h) Optical Imaging

1. References

2. F. Reinitzer, *Monatsch Chem.* **9,** 421 (1888).
3. G.W. Gray, *Molecular Structure and the Properties of Liquid crystals,* (Academic Press Inc., London, 1962).
4. C. Robinson, *Liquid Crystals* (Gordan and Breach Science Publishers, London,1966).
5. J. L. Ericksen, *Liquid crystals and Ordered Fluids* (Plenum Press, N.Y., 1970).
6. G. W. Gray, P. A. Winsor, eds., *Liquid crystals and Plastic crystals*, Vol. 1 (Ellis Horwood, Chichester, England, 1974).
7. E. B. Priestly, P. J. Wojtowicz, and P. Sheng, eds., *Introduction to Liquid Crystals,* (Plenum Press, New York, 1975).
8. S. Chandrasekhar, *Liquid crystals* (Cambridge University Press, 1977, 1992).
9. D. Demus and L. Ritcher, *Textures of Liquid crystals* (Verlag Chemie, New York, 1978).
10. F. D. Saeva, ed., *Liquid crystals: The Fourth State of Matter* (Marcel Dekker Inc. 1979).
11. G. R. Luckhurst, and G. W. Gray, eds., *The Molecular Physics of Liquid Crystals*, (Academic Press Inc., London, 1979).
12. H. Kelker, and R. Hatz, *Handbook of Liquid crystals* (Verlag Chemie, Weinheim, 1980).
13. L. Bata, ed., *Advances in Liquid crystal Research and Applications* (Pergamon, Oxford, 1980).
14. L. M. Blinov, *Electro-optical and Magneto-optical Principles of Liquid crystals*, (Wiley, Chichester, 1983).
15. G. W. Gray, J. W. Goodby, *Smectic Liquid Crystals:Textures and structures,* (Leonard Hill, London, 1984). (b) J. W. Goodby, R. J. Mandle, et al, *liq.cryst.,* **42,** 593, (2015).
16. A. C. Griffin, ed., Ordered Fluids and Liquid Crystals, (Plenum Press, New York,1984)
17. J. L. Ericksen, D. Kinderlehrer, eds., *Theory and Applications of Liquid crystals* (Springer Verlag , New York , 1987).
18. G. W. Gray, ed., *Thermotropic Liquid Crystals* (Wiley, New York , 1987).
19. P. S. Pershan, *Structure of Liquid Crystals* (World Scientific 1988).
20. G. Vertogen, W. H. de Jeu, *Thermotropic Liquid crystals, Fundamentals*, (Springer-Verlag, New York 1988).
21. V. A. Belyakov, V. E. Dmitrienko, *Optics of Chiral Liquid Crystals,* (Academic Publishers, Glasgow, Harwood, 1989).
22. L. Pohl, U. Finkenzeller, *Physical Properties of Liquid Crystals: Applications and Uses*, vol.1, ed., B. Bahadur (World Scientific 1990 Chapter 4 p. 139).

23. P. G. de Gennes, J. Prost, *The Physics of Liquid crystals*, (Clarendon Press, Oxford, 1993).
24. F. Biscarini, C. Chiccoli, P. Pasini, F.Semeria, C. Zannoni, *Phys. Rev. Lett.,* **75** 1803, (1995).
25. S. Chandrasekhar, *Mol. Cryst. Liq. Cryst.,* **124,** 1 (1985).
26. G. W. Gray, K. J. Harrison, J. A. Nash, *Electron Lett.,* **9**, 130, (1973).
27. R. Eidenschink, D. Erdmann, J. Krause, L. Pohl, *Angew. Chem. Int. Ed. Engl.*, **16**, 100 (1977).
28. G. W. Gray, K. J. Harrison, J. A. Nash, *J. Chem. Soc. Chem. Commun.,* **1974**, 431 (1974).
29. S. M. Kelly, *Liquid Crystals,* **10**,261, 273, (1991).
30. H. Takatsu, K. Takeuchi, H. Sato, *Mol. Cryst. Liq. Cryst.,* **100**, 345 (1983).
31. M. A. Osman, T. Huynh-Ba, *Mol. Cryst. Liq. Cryst.,* **82** 331,(1983).
32. S. Singh, Phys. Rep., **324** 107, (2000). (b) J. R. Bruckner, F. Giesselmann, *crystals,* **9**, 568 (2019)
33. J. C. Toledano, P. Toledano, *The Landau Theory of Phase Transitions*, (World Scientific, Singapore, 1987).
34. P. J.Collings, J. S. Patel, eds., *Handbook of Liquid Crystal Research* (Oxford Univ. Press, Oxford, 1997)
35. S. Elston, R. Sambles, eds., *The Optics of Thermotropic Liquid Crystals* (Taylor and Francis Ltd., London, 1998).
36. P. J. Collings, M. Hird, *Introduction to Liquid Crystals: Chemistry and Physics* (Taylor and Francis Ltd, London, 1977) (b) T. Ganicz, W. Stanczyk, *materials*, **2,** 95, (2009).
37. M. P. Taylor, R. Hentschke, J. Herzfeld, Phys. Rev. Lett. **62**, 800 (1989)
38. K. Sokalski, *Physica A,* **113**, 133 (1982).
39. C. D. Mukherjee, T. R. Bose, D. Ghosh, M. K. Roy, M. Saha, *Mol. Cryst. Liq. Cryst.,* **124,** 139 (1985).
40. H. Wang, M. Y. Jin, R. C. Jarnagin, T. J. Bunning, W. Adams, B. Cull, Y. Shi, S. Kumar, E. T. Samulski, *Nature,* **238,** 244 (1996).
41. B. Mulder, *Phys. Rev.,* **A35**, 3095 (1987).
42. R. Holyst, A. Poniewierski, *Phys. Rev.,* **A39,** 2742 (1989).
43. A. M. Somoza, P. Tarazona, *Phys. Rev. Lett.,* **61,** 2566 (1988).
44. M. C. Mahato, M. Raj Lakshmi, R. Pandit, H. R. Krishnamurthy, *Phys. Rev.,* **A38**, 1049 (1988).
45. R. G. Preist, *Mol. Cryst. Liq. Cyst.,* **37**, 101 (1976).
46. R. B. Griffiths, Phys. Rev. Lett. **24**, 175 (1970); M. Marynissen, J. Thoen, W. Van Dael, *Mol. Cryst. Liq. Cryst.,* **124** 195 (1985).
47. R. Alben, *Solid State Commun.,* **13,** 1783 (1973).
48. B. I. Halperin, T. C. Lubensky, S. K. Ma, *Phys. Rev. Lett.,* **32,** 292 (1974).

49. I. Lelidis, G. Durand, *J. Phys. II (Paris)*, **6**, 1359 (1996).
50. M. A. Anisimov, V. P. Voronov, A. O. Kulkov, F. Kholmurodov, *J. Phys. (Paris)*, **46**, 2137 (1985).
51. M. A. Anisimov, *Critical Phenomena in Liquids and Liquids Crystals* (Gordan and Breach, 1991)
52. W. H. de Jeu, *NATO School on Phase Transitions in Liquid Crystals*, Erice, Italy (May, 1991)
53. C. Dasgupta, B. I. Halperin, *Phys. Rev. Lett.*, **47**, 1556 (1981).
54. T. C. Lubensky, *J. Chim. Phys.*, **80**, 31 (1983).
55. D. R. Nelson, J. Toner, *Phys. Rev.*, **B24**, 363 (1981).
56. J. Toner, *Phys. Rev.*, **B26**, 462 (1982).
57. C. Dasgupta, *Int. J. Mod. Phys.*, **B9**, 2219 (1995).
58. B. R. Patton, B. S. Andereck, *Phys. Rev. Lett.*, **69**, 1556 (1992).
59. J. G. Kirkwood, E. Monroe, *J. Chem. Phys.*, **9**, 514 (1941).
60. E. M. Averyanov, V. A. Gunyakov, *Opt. Spectrosc.*, **66**, 72 (1989).
61. J. W. Emsley, G. R. Luckhurst, H. S. Sachdev, *Liquid Crystals*, **5**, 953 (1989).
62. M. P. Fontana, B. Rosi, N. Kirov, I. Dozov. *Phys. Rev. A*, **33**, 4132 (1986).
63. M. D. Lipkin, D. W. Oxtoby, *J. Chem. Phys.*, **79,** 1939 (1983).
64. T. J. Sluckin, P. Shukla, *J. Phys.*, **A16**, 1539 (1983),
65. P. Patel, S. S. Keast, M. E. Neubert, S. Kumar, *Phys. Rev. Lett.*, **69**, 301 (1992),
66. J. Prost, *J. Phys., (Paris)* **40**, 581 (1979),
67. J. Prost, P. Barois, *J. Chim. Phys.*, **80,** 65 (1983),
68. J. Wang, T. C. Lubensky, *Phys. Rev.*, **A29**, 2210 (1984).
69. G. Friedel, *Ann. Physique*, **18**, 273 (1922).
70. S. Chandrasekhar, B.K. Sadashiva, K.A. Suresh, *Pramana*, **9**, 471 (1977).
71. A. M. Levelut, *J. Chim. Phys.*, **88**, 149 (1983).
72. C. Destrade, N. H. Tinh, H. Gasparoux, J.Malthete, A. M. Levelut, *Mol. Cryst. Liq. Cryst.*, **71**, 111 (1981). (b) A. Gowda, M. Kumar, S. Kumar, *liq. cryst.*, **44**, 1990 (2017).
73. H. P. Hinov, *Mol. Cryst. Liq. Cyrst.*, **136**, 221 (1986).
74. S. Chandrasekhar, S. Krishna Prasad, *Contemp. Phys.*, **40**, 237 (1989).
75. J. D. Brooks, G. H. Taylor, *Carbon*, **3**, 185 (1965).
76. J. E. Zimmer, J. L. White, *Mol. Cryst. Liq. Cryst.*, **38**, 177 (1977).
77. J. Malthete, A. Collet, *Nouv. J. Chem.*, **9**, 151 (1985).
78. H. Zimmerman, R. Poupko, Z. Luz, J. Billard, *Z. Naturforsch. a*, **40,** 149 (1985).
79. E. I. Kats, *Sov. Phys. JETP*, **48,** 916 (1978).
80. F. Yang, J. R. Sambles, *Liquid Crystals*, **13,** 1 (1993).
81. W. Maier, G. Meier, *Z. Naturforsch A*, **16** , 262 (1961).
82. F. Noack, *Mol. Cryst. Liquid Cryst.*, **113**, 247 (1984).
83. F. C. Frank, *Disc. Faraday Soc.*, **25**, 19 (1958).

84. H. Schadt, B. Schedule, J.Nehring, *J. Chem. Phys.*, **71**, 5140 (1979).
85. F. Rondelez, J. P. Hulin, *Solid State Commun.*, **10**, 1009 (1972).
86. J. P. Huralt, *J. Chem. Phys.*, **59**, 2068 (1973).
87. M. Delaye, R. Ribotta, G. Durand, *Phys. Lett.*, **44A**, 139 (1973).
88. N. A. Clark, R. B. Meyer, *App. Phys. Lett.*, **22**, 493 (1973).
89. W. H. de Jeu, *Physical Properties of Liquid Crystalline Materials* (Gordan and Breach Science Publishers, New York, London, 1980)
90. U. Finkenzeller, T. Geelhaar, G. Weber, L. Pohl, *Liquid Crystalline Reference compounds*, Proc. of the 12th Int. Liquid Crystal Conf., Freiburg, West Germany (1988) p.84.
91. F. G. Smith, J. H. Thomson, *Optics*, 2nd ed. (John Wiley and Sons Ltd. Chichester, (1988).
92. S. Singh, *Phys. Rep.*, **277**, 283 (1996).
93. A. Beyer, U. Finkenzeller, Merck Liquid Crystals (January 1995)
94. C. Zannoni, in: G. R. Luckhurst, G. W. Gray (Eds.), *The Molecular Physics of Liquid Crystals*, Acad. Press, New York, (1979) (Chapter 3).
95. Y. Singh, *Phys. Rep.*, **207**, 351 (1991).
96. S. Goshen, D. Mukamel, S. Shtrikman, *Mol. Cryst. Liq. Cryst.*, **31,** 171 (1975).
97. J. P. Straley, *Phys. Rev. A*, **10,** 1881 (1974).
98. Y. Singh, K. Rajesh, V. J. Menon, S. Singh, *Phys. Rev. E*, **49,** 501 (1994).
99. C. W. Oseen, *Trans. Faraday. Soc.*, **29**, 883 (1933).
100. R. D. Polak, G. P. Crawford, B.C. Kostival, J. W. Doane, S. Zummer, *Phys. Rev. E*, **49**, R978 (1994).J. Charvolin, J. F. Sadoc, *J. Phys. Chem.*, **92**, 5787 (1988).
101. J. Nehring, A. Saupe, *J. Chem. Phys.*, **54**, 337 (1971).
102. F. M. Leslie, I. W. Stewart, M. Nakagawa, *Mol. Cryst. Liq. Cryst.* **198**, 443 (1991).
103. S. Chandrasekhar, G. S. Ranganath, *Adv. Phys.* **35**, 507 (1986).
104. W. H. de Jeu, P. Bordewijk, *J. Chem. Phys*., **68**, 109 (1978).
105. A. A. Sonin, *The Surface of Liquid Crystals*, (Gordon and Breach), Luxembourg, (1995).
106. T. Uchida, *Surface Alignment of Liquid crystals in Liquid Crystals-Applications and Uses*, vol. 3, ed., B. Bahadur, (World Scientific, New Jersey, (1990).
107. A. Rapini, M. Papoular, *J.* Phys. (Paris) Colloq. **30**,C-4 (1969).
108. B. O. Roos, K. Andersson, M. P. Fulscher, *Chem. Phys. Letters*, **192**, 5 (1992).
109. S. T. Wu, *J. Appl. Phys.*, **69**, 2080 (1991).
110. J. P. Crawford, J. Naciri, R. Sashidar, P. Keller, B. R. Ratna, *Mol. Cryst. Liquid Cryst.*, **263**, 223 (1991).

111. M. G. Clark, K. S. Harrison, E. P. Raynes, *Physics Technology*, *Institute of Physics Publishing*, 11, 108.
112. I. Lelidis, G. Durand, *Phys. Rev. Lett.*, **48**, 3822 (1993).
113. S. T. Wu, C. S. Hsu, *SPIE*, **3015**, 8 (1997).
114. B. Tjipto-Margo, D. E. Sullivan, *J. Chem. Phys*., **74**, 3316 (1981)
115. P. W. Atkins, R. S. Friedman, *Molecular Quantum Mechanics*, 3rdedn. Oxford University Press, Oxford (1997).
116. W. Kohn, L. J. Sham, *Phys Rev.*, **140**, A1133 (1965).
117. R. O. Jones, O. Gunnarsson, *Rev Mod Phys* **61**, 689 (1989).
118. P. Hohenberg, W. Kohn, *Phys Rev* **136**, B864 (1965).

CHAPTER 2

Methodology

2.1 Quantum Mechanics

Quantum mechanics calculate the properties of atoms, molecules, clusters, surfaces, crystalline solids, and disordered solids by solving the quantum mechanical equations that describe the positions and energies of electrons around nuclei. Quantum mechanics is capable of calculating the total energies of molecules with different distances between the atoms. But the calculations are still too time-consuming to calculate the many vibrational modes of large molecules. In chemistry, molecular mechanics is a set of tools for calculating the shapes and properties of molecules. Molecular mechanics is semi-empirical. Quantum Mechanics is a theory to describing a single particle. A molecule is made up of many atoms with many protons, neutrons, and electrons; therefore, Quantum Mechanics does not describe molecules. Quantum Mechanics includes either the Schroedinger equation (non-relativistic) or perhaps the Dirac or even the Klein-Gordon equations (relativistic), while Quantum Field theory includes or can include all three. An electron is described by the Dirac equation while a photon by the Klein-Gordon equation. Quantum Electrodynamics is a theory that explains how electrons and photons interact. Quantum mechanical (QM) methods are suitable for theoretically determining the molecular, electronic structures and optical properties of the molecules. The Schrödinger equation solution is mostly portable with the QM theory because QM theory contributes to the biological system's QM calculations and etc. The procedure involved in its rigorous formulation is known as Ab Initio molecular orbital theory. Ab Initio means from the beginning. The primary aim is to calculate the molecular properties of the molecule without considering any experimental parameters. We can describe the molecular system

at the atomic level (molecular mechanics) and the electronic level (QM) by molecular modeling. QM calculation is one of the oldest and most used mathematical formalisms of theoretical chemistry. According to QM, all possible information on a molecular system can be obtained from wave function, Ψ, which is obtained by solving the Schrödinger wave equation. The Schrödinger equation is the fundamental equation in QM and provides the basis for providing a complete electronic description of the molecule [1, 2].

Quantum chemical methods have been divided into two main classes: semi-empirical methods (such as PM7, AM1, MNDO etc.) and non-empirical (*ab initio*, DFT etc.) methods. Semi-empirical methods use some parameters derived from experimental data to simplify the calculations, and it is less demanding than *ab initio* methods. In contrast, *ab initio* calculation uses the correct Hamiltonian. It does not use the experimental data other than some physical constants' values such as the speed of light, the masses, charges of the electrons and nuclei, Plank's constant, etc. [3-5].

2.2 Hartree-Fock Approximations

The Hartree-Fock (H-F) is a method of approximation for measuring the wave function at the stationary state. The H-F method is also known as the self-consistent field method (SCF). The Hartree equation as an approximation solution of the Schrödinger equation. The H-F theory by considering a single determent for the wave function and neglect the electron correlation. Therefore H-F theory gives an inadequate description of the electronic structure. The H-F theory is insufficiently accurate to correlate accurate quantitative predictions.

In H-F theory, the energy has the form:

$$E_{HF} = V + \langle hP \rangle + 1/2\langle PJ(P) \rangle - 1/2\langle PK(P) \rangle \qquad 2.1$$

Where all the terms have the following meanings: V is nuclear repulsion energy.

P is the density matrix. $\langle hP \rangle$ is the one-electron (kinetic plus potential) energy. $1/2\langle PJ(P) \rangle$ is the classical coulomb repulsion of the electrons. $-1/2\langle PK(P) \rangle$ is the exchange energy resulting from the quantum (fermion) nature of electrons.

In the Kohn-Sham formulation of DFT, the exact exchange (H-F) for a single determinant has changed by a more general expression. The exchange-correlation functional, which can include terms calculating for both the exchange and the electron correlation energies, the exchange-correlation functional not present in H-F theory.

$$E_{KS} = V + \langle hP \rangle + 1/2\langle PJ(P) \rangle + E_X[P] + E_C[P] \qquad 2.2$$

Where $E_X[P]$ is the exchange of functional energy, and $E_C[P]$ is the correlation functional energy.

By the Kohn-Sham formulation, the H-F theory can be regarded as a particular case of DFT, with $E_X[P]$ given by the exchange integral -1/2<PK(P)> and E_C=0. The functionals commonly used in DFT are integrals of a few function of the density and possibly the density gradient:

$$E_X[P] = \int f(\rho_\alpha(r), \rho_\beta(r), \nabla\rho_\alpha(r), \nabla\rho_\beta(r))dr \qquad 2.3$$

Where the function f has been used for E_X and E_C. The pure DFT methods, Gaussian supports hybrid methods in which the exchange functional is a linear combination of the HF exchange and a functional integral of the above form. Proposed functionals lead to integrals that cannot be evaluated in closed form and are solved by numerical quadrature [6].

Hartree–Fock exact exchange functional represented by the Eq. 2.4.

$$E_X^{HF} = -\frac{1}{2}\sum_{i,j}\int\int \psi_i^*(r_1)\psi_j^*(r_2)\frac{1}{r_{12}}\psi_j(r_1)\psi_i(r_2)dr_1dr_2 \qquad 2.4$$

2.3 Density Functional Theory

The density functional theory (DFT) presents the most successful approach to compute the electronic structure of solid, liquid, and gas state of matter. The DFT applicability ranges from atoms to molecules, and solids to nuclei and quantum and classical fluids. The original formulation of the density functional theory provides the ground state properties of a system, and the electron density plays a vital role. The DFT predicts a great variety of molecular features: vibrational frequencies, molecular structures, ionization energies, atomization energies, magnetic and electric properties, reaction paths, etc. The DFT has been generalized to deal with many different situations:

multicomponent systems such as nuclei and electron-hole droplets, time-dependent phenomena and excited states, spin-polarized systems, free energy at finite temperatures, superconductors with electronic pairing mechanisms, relativistic bosons, electrons, molecular dynamics, etc. [4] The time-independent Schrödinger equation is

$$\hat{H}\Psi_i(\vec{x}_1,\vec{x}_2,...\vec{x}_N,\vec{R}_1,\vec{R}_2,...\vec{R}_M) = E_i\Psi_i(\vec{x}_1,\vec{x}_2,...\vec{x}_N,\vec{R}_1,\vec{R}_2,...\vec{R}_M) \quad 2.5$$

$$\hat{H} = -\frac{1}{2}\sum_{i=1}^{N}\nabla_i^2 - \frac{1}{2}\sum_{A=1}^{M}\frac{1}{M_A}\nabla_A^2 - \sum_{i=1}^{N}\sum_{A=1}^{M}\frac{Z_A}{r_{iA}} + \sum_{i=1}^{N}\sum_{j>i}^{N}\frac{1}{r_{ij}} + \sum_{A=1}^{M}\sum_{B>A}^{M}\frac{Z_A Z_B}{R_{AB}} \quad 2.6$$

Here A and B compute over the M nuclei while *i* and *j* indicate the N electrons in the system.

The first two terms express the kinetic energy of the electrons and nuclei. Another three terms indicate the attractive electrostatic interaction between the electrons and nuclei and, respectively, potential due to the electron-electron and nucleus-nucleus interactions.

The DFT methodology contrast to a wave function that describes the energy as a functional of the electron density. Kohn et al. have derived a set of one-electron equations that enable one to determine the electron density and, therefore, the system's total energy. The exchange-correlation (E_{XC}) functional is unknown, and therefore, approximate equations have been set-up to estimate its contribution. Generally, E_{xc} breaks into an exchange functional (E_X) energy and a correlation functional (E_C) energy. The exchange functional essentially describes two ferromagnetic spins' interactions in different orbital, whereas the correlation energy is the pairing energy of electrons in the same orbital [8, 9].

2.3.1 The Physical Significance of Hohenberg and Kohn Theorem

(a) The ground state density of the system has been calculated with the help of variational methods.

(b) The energy of a stationary quantum mechanical system has a function of ground state energy.

The energy functional of DFT is the sum of two terms. First, representing the interaction energies of all the electrons with external potential $V_{ext}(r)$, it is contributed by Coulomb interaction with nuclei. The second term $F[\rho(r)]$ represents the summation of all the electrons' kinetic energies and the influence of inter electronic exchange represented by Eq. 2.7 [10].

$$E[\rho(r)] = \int V_{ext}(r)\rho(r)dr + F[\rho(r)] \qquad 2.7$$

There is a limitation of the electron density by way of the number of electrons (N) is fixed by the equations given which are given below [11]

$$N = \int \rho(r)dr \qquad 2.8$$

$$N - \int \rho(r)dr = 0 \qquad 2.9$$

To minimize or ground state, energy has been introduced by the Lagrange multiplier (μ) given by the Eq. 2.10.

$$\delta E[\rho(r) - \mu\delta \int \rho(r)dr = 0 \qquad 2.10$$

$$\int \frac{\delta E[\rho(r)}{\delta\rho(r)}\delta\rho(r)dr - \mu\int \delta\rho(r)dr = 0 \qquad 2.11$$

The given equation is representing the chemical potential of electrons, which has correlated with the electronegativity of the system.

According to the Kohn and Sham theorem $F[\rho(r)]$ contains a set of three terms represent by the Eq. 2.12.

$$F[\rho(r)] = T_0[\rho(r)] + E_H[\rho(r)] + E_{XC}[\rho(r)] \qquad 2.12$$

Where the kinetic energy of the electron is indicating by $T_0[\rho]$ and represented by the Eq. 2.13, which does not include electron-electron correlations [12].

$$T_0[\rho] = \sum_{i=1}^{N} \int \psi_i^*(r) \left(-\frac{\Delta^2}{2} \right) \psi_i(r) dr \qquad 2.13$$

The second term $E_H[\rho(r)]$ is called Hartree electrostatic energy represented by the Eq. 2.14, which arises from the classical interaction between the two charge densities.

$$E_H[\rho(r)] = \frac{1}{2} \int\int \frac{\rho(r_1)\rho(r_2)}{|r_1 - r_2|} dr_1 dr_2 \qquad 2.14$$

The third term is known as $E_{xc}[\rho(r)]$ as exchange-correlation energy. Hence the total energy of the system can be written as

$$E[\rho(r)] = \int V_{ext}(r)\rho(r)dr + T_0[\rho(r)] + E_H[\rho(r)] + E_{XC}[\rho(r)] \qquad 2.15$$

According to the Kohn and Sham, the density $\rho(r)$ of the system as square moduli of a set of one-electron orthogonal orbitals is given below in Eq. 2.16.

$$\rho(r) = \sum_{i=1}^{N} |\psi_i(r)|^2 \qquad 2.16$$

For the one-electron K-S equation is represented by Eq. 2.17.

$$-\left\{ \frac{\Delta_1^2}{2} - \left(\sum_{A=1}^{M} \frac{Z_A}{r_{1A}} \right) + \int \frac{\rho(r_2)dr_2}{r_{12}} + V_{XC}[r_1] \right\} \psi_i(r_1) = \varepsilon_i \psi_i(r_1) \qquad 2.17$$

Where $V_{xc}(r) = \frac{\delta E_{xc}[\rho(r)]}{\delta \rho(r)}$ is the functional derivative of exchange-correlation energy. For the K-S equation solution, a self-consistent approach executes the number of times for convergence of the system.

The K-S theory gives the exchange-correlation functional. In Local Density Approximation (LDA) the density is considered as the uniform electron gas. In LDA, the functional $E_{xc}[\rho]$ has been taken from the Dirac formula and represented by the Eq. 2.18.

$$E_{XC}^{LDA}[\rho(\rho)] = \int \rho(r)\varepsilon_{XC}(\rho)dr \qquad 2.18$$

Where $\varepsilon XC(\rho)$ is the sum of exchange-correlation energy per electron consistent with the electron gas of density ρ. Most probably α(up) and β(down)

In general, for a spin-unpolarized system, a local density approximation for the exchange-correlation energy is written as

$$E_{XC}^{LDA}[\rho] = \int \rho(r)\varepsilon_{xc}(\rho(r))dr \qquad 2.19$$

Where ρ is the electronic density, and ε_{xc} is the exchange-correlation energy per particle of a homogeneous electron gas of charge density ρ. The exchange-correlation energy is the summation of exchange and correlation terms linearly.

$$E_{XC} = E_x + E_C \qquad 2.20$$

The extension of density functional to spin-polarized systems is straightforward for exchange, where the exact spin-scaling is known, but further approximations must be employed for correlation. A spin-polarized system in DFT operates with two spin densities, ρ_α and ρ_β with $\rho = \rho_\alpha + \rho_\beta$, and the form of the local-spin-density approximation (LSDA) is represented by Eq. 2.21.

$$E_{XC}^{LSDA}[\rho_\alpha, \rho_\beta] = \int dr\rho(r)\varepsilon_{XC}(\rho_\alpha, \rho_\beta) \qquad 2.21$$

Becke suggested an extensively used correlation (B88) for the LSDA exchange energy is represented by the Eq. 2.22.

$$E_X^{B88} = E_X^{LDA} + \Delta E_X^{B88} \qquad 2.22$$

$$\Delta E_X^{B88} = -\beta\rho^{1/3}\frac{x^3}{1+6\beta x\sinh^{-1}x} \qquad 2.23$$

the fitting of known atomic data estimates β

$$x = \frac{|\Delta\rho|}{\rho^{4/3}} \qquad 2.24$$

Commonly used correlation energy functional E_C^{VWN} is due to Vosko, Wilk, and Nusair [13] and represents the correlation energy per electron in gas $\varepsilon_C\left[\rho_1^\alpha \rho_1^\beta\right]$ with spin densities ρ_1^α and ρ_1^β

$$E_C^{VWN} = \int \rho_1(r_1)\varepsilon_c\left[\rho_1^\alpha(r_1), \rho_1^\beta(r_1)\right]dr_1 \qquad 2.25$$

A combination of Slater exchange and Vosko-Wilk-Nusair correlation both are directly derived from the homogenous electron gas (HEG) equations, gives the Local Density Approximation. However, to correct the non-local terms, other (better) exchange and correlation functional have been developed. Lee, Yang, and Parr (LYP correlation functional) [14] gives the popular approaches for electron correlation and other approaches are provided by Perdew and Wang (PW91 correlation functional), [15]; however, there is much more functionality available but each with their qualities and drawbacks.

The Becke benchmarked DFT methods against a test set of experimentally known ionization energies, electron affinities, and proton affinities with high accuracy[16]. He came up with a three-parameter (hybrid) DFT to estimate the exchange and correlation functions' contributions.

Becke-3-LYP (B3LYP) uses a different mixing scheme involving three mixing parameters is represented by the Eq. 2.26.

E_{XC} = 0.8*E_X(LSDA) + 0.2*E_X(HF) + 0.72*DE_X(B88) + 0.81*E_C(LYP) + 0.19*E_C(VWN) 2.26

Essentially the hybrid density functional method B3LYP has the following form is represented by the Eq. 2.27.

$$E_{XC}^{B3LYP} = (1-a_0)E_X^{LSDA} + a_0 E_X^{HF} + a_X \Delta E_X^{B88} + a_C E_C^{LYP} + (1-a_C)E_C^{VWN} \quad 2.27$$

Here, E_X^{LSDA} is the exchange energy under the local spin density approximation, E_X^{HF} is the K-S orbital based HF exchange energy functional, E_C^{LYP} is the Lee-Yang-Paar correlation function, E_C^{VWN} is the vosko, Wilk, Nusair correlation functional, a_0, a_x, and a_c are the empirical coefficients obtained by least-square fitting to experimental evidence [4].

The commonly used B3LYP method foils to predict dispersion energy. DFT application is limited and used for the systems where the dispersion part is the dominant part. In that case, the calculated interaction energy values are always underestimated. A breakthrough in computational chemistry, in general, appeared when Becke developed the hybrid density functional procedures [16-17].

2.4 M062X

The Density Functional Theory (DFT) method M062X is also known as Minnesota functionals (Myz). It is exchange-correlation energy functional in the DFT. The M062X has a 54% Hartree Fock (HF) exchange. Prof. Donald Truhlar develops this method at the University of Minnesota. The M062X functional is based on the meta-GGA approximation. The M062X functional was used in quantum chemistry and solid-state physics calculations. The Myz functionals are mostly used in quantum chemistry. According to the literature survey, the old Minnesota functionals are given the poor performance on atomic densities. However, nowadays, Minnesota functionals are found to be suitable for computational calculations. The Minnesota functionals are most ideal for the diatomic densities as a comparison with atomic densities. The Minnesota functionals are available in all computational programs. The revM06-L functional, not available in Gaussian 09 or Gaussian 16 [18, 19].

2.5 Born-Oppenheimer Approximation

Due to the higher masses of nuclei, move much slower than the electrons. We can consider the electrons as moving in the field of fixed nuclei. The nuclear kinetic energy is zero, and their potential energy is exclusively constant. Thus, the electronic Hamiltonian reduces to

$$\hat{H}_{elec} = -\frac{1}{2}\sum_{i=1}^{N}\nabla_i^2 - \sum_{i=1}^{N}\sum_{A=1}^{M}\frac{Z_A}{r_{iA}} + \sum_{i=1}^{N}\sum_{j>i}^{N}\frac{1}{r_{ij}} = \hat{T} + \hat{V}_{Ne} + \hat{V}_{ee} \quad 2.28$$

The solution of the Schrodinger equation with $\hat{H}_{elec}$ is the electronic wave function ψ_{elec} and the electronic energy E_{elec}. The total energy E_{tot} is the sum of E_{elec} and the constant nuclear repulsion term E_{nuc} [20].

$$H_{elec}\Psi_{elec} = E_{elec}\Psi_{elec} \quad 2.29$$

$$E_{tot} = E_{elec} + E_{nuc} \quad 2.30$$

$$E_{nuc} = \sum_{A=1}^{M}\sum_{B>A}^{M}\frac{Z_A Z_B}{R_{AB}} \quad 2.31$$

2.6 Basis Set

Basis sets have the first time demonstrated by J. C. Slater. The usual expression for a basis function is given as:

$$\text{Basis Function} = N * e^{(-\text{alpha} * r)} \quad 2.32$$

Where: N = Normalization constant, alpha = Orbital exponent, r = radius in angstroms

The basis set is a set of functions that serves as an electronic wave function in the HF or DFT methods. A basis is a set of mathematical functions that are used to describe the shape of orbitals in an atom, which is used to approximate theoretical calculation or molecular modeling. The basis set has been used in the theoretical and computational chemists. The basis set may be composed of atomic orbital's. The atomic orbital's plays an essential role in the quantum chemistry simulation. The plane wave has been used in the solid-state community. Several types of atomic orbital's are Gaussian type orbital's numerical atomic orbital's or Slater type orbital's. In the basis set, the wave function has indicated as a vector. The one-electron operators correspond to the matrices with rank two tensors; thereby, two electrons operators have rank four tensors. During molecular calculation, the basis is composed of atomic orbital's with the nucleus at the center of the molecules. The most common basis set is Slater type orbital's (STO), which are the

solution of the Schrödinger equation of hydrogen-like atoms. The smallest basis set, also known as a minimal basis set (a basis set that illustrates only the essential aspects of the orbital's). In HF calculation, each atom of the molecule has a single basis function used by each orbital's. [21-23]

2.6.1 6-31G

In a 6-31G basis set, the carbon has one basic function and representing the 1s atomic orbital's. The polarization basis function has been expressed by an asterisk (*). The double asterisk (**) indicated polarization functions on hydrogen and helium. The 6-31G** basis set is exceptionally usual, where the hydrogen atom acts as a bridging atom [24-25].

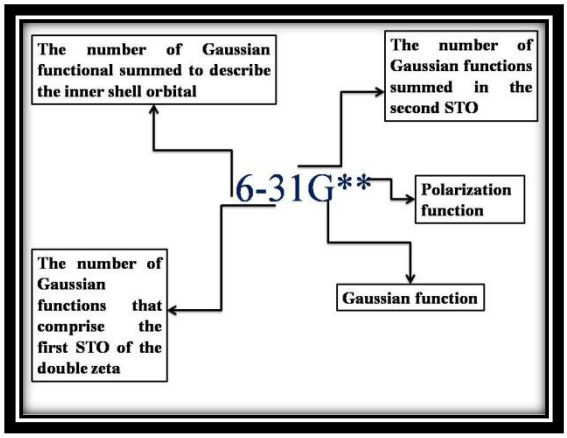

Figure 2.1. Description of 6-31G** basis set

The Pople basis set is other families of basis sets written as 6-31G. It has indicated that each core orbital mentioned by a single contraction of six GTO primitives, which defines each core orbital and two contractions, of which one with three primitives and other with one primitive describe each valence shell orbital. These types of basis sets are prevalent for organic molecules. It has denoted as 6-31G* or 6-31G**, as shown in Fig. 2.1. A single asterisk (*) indicates a set of d primitives has been added to atoms other than hydrogen, while double asterisks (**) means a set of p primitives has been added to hydrogen as well. These are called polarization functions because they give the wave function more flexibility to change shape. One or two plus signs can also be added, such as 6-31+G* or 6-31++G*. A single plus sign indicates that diffuse functions have been

added to atoms other than hydrogen. The second plus sign indicates that diffuse functions are being used for all atoms [26-27].

2.7 Working Scheme

All the molecules are optimized by the Gaussian 09 Software package [28] with the help of density functional theory (DFT) method B3LYP [14,16] and M062X [18] by 6-31G** basis set [26-27]. After the simulation of all the molecules, we are applying the electric field (a.u) to the homologous series along the molecular axis (x-axis) and perpendicular axis (y-axis), as shown in figure 2. The range of applied electric field is 0.0000 (a.u) to 0.1000 (a.u) at the interval of 0.0020 (a.u) where 1 a.u=5.14 x 10^{11} V/m [29] where 1 a.u.= 6.5 x 10^{15} Hz. After an applied electric field, we have calculated the molecular polarizability of the molecular series. The x-axis is considered extraordinary molecular polarizability (αe), and along the y-axis is considered ordinary molecular polarizability (α_o). With the help of α_e and α_o, we have calculated the birefringence (2.40), order parameter (2.39), refractive index (2.45), and magic angle (2.41)as per the equations given below. Where α, μ, and β equivalent to the components of the polarizability (2.33), dipole moment (2.35), and first-order hyperpolarizability (2.34) [30-31].

$$\alpha = \frac{1}{3}(\alpha_{xx} + \alpha_{yy} + \alpha_{zz}) \quad 2.33$$

$$\beta = \left[(\beta_{xxx} + \beta_{xyy} + \beta_{xzz})^2 + (\beta_{yyy} + \beta_{xxy} + \beta_{yzz})^2 + (\beta_{zzz} + \beta_{xxz} + \beta_{yyz})^2\right]^{1/2} \quad 2.34$$

$$\mu = (\mu_x{}^2 + \mu_y{}^2 + \mu_z{}^2)^{1/2} \quad 2.35$$

$$\Delta\alpha = 2^{-1/2}\left[(\alpha_{xx} - \alpha_{yy})^2 + (\alpha_{yy} - \alpha_{zz})^2 + (\alpha_{zz} - \alpha_{xx})^2\right]^{1/2} \quad 2.36$$

$$\Delta\tilde{\alpha} = \alpha_e - \alpha_o \quad 2.37$$

$$\Delta\tilde{\alpha} = S\Delta\alpha \quad 2.38$$

Order Parameter (S):-

$$S = \frac{\alpha_e - \alpha_o}{\alpha_e + \alpha_o} \quad 2.39$$

Birefringence (Δn):-

$$\Delta n = \frac{(\alpha_e - \alpha_o)}{6.3631}\left[R^3 - \left(\frac{2\alpha_o + \alpha_e}{20.244}\right)\right]^{-1} \quad 2.40$$

Where, R is the radius of the liquid crystal molecule.

Magic angle (θ):-

$$\theta = \cos^{-1}\left[\frac{(2S+1)}{3}\right] \quad 2.41$$

Refractive index (n):-

$$\alpha = \frac{2\alpha_o + \alpha_e}{3}, \quad \gamma_e = \alpha + \frac{2(\alpha_e - \alpha_o)}{3S}, \quad \gamma_o = \alpha - \frac{(\alpha_e - \alpha_o)}{3S} \quad 2.42$$

$$n_e = \frac{7}{2\sqrt{10}} + \frac{(2\sqrt{10}/5)\pi N\alpha}{1 - \frac{4\pi N\alpha}{3}} + \frac{(4\sqrt{10}/15)\pi NS(\gamma_e - \gamma_o)}{1 - \frac{4\pi N\alpha}{3}} \quad 2.43$$

$$n_o = \frac{7}{2\sqrt{10}} + \frac{(2\sqrt{10}/5)\pi N\alpha}{1 - \frac{4\pi N\alpha}{3}} - \frac{(2\sqrt{10}/15)\pi NS(\gamma_e - \gamma_o)}{1 - \frac{4\pi N\alpha}{3}} \quad 2.44$$

$$n = \frac{7}{2\sqrt{10}} + \frac{(2\sqrt{10}/5)\pi N\alpha}{1 - \frac{4\pi N\alpha}{3}} \quad 2.45$$

Where N is the number of liquid crystal molecules.

2.8 Electric Field on Liquid Crystal

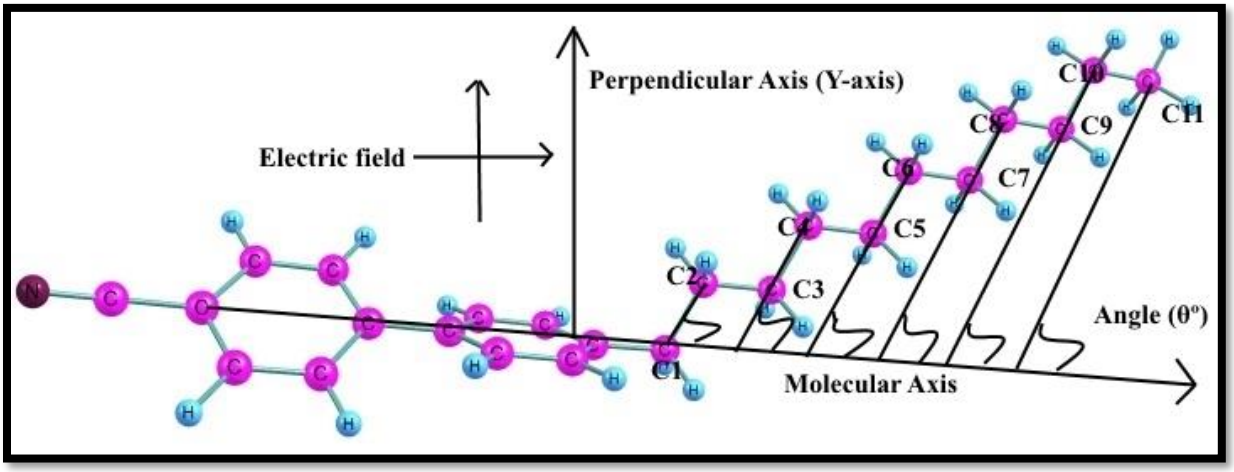

Figure 2.2 11CB liquid crystal under the influence of an external electric field

The presence of an influence the wave function leads to the induced dipole and quadrupole moment, as shown in Fig. 2.2 and Fig. 2.3. For the dipole moment, this may be written as

$$\mu = \mu_0 + \alpha F + \frac{1}{2}\beta F^2 + \frac{1}{6}\gamma F^3 + ... \qquad 2.46$$

Where μ_0 is the permanent dipole moment, α is the polarizability, β is the first hyperpolarizability, γ is the second hyperpolarizability, etc.

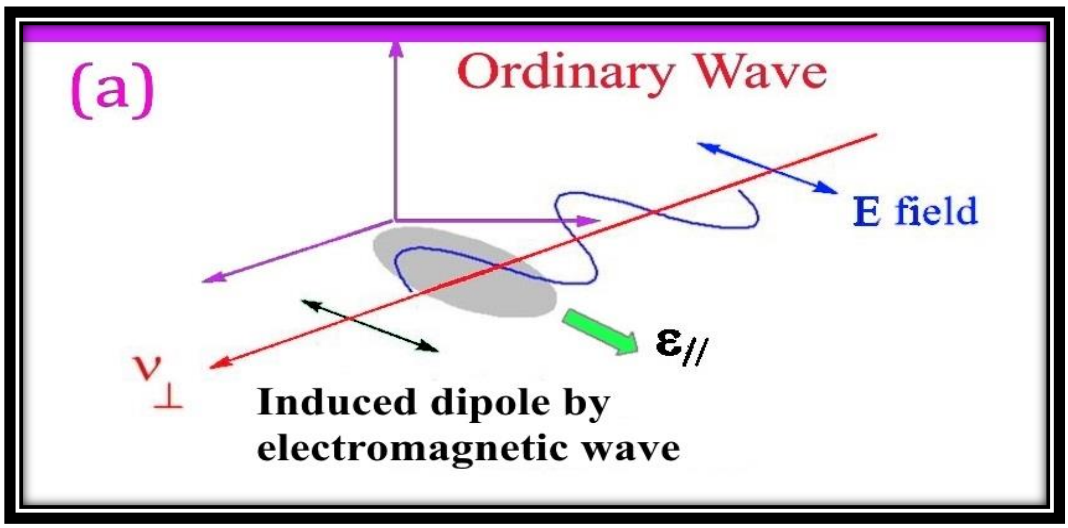

Figure 2.3 An ordinary wave of the electric field applied on the LC molecule

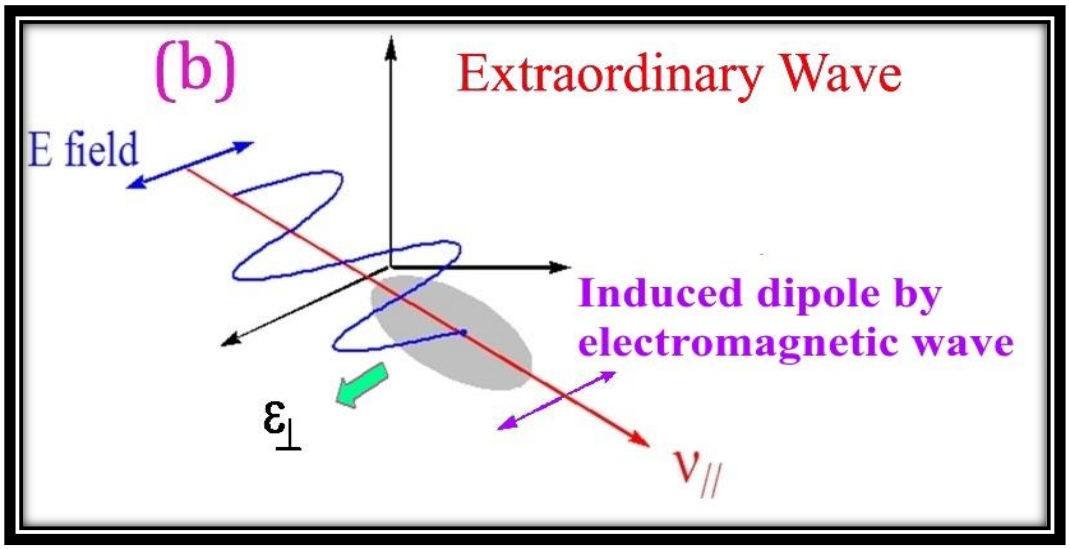

Figure 2.4 An extraordinary wave of the electric field applied on the LC molecule

For a homogeneous field (i.e., field gradient and higher derivatives are zero), the molecule's total energy may be written as Taylor expansion, where all the derivatives have evaluated at F=0. There will be derivates of each field component that leads to a broad no. of indices and summations in a proper mathematical formulation. To avoid this notational cluttering, we are adopted a slightly nonstandard notation where the field is expressed by a vector notation, implying that derivatives should be taken along all the individual field components.

$$E(F) = E(0) + \frac{\partial E}{\partial F}|_{F=0} F + \frac{1}{2}\frac{\partial^2 E}{\partial F^2}|_{F=0} F^2 + \frac{1}{6}\frac{\partial^3 E}{\partial F^3}|_{F=0} F^3 + \frac{1}{24}\frac{\partial^4 E}{\partial F^4}|_{F=0} F^4 + \ldots\ldots\ldots\ldots 2.47$$

Where $\partial E/\partial F = -\mu$, where the expression gives μ in eq(a). Differentiation of eq (b) concerning F gives.

$$\mu = \frac{\partial E}{\partial F}|_{F=0} - \frac{\partial^2 E}{\partial F^2}|_{F=0} F - \frac{1}{2}\frac{\partial^3 E}{\partial F^3}|_{F=0} F^2 - \frac{1}{6}\frac{\partial^4 E}{\partial F^4}|_{F=0} F^3 + \ldots\ldots\ldots \quad 2.48$$

Comparing Eqs. (2.46) and (2.48) shows that the first derivative is the dipole moment μ_0, the second derivative is the polarizability α, the third derivative is the hyperpolarizability β, etc.

$$\mu_0 = \frac{\partial E}{\partial F}|_{F=0}; \alpha = -\frac{\partial^2 E}{\partial F^2}|_{F=0}; \beta = -\frac{1}{2}\frac{\partial^3 E}{\partial F^3}|_{F=0}; \gamma = -\frac{1}{6}\frac{\partial^4 E}{\partial F^4}|_{F=0}\ F^3 \qquad 2.49$$

The molecular polarizability is enhanced with an increased number of electrons and increases as the electrons become less tightly held by the nuclei. The non-linear polarization of the molecule, that is a function of the applied electric field and is revealed by the power series expansion. Molecular geometry has not allowed changing during the calculation of polarizability. The electric field has started at 0.000 a.u. With an increment of 0.0020 a.u. Polarizability has been calculated from the trace of polarizability tensor [32].

References

1. W. Koch and M.C. Holthausen, *A Chemist's Guide to Density Functional Theory*, WILEYVCH (2001).
2. R. G. Parr and W. Yang, *Density-Functional Theory of Atoms and Molecules*, Oxford University Press, New York (1989).
3. E. Schroedinger, *Ann. Physik,***79**, 361 (1926).
4. A. R. Leach, *Molecular modeling: Principle and applications*, Prentice Hall, 2001.
5. L. I. Shiff, *Quantum Mechanics*, McGraw- Hill, NewYork., 3rd edition (1968).
6. D. P. Woodruff, *The chemical physics of solid surface*, 9th edition, Elsevier science, 2001.
7. C. Edimiston, K. Ruedenberg, *Rev. Mol. Phys.*, **34**, 457 (1963); J. *Chem. Phys.,***43**, 597 (1965).
8. I. N. Levine, *Quantum Chemistry*, Chapter-8, "Perturbation Theory", Pearson, Fifth edition (2000).
9. L. Pauling, E. B. Wilson, *Introduction to Quantum Mechanics,* McGraw-Hill, New York (1935).
10. P. Hohenberg, W. Khon, *Phys. Rev.,***136**, B864 (1964).
11. E. K. U. Gross, R. M. Dreizler, *Dendity functional theory*, NATO ASI, Plenum, New York, 337, (1995).

12. W. Khon, L. Sham, *J. Phys. Rev.,* 140, 1133 (1965).
13. S. H. Vosko, L. Wilk, M. Nusair, *Can. J. Phys*., **58**, 1200 (1980).
14. C. Lee, W. Yang, R. G. Parr, *Phys. Rev*., **B37**, 785 (1988).
15. J. P. Perdew, Y. Wang, *Phys. Rev*., **B45**, 13244 (1992).
16. A. D. Becke, *J. Chem. Phys*., **98**, 5648 (1993).
17. R. G. Parr, W. Yang, *Density Functional Theory*, Oxford University Press (1989).
18. Y. Zhao, D. G. Truhlar *Theor Chem Acc*., **120** (1–3), 215 (2006).
19. M. J., Field, L. D., Moleculaire, C. Grenoble, *Practical introduction to the simulation of molecular systems*. Second edn. Cambridge University Press (2007).
20. M. Born, J. R. Oppenheimer. *Annalen der Physik,* **389** (20), 457 (1927).
21. T. Helgaker, P. R. Taylor, *Modern electronic structure theory*, part II, World scientfic, (1995).
22. W. J. Hehre, R. F. Stewart, J. A. Pople, *J. Chem. Phys.*, **51**, 2657 (1969).
23. F. Jensen, Atomic orbital basis sets, *WIREs Comput. Mol. Sci*. **3** (3), 273 (2013).
24. R. Ditchfield, W. J. Hehre, J. A. Pople, J. Chem. Phys., **54** (1971) 724.
25. P. C. Hariharan, J. A. Pople, Theor. Chem. Acc., 28 (1973) 213-22.
26. P. J. Hay, W. R. Wadt, *J. Chem. Phys.* **82**, 299 (1985).
27. H. D. Cohen, C.C. J. Roothaan, *J. Chem. Phys.* **43**, S34 (1965).
28. M. J. Frisch, G. W. Trucks, H. B. Schlegel, G. E. Scuseria, M. A. Robb, et al. Gaussian 09, Revision A.02, Gaussian, Inc., Wallingford CT, (2010).
29. Y. Wang, F. Wang, J. Li, Z. Huang, S. Liang, J. Zhou, et al. *Energies*, **10** (4), 510. (2017).
30. N. Kumar, P. Singh, P. Upadhyay, S. Chaudhary, et al. *Eur. Phys. J. Plus.* **135,** 388 (2020).
31. N. Kumar, P. Singh, K. B. Thapa, D. Kumar, *IOP SciNotes.* **1,** 015202 (2020).
32. F. Jensen, *An Introduction to Computational Chemistry*, Wiley; 2 edition (2007).

Chapter 3

Spectroscopy Existing Behind the Electro-Optical Properties with an Even-Odd Effect of nCB Liquid Crystal Molecules

3.1 Introduction

The electro-optical response depends on the physical property and molecular structure of the LC molecules. The cyanobiphenyl (nCB) LC's are highly polar, so it has very high thermal and electrochemical stability. The external electric field sufficiently affects rod shape LC's optical properties through both ends of molecules' polarization. Under an external electric field, the one end of the nCB molecule has favorable charges. In contrast, the other end is negatively charged and formed an electric dipole. The LC molecules director will reorient along the direction of the applied external electric field [1-2]. The molecular polarizability increases with an increment of carbon atom number of the alkyl chain of the tail of the nCB LC molecules [3]. The nCB LC's family first synthesized by Gray et al. [4-5] for the display technology's electro-optical application. The nCB LC is colorless and stable to the moisture that is the best feature of these molecules. The nCB LC have a unique property for the alkyl chain length is changed, then the molecular properties of the mesophase changes [6-7]. The nCB LC molecules are indicated an even-odd effect under the extension of the alkyl chain. The optical polarizability of the nCB LC molecule has followed the even-odd effect and gives the interchange polarizability. The order parameter also exhibits the even-odd effects for the even-odd number of the alkyl chain's carbon atom in the tail of the nCB LC [8].

The birefringence is an electro-optical phenomenon used to determine the Kerr effect under the electric field's impact. The birefringence is a fundamental property of the LC, which gives LC's valuable information to use in various optical device applications. The electric field to the LC molecules has a rapid method to calculate birefringence and polarizability for the display technology's electro-optical application. The electro-optical effect is used to study the pretransitional behavior (related to the order parameter) of the nCB LC. The nCB LC has a positive Kerr constant because of the intense, permanent dipole moment and highly conjugated π-electrons [9-11]. The polarization of LC molecules induced by an applied electric field to the molecule depends on the applied field's direction. The electric field corresponds to an essential parameter to determine the electro-optic property of the LC molecules [12-13]. Rod shape LC molecules are lesser tilted as a comparison to the bent-core type LC molecules. The electrically induced tilt effects are observed in several types of bent-core and hockey-stick type LC molecules [14]. The polarization and bending plane of the molecules are parallel in the absence of an electric field, and it will be perpendicular to the plane in the presence of an electric field. The smectic phase of the LC molecule tilted continuously with the increased electric field [15-18]. The switching behavior of the even-odd numbered carbon atom in the tail of the LC is different [19]. The notation of nCB refers to the number of carbon atoms in the alkyl chain of nCB LC molecules. The Kerr constant measured with exploiting of birefringence under the impact of electric field. The birefringence is equal to the product of light wavelength, Kerr constant, and the square of the electric field ($\Delta n=\lambda KE^2$), where λ=wavelength of light, E= strength of the electric field, K=Kerr constant [20-22]. Karat et al. [23] reported that even members of the nCB series make a larger angle with the long molecular axis. It will reduce the anisotropy of the molecule and thereby minimize the order parameter and nematic to the isotropic phase transition temperature. However, the odd member of the nCB series makes the least angle with the molecule's long molecular axis. Thus, it will enhance the molecule's anisotropy, thereby increasing the order parameter and transition temperature. The present work also reveals the order parameter, and birefringence decreases for the even member. However, the order parameter and birefringence increase for the odd member of the nCB LC series. The nCB LC is a widely studied molecule, and all the optical parameters are readily

available for comparison. With the help of the described method, we are explained that the electric field is another method to achieve the all-optical properties and phase transitions. Which is shown in Fig. 3.1 by the variation of temperature to the LC. Electric polarizability is the most crucial factor in finding optical parameters.

3.2 Computational Methodology

All the molecules are optimized by the Gaussian 09 software package [24] with the help of density functional theory (DFT) method B3LYP [25-26] and M062X [27] with 6-31G** basis set [28-29]. After optimization of all the molecules, we have applied the electric field to nCB LC along the molecular axis (x-axis) and perpendicular (y-axis) to it from 0.0000 (a.u.) to 0.2000 (a.u.) at the interval of 0.0020 (a.u). After the applied electric field, we have calculated the molecular polarizability of the nCB LC molecules. The X-axis has considered as extraordinary molecular polarizability (α_e), and Y-axis has considered as ordinary molecular polarizability (α_o). With the help of α_e and α_o, we have calculated the order parameter (3.1), birefringence (3.2), and refractive index (3.4) as per the given formula. The finite-field approach framework predicts the total molecular energy under the impact of the electric field is given below [30,31];

$$E = E_o - \mu_i F_i - \frac{1}{2}\alpha_{ij}F_iF_j - \frac{1}{6}\beta_{ijk}F_iF_jF_k$$

Where E_o is the total energy in the absence of the electric field. Fi, μi, αij, and βijk equivalent to the electric field components, dipole moment, polarizability, and first-order hyperpolarizability. Respectively directions specified along with the subscripts i, j and k=x, y and z. The α, β, μ, and Δα are represented as numerical differentiation with an electric field of magnitude 0.002 (a.u). respectively equations are given below [32-34];

$$\alpha = \frac{1}{3}(\alpha_{xx} + \alpha_{yy} + \alpha_{zz})$$

$$\beta = \left[(\beta_{xxx} + \beta_{xyy} + \beta_{xzz})^2 + (\beta_{yyy} + \beta_{xxy} + \beta_{yzz})^2 + (\beta_{zzz} + \beta_{xxz} + \beta_{yyz})^2\right]^{1/2}$$

$$\mu = (\mu_x{}^2 + \mu_y{}^2 + \mu_z{}^2)^{1/2}$$

$$\Delta\alpha = 2^{-1/2}\left[(\alpha_{xx} - \alpha_{yy})^2 + (\alpha_{yy} - \alpha_{zz})^2 + (\alpha_{zz} - \alpha_{xx})^2\right]^{1/2}$$

$$\Delta\tilde{\alpha} = \alpha_e - \alpha_o$$

$$\Delta\tilde{\alpha} = S\Delta\alpha$$

where $\tilde{\alpha}$ is mean isotropic polarizability.

Order parameter (S):-

$$S = \frac{\alpha_e - \alpha_o}{\alpha_e + \alpha_o} \qquad 3.1$$

Birefringence (Δn):-

$$\Delta n = \frac{(\alpha_e - \alpha_o)}{6.3631}\left[R^3 - \left(\frac{2\alpha_o + \alpha_e}{20.244}\right)\right]^{-1} \qquad 3.2$$

where R is the radius of the liquid crystal molecule.

Magic angle (θ):-

$$\theta = \cos^{-1}\left[\frac{(2S+1)}{3}\right] \qquad 3.3$$

Refractive index (n):-

$$\alpha = \frac{2\alpha_o + \alpha_e}{3}, \quad \gamma_e = \alpha + \frac{2(\alpha_e - \alpha_o)}{3S}, \quad \gamma_o = \alpha - \frac{(\alpha_e - \alpha_o)}{3S}$$

$$n_e = \frac{7}{2\sqrt{10}} + \frac{\left(2\sqrt{10}/5\right)\pi N\alpha}{1-\frac{4\pi N\alpha}{3}} + \frac{\left(4\sqrt{10}/15\right)\pi NS(\gamma_e - \gamma_o)}{1-\frac{4\pi N\alpha}{3}}$$

$$n_o = \frac{7}{2\sqrt{10}} + \frac{\left(2\sqrt{10}/5\right)\pi N\alpha}{1-\frac{4\pi N\alpha}{3}} - \frac{\left(2\sqrt{10}/15\right)\pi NS(\gamma_e - \gamma_o)}{1-\frac{4\pi N\alpha}{3}}$$

$$n = \frac{7}{2\sqrt{10}} + \frac{\left(2\sqrt{10}/5\right)\pi N\alpha}{1-\frac{4\pi N\alpha}{3}} \qquad (3.4)$$

where N=1, is the number of liquid crystal molecules studied with the variation of temperature and external electric field to find out the different phases of LC series. The LC's temperature range is 300K to 400K used to study the LC series phases, as shown in Fig. 3.1.

3.3 Results and Discussion

3.3.1 Effect of the temperature with an extension of alkyl chain length

This subsection describes the different phase transition of nCB liquid crystal with the variation of temperature. The red line is indicating the crystalline to the nematic phase transition from 1CB to 7CB. The 8CB to 12CB showing crystalline to smectic phase A transition indicated by the pink line. The 8CB to 9CB leading smectic A to nematic phase transition marked by the green line. Nematic to the isotropic phase transition of 1CB to 9CB shown by the blue line, and lastly, smectic A to the isotropic phase transition of 10CB to 12CB indicated by the brown line. The temperature variation expresses the even-odd effect for the phase transition of the nCB series [35-36]. Which is also shown

by the application of the electric field on the nCB series**.** Dalmolen et al. [37], Dunmur et al. [40], and Lin et al. [46] are reported the nCB series expresses an even-odd effect under the impact of the temperature of LC. The nCB LC molecules reveal an even-odd effect under the temperature's influence by extending alkyl chain length. Karat et al. [24] already reported that even member of the nCB series is making a larger angle with the long molecular axis. Thus, it will reduce the molecule's anisotropy and thereby minimize the nematic to the isotropic phase transition temperature. However, the odd member of the nCB series is making a lower angle with the molecule's long molecular axis. Thus, it will be enhancing the anisotropy of the molecule, thereby increasing the transition temperature as shown in Fig. 3.1. The C-C symmetric scissoring in the benzene ring is responsible for crystalline to the nematic phase transition. Because the IR frequency corresponds to the absorbance is continual increases from 1CB to 7CB as shown in Table 1.1 to 1.7. However, the absorbance decreases for the 8CB because it is expressed crystalline to the smectic A phase transition indicates by the pink line. The C-C and C-H atom's stretching has contributed to the anisotropy of polarizability for the new compound compared with the previous molecule [41].

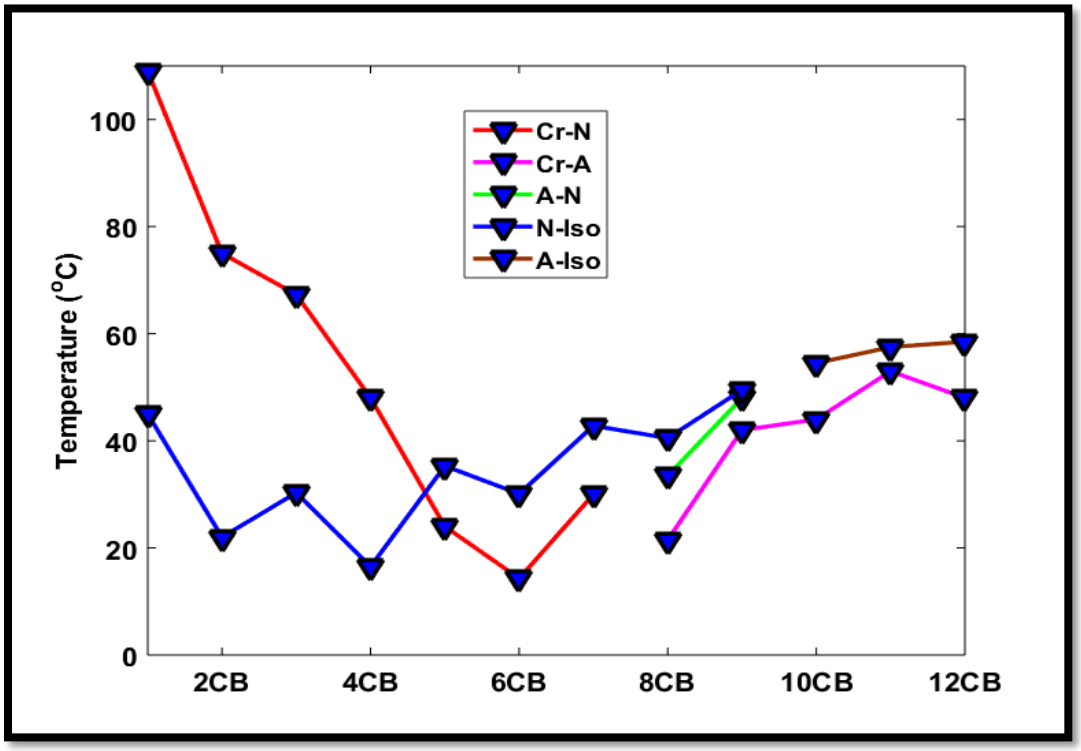

Figure 3.1 Effect of temperature under the expansion of alkyl chain length {red line indicates crystalline to nematic phase (Cr-N), the blue line indicates nematic to isotropic phase transition (N-iso), the green line suggests smectic A to nematic phase transition (A-N), the pink line indicates crystalline to smectic A phase transition (Cr-A), the brown line indicates smectic A to isotropic phase transition (A-Iso) [35]}

Table 3.1. Molecular spectroscopy of 1CB

S. No.	Frequency (cm^{-1})	Vibrations of 1CB	Infrared absorbance
1.	**593**	C-H atom wagging	12.6801
2.	**827**	C-H atom wagging	41.7097
3.	**1066**	H atom wagging in linkage group	15.2187
4.	**1211**	Scissoring in H atom	10.9267
5.	**1532**	In-plane H atom wagging in both benzene ring	45.3713
6.	**1647**	In-plane H atom wagging in both benzene ring	67.9165
7.	**2266**	C-N atom stretching	62.5656
8.	**3028**	C-H symmetric stretching in the alkyl chain	33.7266
9.	**3089**	C-H asymmetric stretching in the alkyl chain	19.9984
10.	**3186**	C-H asymmetric stretching in benzene ring2	24.9623

Table 3.2. Molecular spectroscopy of 2CB

S. No.	Frequency (cm^{-1})	Vibrations of 2CB	Infrared absorbance
1.	**568**	C-H atom wagging	13.8951
2.	**838**	C-H atom wagging	56.3054
3.	**1081**	H atom wagging in linkage group	19.4971
4.	**1431**	Stretching in C-H atom	10.7469
5.	**1532**	H atom rocking in both benzene ring	42.2867

6.	**1646**	H atom rocking in both benzene ring	66.2492
7.	**2267**	C-N atom stretching	63.7949
8.	**3035**	C-H symmetric stretching in the alkyl chain	35.8324
9.	**3110**	C-H asymmetric stretching in the alkyl chain	47.4022
10.	**3184**	C-H asymmetric stretching in benzene ring2	22.9844

Table 3.3. Molecular spectroscopy of 3CB

S. No.	**Frequency (cm^{-1})**	**Vibrations of 3CB**	**Infrared absorbance**
1.	**565**	C-H atom wagging	12.7295
2.	**845**	C-H atom wagging	30.7864
3.	**1017**	C-C symmetric scissoring in the benzene ring	10.9862
4.	**1431**	Stretching in C-H atom	10.8979
5.	**1532**	H atom rocking in both benzene ring	45.2558
6.	**1646**	H atom rocking in both benzene ring	71.9543
7.	**2267**	C-N atom stretching	65.1890
8.	**3030**	C-H symmetric stretching in the alkyl chain	81.8526
9.	**3098**	C-H asymmetric stretching in the alkyl chain	54.7674
10.	**3184**	C-H asymmetric stretching in benzene ring2	22.5195

Table 3.4. Molecular spectroscopy of 4CB

S. No.	**Frequency (cm^{-1})**	**Vibrations of 4CB**	**Infrared absorbance**
1.	**567**	C-H atom wagging	14.4115
2.	**841**	C-H atom wagging	32.7990
3.	**1017**	C-C symmetric scissoring in the benzene ring	10.6536

4.	**1431**	Stretching in C-H atom	10.6063
5.	**1531**	H atom rocking in both benzene ring	47.1805
6.	**1646**	H atom rocking in both benzene ring	75.5904
7.	**2266**	C-N atom stretching	66.0374
8.	**3029**	C-H symmetric stretching in the alkyl chain	49.9012
9.	**3098**	C-H asymmetric stretching in the alkyl chain	56.5727
10.	**3184**	C-H asymmetric stretching in benzene ring2	18.9294

Table 3.5. Molecular spectroscopy of 5CB

S. No.	**Frequency (cm^{-1})**	**Vibrations of 5CB**	**Infrared absorbance**
1.	**569**	C-H atom wagging	14.2067
2.	**843**	C-H atom wagging	38.8640
3.	**1017**	C-C symmetric scissoring in the benzene ring	11.3704
4.	**1531**	H atom rocking in both benzene ring	47.7280
5.	**1646**	H atom rocking in both benzene ring	77.6846
6.	**2266**	C-N atom stretching	66.6334
7.	**3026**	C-H symmetric stretching in the alkyl chain	51.4412
8.	**3096**	C-H asymmetric stretching in the alkyl chain	60.4378
9.	**3184**	C-H asymmetric stretching in benzene ring2	19.0613

Table 3.6. Molecular spectroscopy of 6CB

S. No.	**Frequency (cm^{-1})**	**Vibrations of 6CB**	**Infrared absorbance**
1.	**569**	C-H atom wagging	14.3463
2.	**845**	C-H atom wagging	32.6777

3.	**1017**	C-C symmetric scissoring in the benzene ring	11.5199
4.	**1531**	H atom rocking in both benzene ring	48.4753
5.	**1646**	H atom rocking in both benzene ring	78.8627
6.	**2266**	C-N atom stretching	66.9738
7.	**3027**	C-H symmetric stretching in the alkyl chain	69.0056
8.	**3096**	C-H asymmetric stretching in the alkyl chain	60.9689
9.	**3184**	C-H asymmetric stretching in benzene ring2	18.6464

Table 3.7. Molecular spectroscopy of 7CB

S. No.	**Frequency (cm^{-1})**	**Vibrations of 7CB**	**Infrared absorbance**
1.	**569**	C-H atom wagging	14.4318
2.	**844**	C-H atom wagging	30.2113
3.	**1017**	C-C symmetric scissoring in the benzene ring	11.9051
4.	**1531**	H atom rocking in both benzene ring	48.7830
5.	**1646**	H atom rocking in both benzene ring	79.8968
6.	**2266**	C-N atom stretching	67.2729
7.	**3027**	C-H symmetric stretching in the alkyl chain	52.4092
8.	**3076**	C-H asymmetric stretching in the alkyl chain	78.0385
9.	**3184**	C-H asymmetric stretching in benzene ring2	18.7277

Table 3.8. Molecular spectroscopy of 8CB

S. No.	**Frequency (cm^{-1})**	**Vibrations of 8CB**	**Infrared absorbance**
1.	**570**	C-H atom wagging	14.0818
2.	**844**	C-H atom wagging	32.6066

3.	**1017**	C-C symmetric scissoring in the benzene ring	11.3718
4.	**1531**	H atom rocking in both benzene ring	49.1511
5.	**1646**	H atom rocking in both benzene ring	80.3690
6.	**2266**	C-N atom stretching	67.4233
7.	**3027**	C-H symmetric stretching in the alkyl chain	68.0403
8.	**3076**	C-H asymmetric stretching in the alkyl chain	84.3813
9.	**3184**	C-H asymmetric stretching in benzene ring2	18.7214

Table 3.9. Molecular spectroscopy of 9CB

S. No.	**Frequency (cm^{-1})**	**Vibrations of 9CB**	**Infrared absorbance**
1.	**570**	C-H atom wagging	14.1481
2.	**844**	C-H atom wagging	32.2473
3.	**1017**	C-C symmetric scissoring in the benzene ring	12.0875
4.	**1531**	H atom rocking in both benzene ring	49.3004
5.	**1647**	H atom rocking in both benzene ring	80.8472
6.	**2266**	C-N atom stretching	67.5816
7.	**3027**	C-H symmetric stretching in the alkyl chain	103.2722
8.	**3064**	C-H asymmetric stretching in the alkyl chain	107.3792
9.	**3184**	C-H asymmetric stretching in benzene ring2	18.9479

Table 3.10. Molecular spectroscopy of 10CB

S. No.	**Frequency (cm^{-1})**	**Vibrations of 10CB**	**Infrared absorbance**
1.	**570**	C-H atom wagging	14.1221
2.	**844**	C-H atom wagging	32.1331

3.	**1017**	C-C symmetric scissoring in the benzene ring	11.3436
4.	**1532**	H atom rocking in both benzene ring	49.3276
5.	**1646**	H atom rocking in both benzene ring	80.9406
6.	**2265**	C-N atom stretching	67.6449
7.	**3026**	C-H symmetric stretching in the alkyl chain	72.6780
8.	**3064**	C-H asymmetric stretching in the alkyl chain	135.1362
9.	**3184**	C-H asymmetric stretching in benzene ring2	19.6324

Table 3.11. Molecular spectroscopy of 11CB

S. No.	**Frequency (cm^{-1})**	**Vibrations of 11CB**	**Infrared absorbance**
1.	**570**	C-H atom wagging	14.2334
2.	**844**	C-H atom wagging	31.6043
3.	**1017**	C-C symmetric scissoring in the benzene ring	9.3491
4.	**1531**	H atom rocking in both benzene ring	49.5608
5.	**1646**	H atom rocking in both benzene ring	81.3196
6.	**2266**	C-N atom stretching	67.7372
7.	**3027**	C-H symmetric stretching in the alkyl chain	109.3245
8.	**3065**	C-H asymmetric stretching in the alkyl chain	163.9189
9.	**3184**	C-H asymmetric stretching in benzene ring2	19.8023

Table 3.12. Molecular spectroscopy of 12CB

S. No.	**Frequency (cm^{-1})**	**Vibrations of 12CB**	**Infrared absorbance**
1.	**570**	C-H atom wagging	14.2432
2.	**844**	C-H atom wagging	31.5740

3.	**1017**	C-C symmetric scissoring in the benzene ring	11.6812
4.	**1531**	H atom rocking in both benzene ring	49.64089
5.	**1646**	H atom rocking in both benzene ring	81.4398
6.	**2266**	C-N atom stretching	67.7678
7.	**3027**	C-H symmetric stretching in the alkyl chain	96.2863
8.	**3065**	C-H asymmetric stretching in the alkyl chain	193.9285
9.	**3184**	C-H asymmetric stretching in benzene ring2	20.5369

3.3.2 Birefringence

We have calculated birefringence with the help of Eq. No. 2 under the external electric field with an extension of the alkyl chain length. Coles [12] reported the birefringence is decreasing under the influence of the external electric field with an extension of alkyl chain length. In this chapter, the birefringence is falling continuously with an extension of the alkyl chain, as shown in Fig. 3.14. Dunmur et al. [40] have reported under the impact of temperature, the dielectric anisotropy, and birefringence decreased. And the nCB series are showing an even-odd effect with the extension of the alkyl chain length. Under the influence of an electric field, the birefringence of nCB LC molecules decreases with the even-odd effect, as shown in Fig. 3.14. The stability of the nematic and smectic phase is given in Fig. 3.2 to Fig. 3.13. Wu et al. [45] reported the birefringence of 5CB is 0.22. The birefringence of 5CB is 0.20, given in Table 3.5. From 1CB to 5CB, the birefringence steadily decreases but does not show the even-odd effect. Still, after the 5CB LC, the birefringence exhibits the perfectly even-odd effect express by the DFT methods B3LYP, as shown in Fig. 3.14. However, the even-odd effect is expressing by the DFT method M062X. The odd carbon atom number of the alkyl chain has a higher birefringence as compared to the even member of the alkyl chain. The birefringence decreases with an increase of carbon atom numbers of the alkyl chain length. The C-H asymmetric stretching corresponds to IR absorbance in the benzene ring, an improvement for the odd member, and falls for the even member of the alkyl chain. The 10CB LC is an

even member of the nCB series. The IR absorbance is increasing instead of decreasing of 10CB LC that is the reason for sharply reducing birefringence given in Table 3.10.

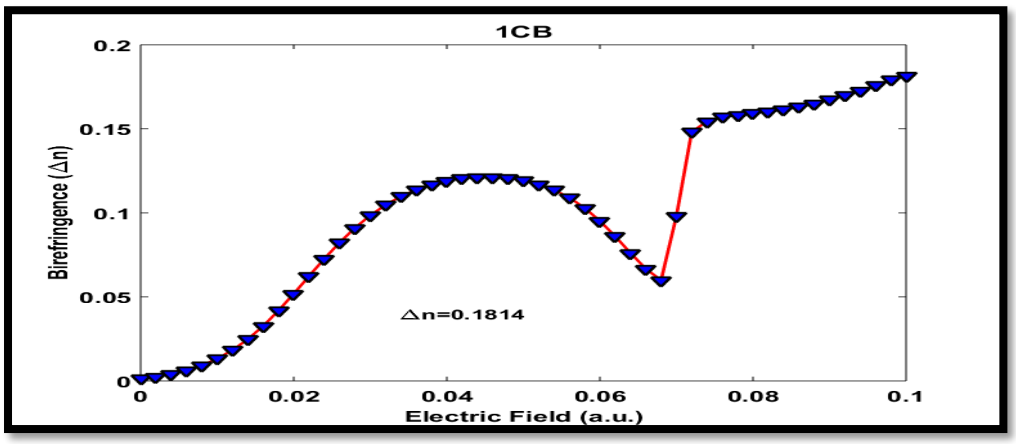

Figure 3.2 Birefringence of 1CB LC under the impact of an electric field

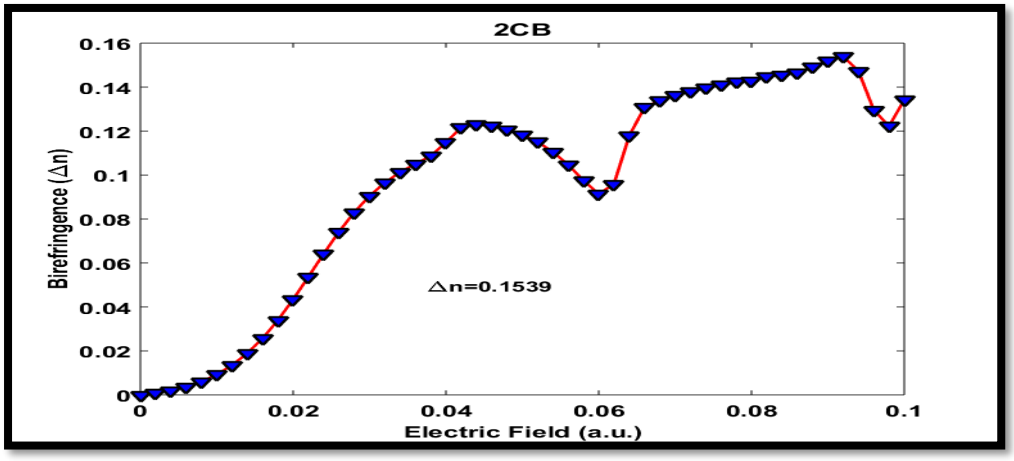

Figure 3.3 Birefringence of 2CB LC under the impact of an electric field

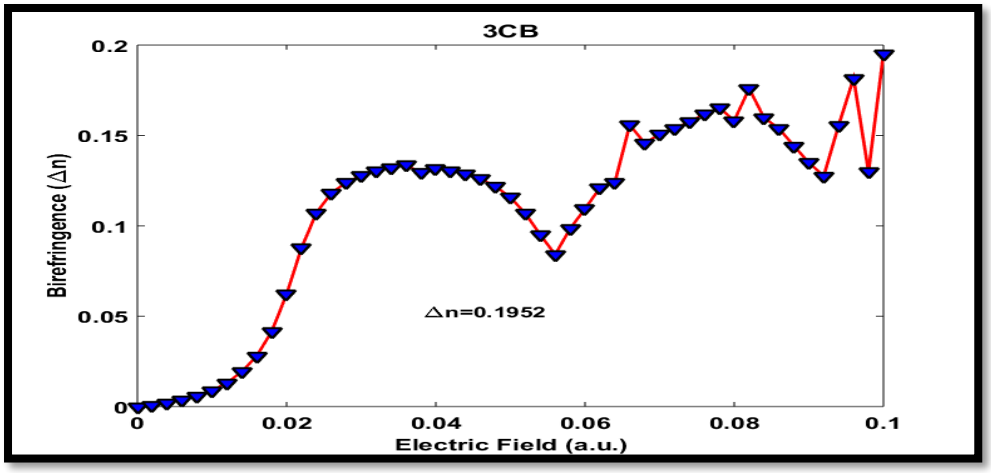

Figure 3.4 Birefringence of 3CB LC under the impact of an electric field

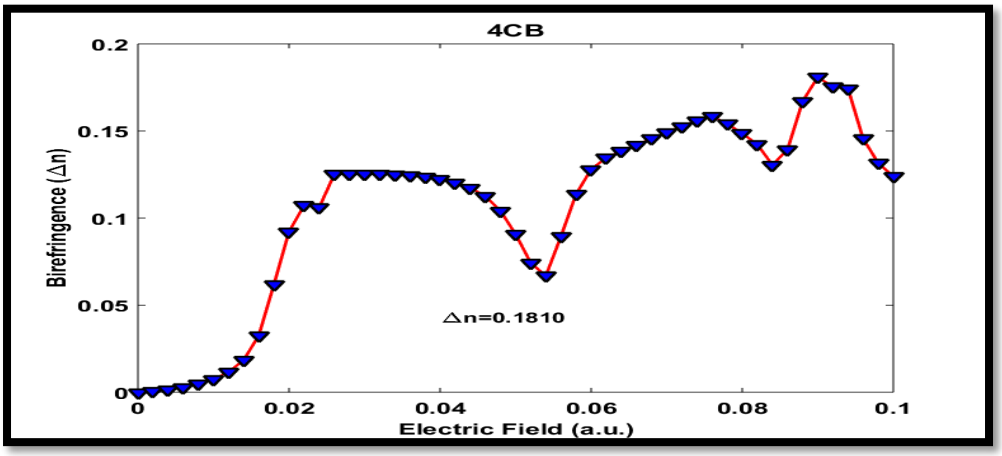

Figure 3.5 Birefringence of 4CB LC under the impact of an electric field

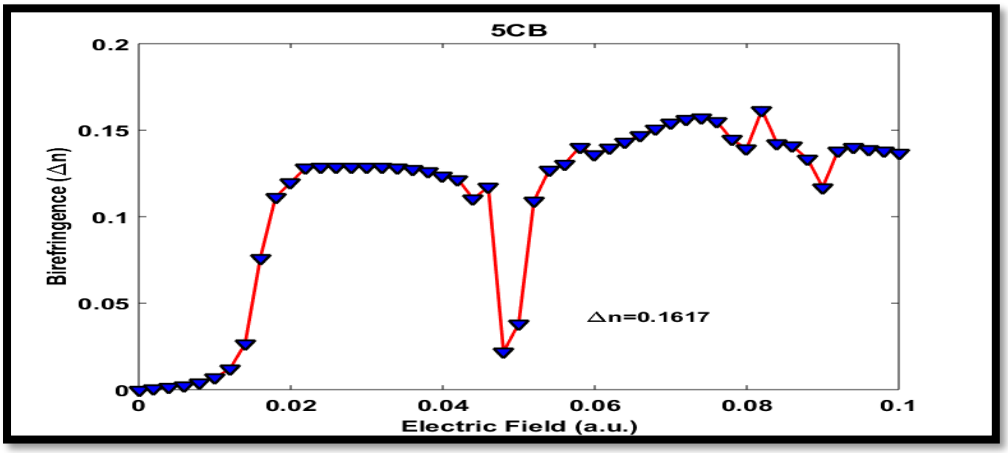

Figure 3.6 Birefringence of 5CB LC under the impact of an electric field

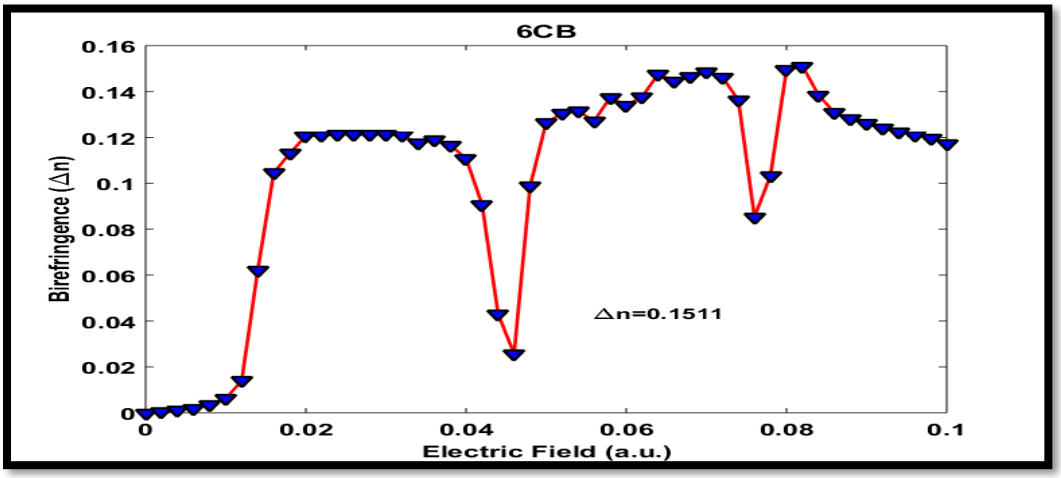

Figure 3.7 Birefringence of 6CB LC under the impact of an electric field

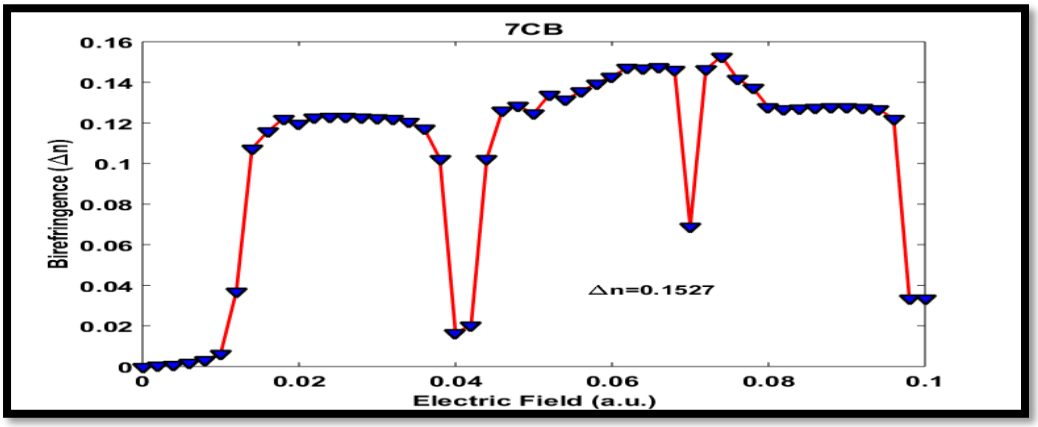

Figure 3.8 Birefringence of 7CB LC under the impact of an electric field

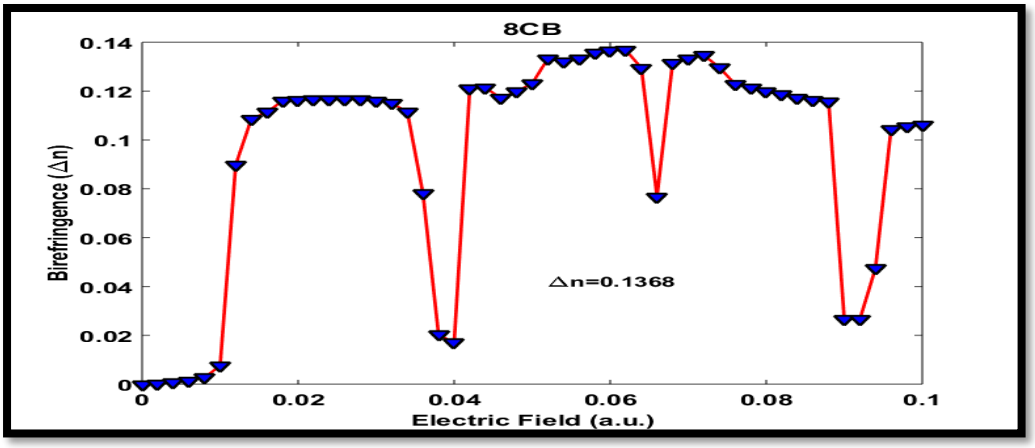

Figure 3.9 Birefringence of 8CB LC under the impact of an electric field

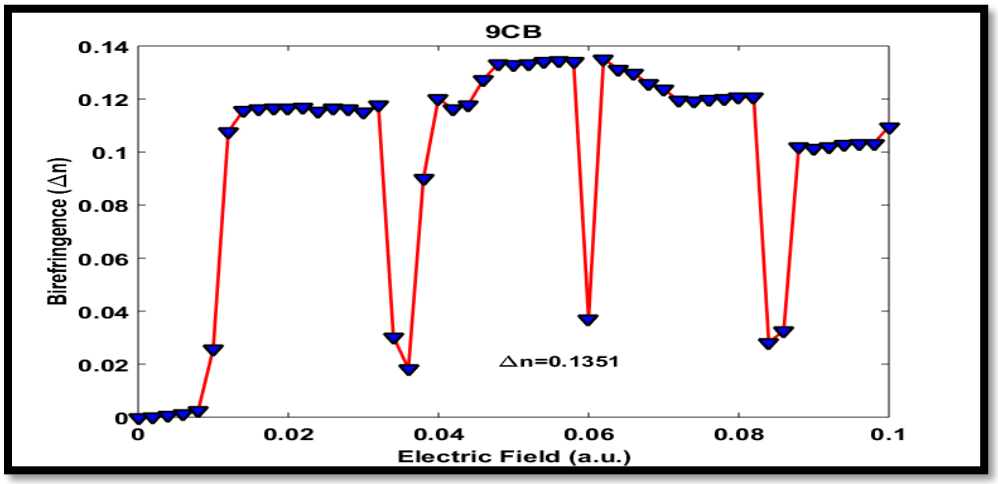

Figure 3.10 Birefringence of 9CB LC under the impact of an electric field

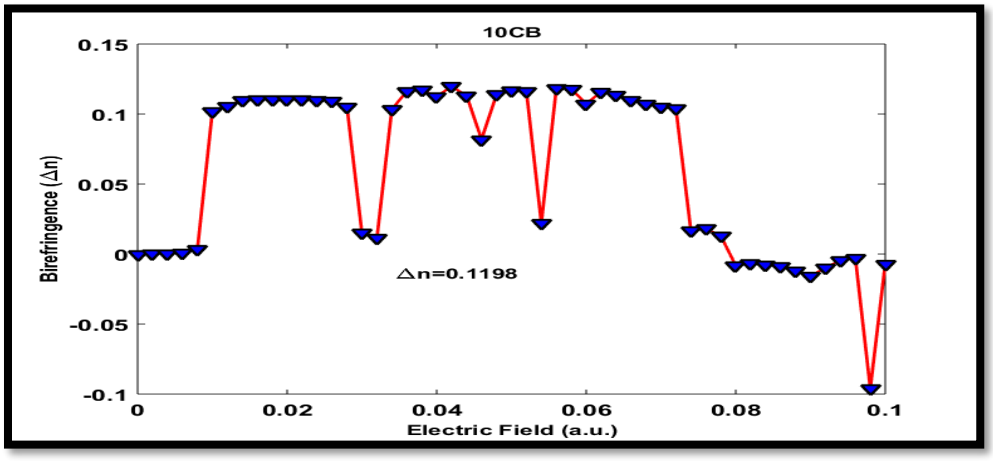

Figure 3.11 Birefringence of 10CB LC under the impact of an electric field

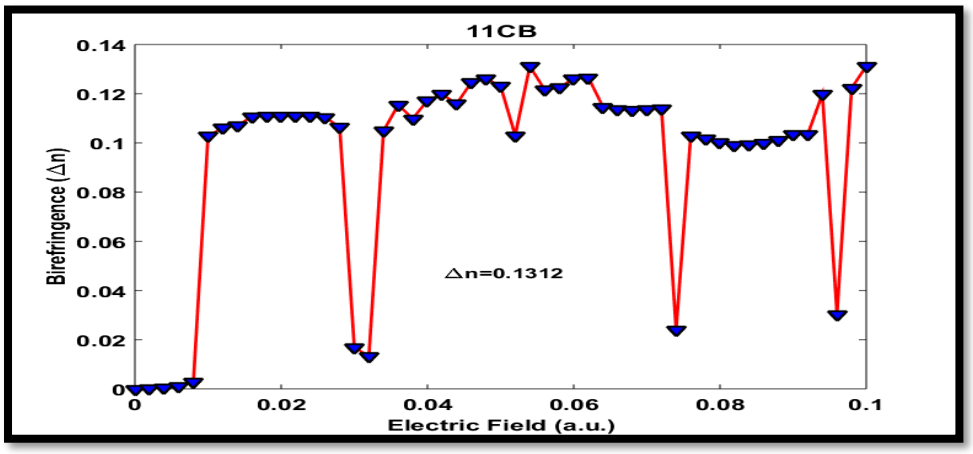

Figure 3.12 Birefringence of 11CB LC under the impact of an electric field

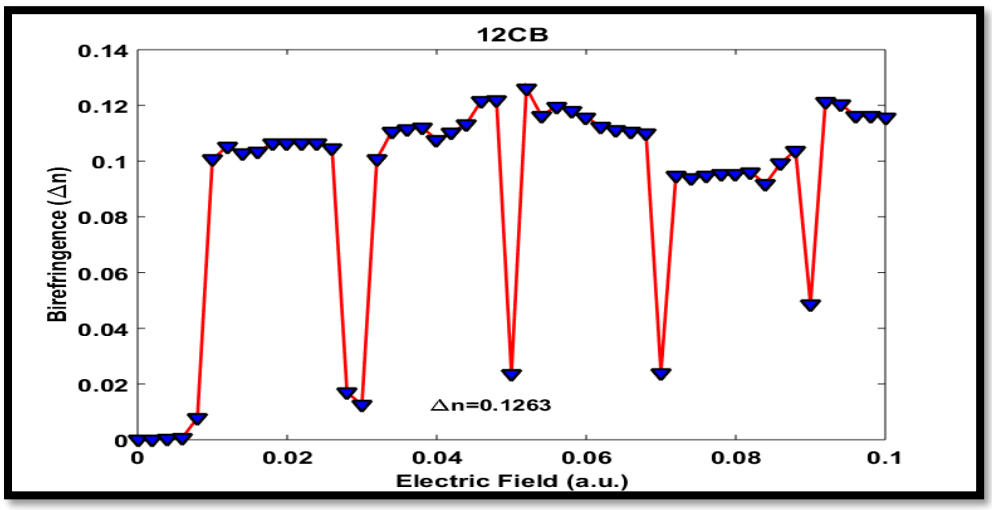

Figure 3.13 Birefringence of 12CB LC under the impact of an electric field

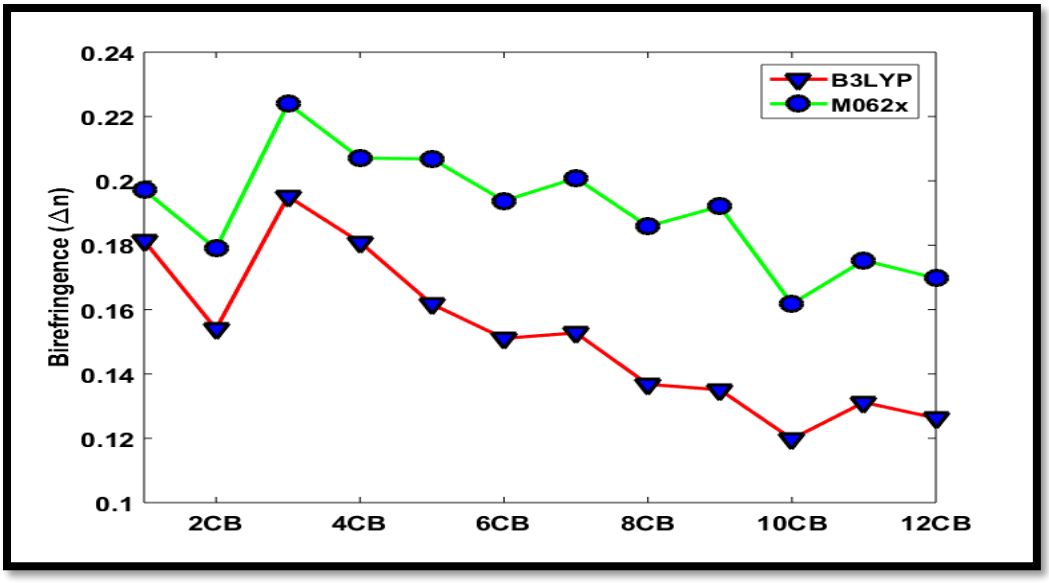

Figure 3.14 Calculated birefringence of nCB series under the external electric field's effect with an extension of the alkyl chain length using B3LYP (red line) and M062X (green line) methods.

3.3.3 Order Parameter

Karat et al. [24] reported the even members of the nCB series is making a larger angle with the long molecular axis. Thus, it will reduce the polarizability of the molecules and thereby minimize an order parameter. This section is also expressing 10CB LC reduces larger molecular polarizability, and it is abruptly decreasing. Horn et al. [36] reported the order parameter of 5CB and 8CB is 0.61 and 0.67. The order parameter of 5CB and 8CB is 0.60 and 0.71. The stability of the order parameter is shown in Fig. 3.15 to Fig. 3.26. Dalmolen et al. [37] and Sherrell et al. [38] are reported the order parameter increases with an extension of alkyl chain length. The order parameter is continuous increases with an extension of the nCB LC molecules' alkyl chain, as shown in Fig. 3.27. The order parameter is also exhibiting the even-odd effect with minor deviation. Park et al. [42] reported that the order parameter is determining from C-N and C-C stretching. The order parameter is continual increases because of the C-N atom stretching, and H atom rocking of the benzene ring corresponds to IR absorbance continuously increases. The C-H atom asymmetric stretching in the alkyl chain is steadily increasing. Which is also responsible

for the increment in the order parameter. The order parameter with an extension of the alkyl chain continuously is going to the crystalline state because the range of liquid crystal is 0.3 to 0.8. Sen et al. [44] reported under the effect of temperature, the order parameter of 5CB is 0.62. The order parameter calculated under the effect of the electric field is 0.60. The order parameter is an optical property of the nCB LC. Based on the order parameter, we can examine the molecular behavior of the nCB LC molecules. The C-H asymmetric stretching of the benzene ring at the frequency of 1532 cm^{-1} shows higher IR absorbance for odd members and lower IR absorbance for even members of the alkyl chain. The C-C symmetric scissoring in the benzene ring is responsible for molecular phases. At the frequency of 2266 cm^{-1}, the C-N atom stretching corresponds to absorbance is continual increases. Which is accountable for an increment of the order parameter.

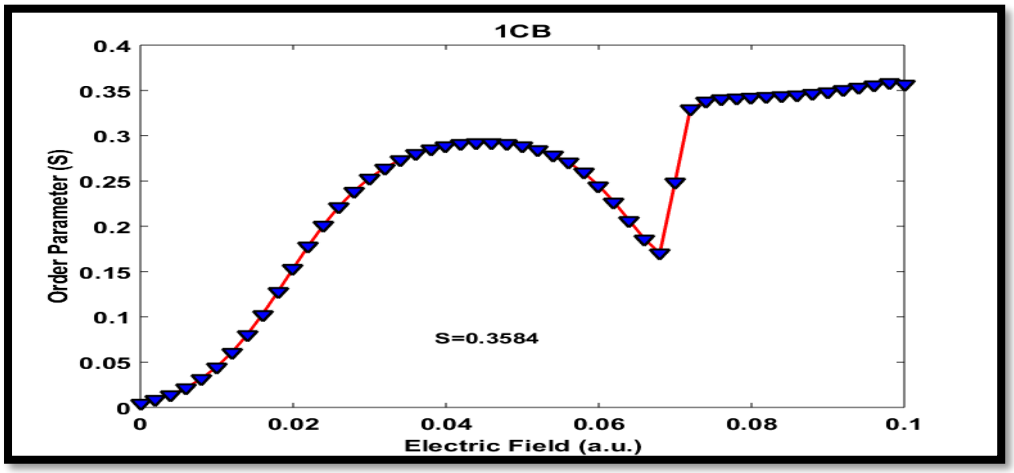

Figure 3.15 Order parameter of 1CB LC under the impact of an electric field

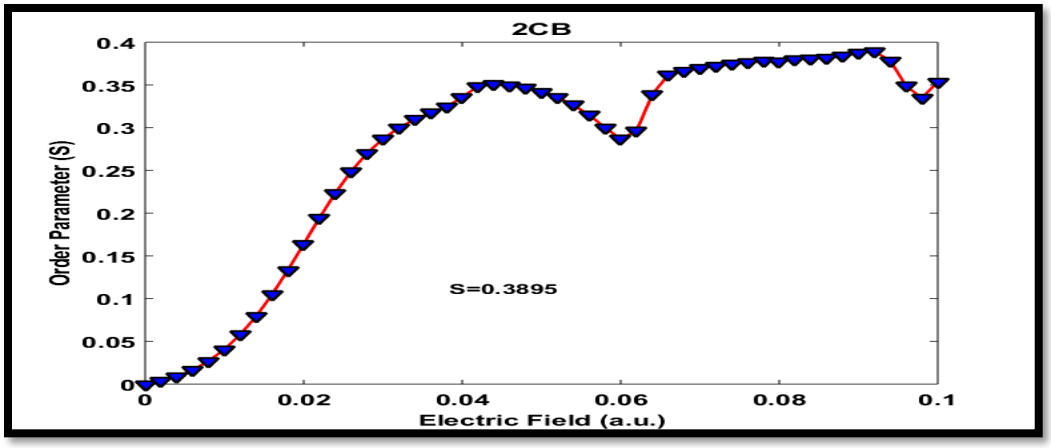

Figure 3.16 Order parameter of 2CB LC under the impact of an electric field

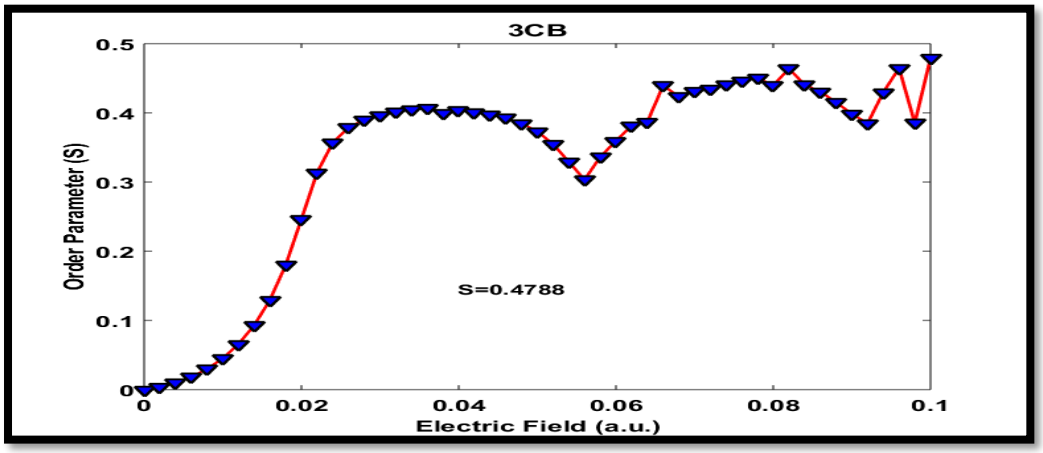

Figure 3.17 Order parameter of 3CB LC under the impact of an electric field

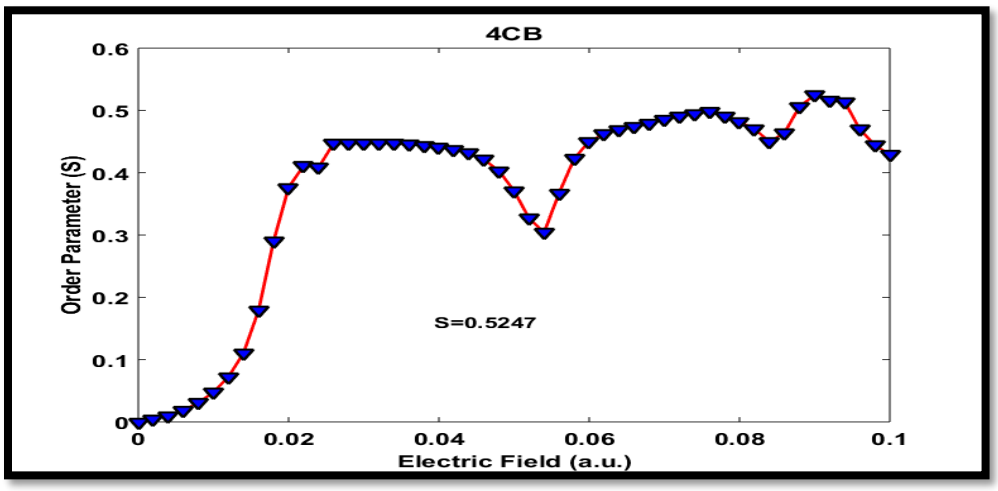

Figure 3.18 Order parameter of 4CB LC under the impact of an electric field

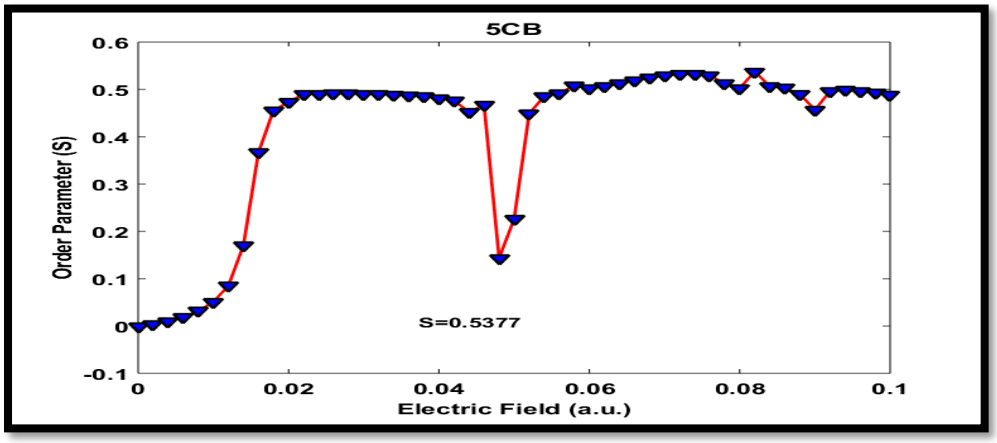

Figure 3.19 Order parameter of 5CB LC under the impact of an electric field

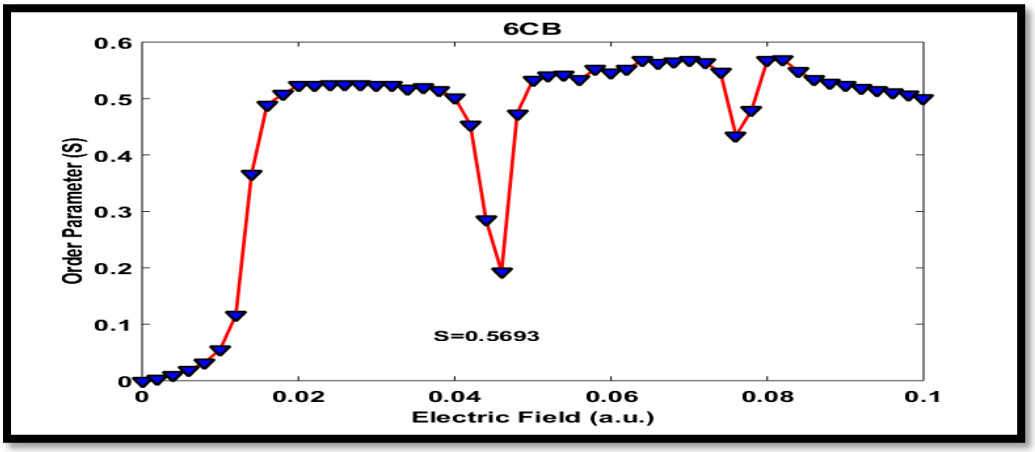

Figure 3.20 Order parameter of 6CB LC under the impact of an electric field

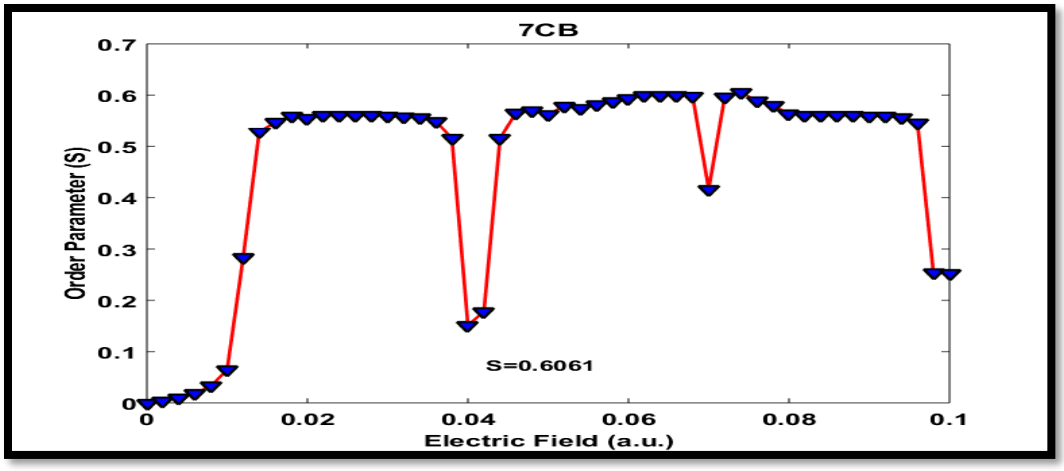

Figure 3.21 Order parameter of 7CB LC under the impact of an electric field

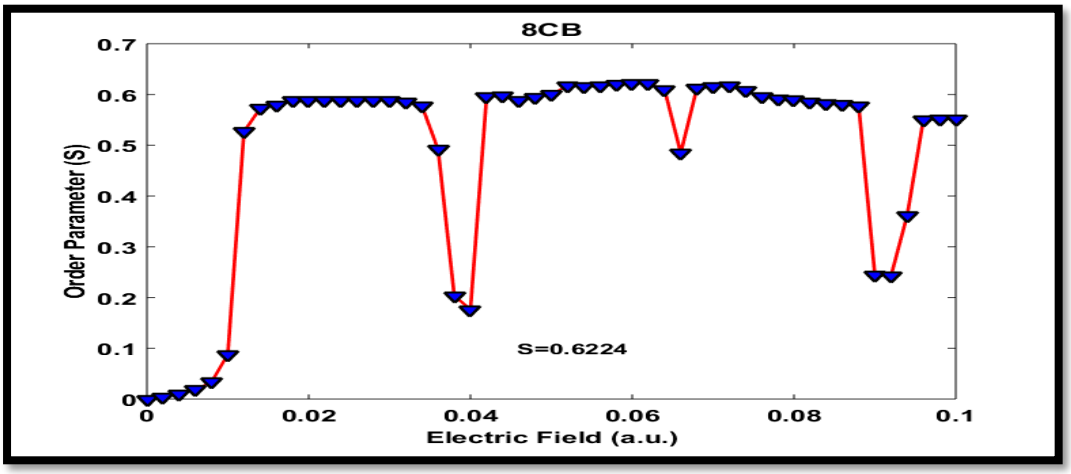

Figure 3.22 Order parameter of 8CB LC under the impact of an electric field

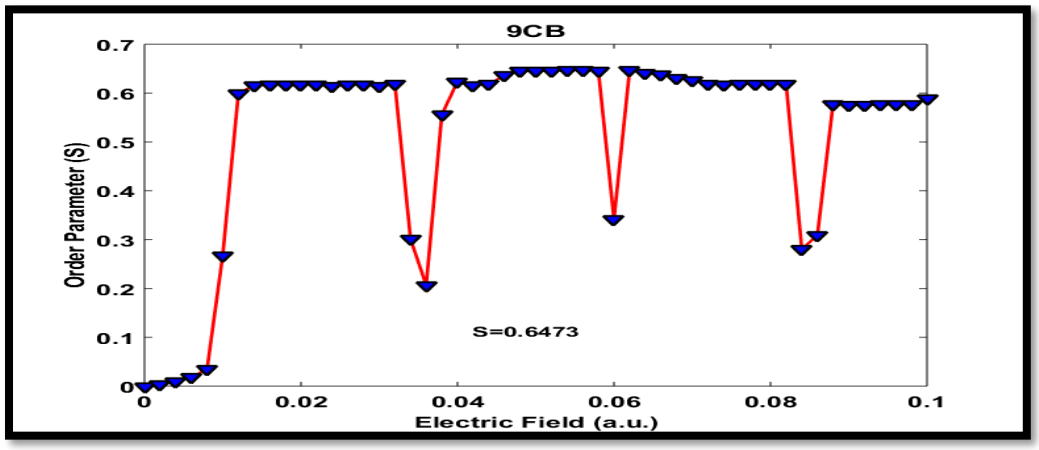

Figure 3.23 Order parameter of 9CB LC under the impact of an electric field

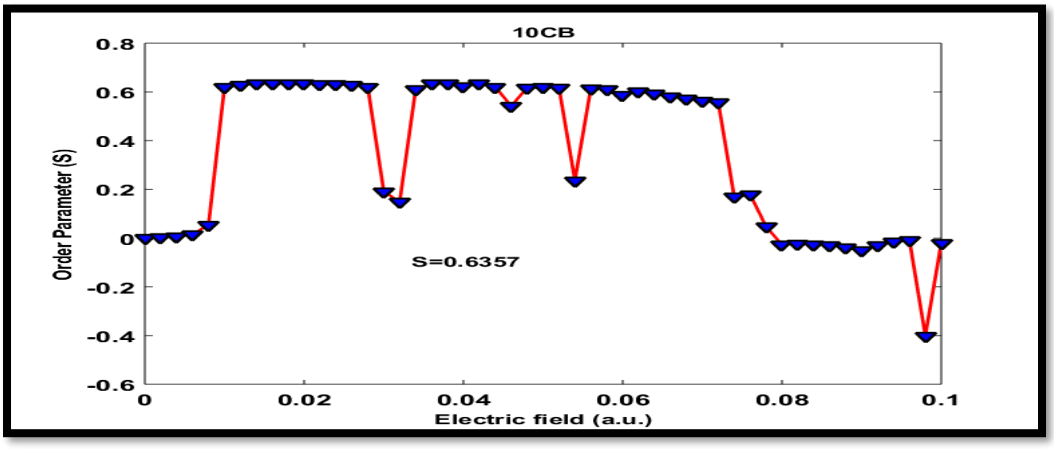

Figure 3.24 Order parameter of 10CB LC under the impact of an electric field

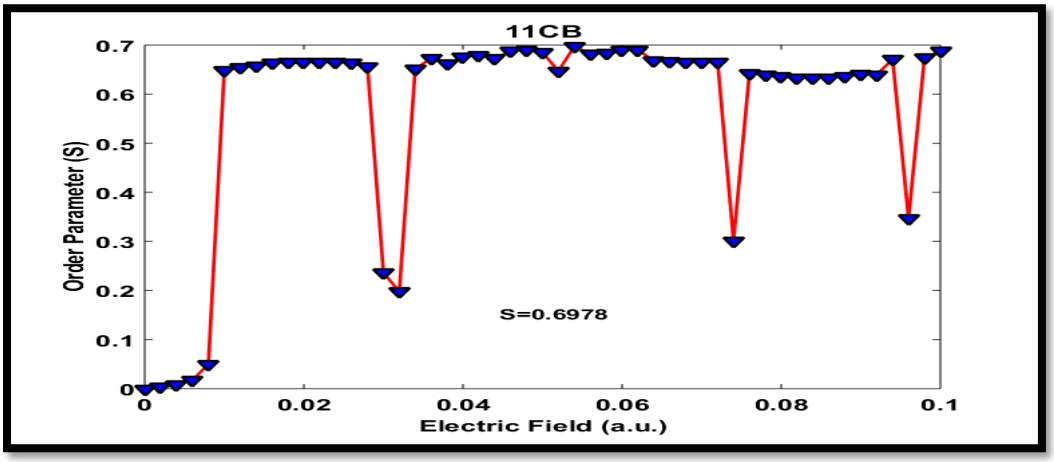

Figure 3.25 Order parameter of 11CB LC under the impact of an electric field

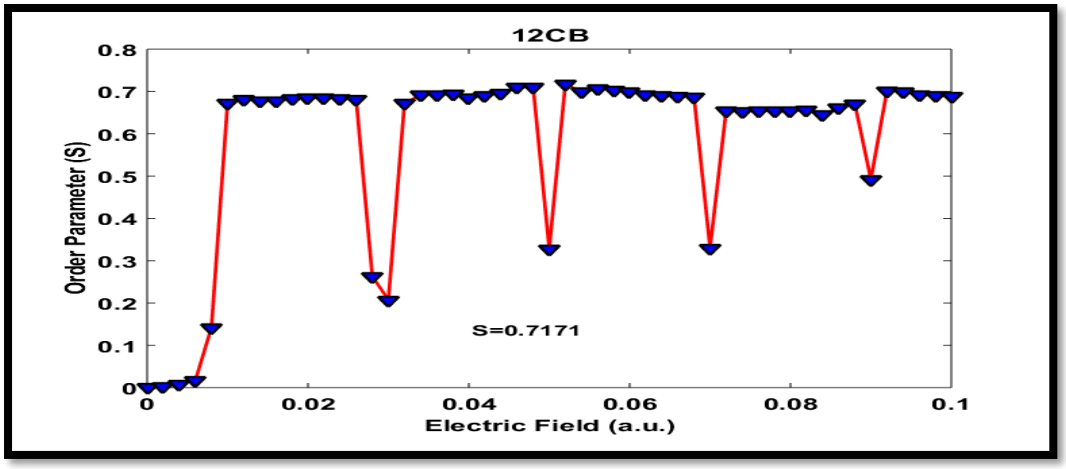

Figure 3.26 Order parameter of 12CB LC under the impact of an electric field

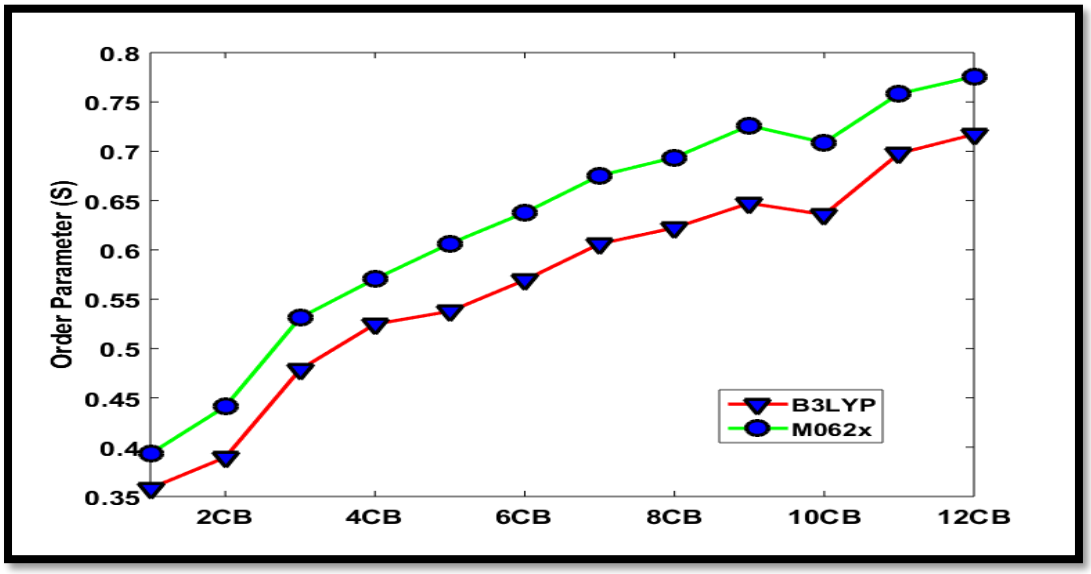

Figure 3.27 Calculated order parameter (S) of nCB series under the effect of the external electric field with an extension of the alkyl chain length using B3LYP (red line) and M062X (green line) methods.

3.3.4 Refractive Index

Chirtoc et al. [39] reported under the impact of temperature, the refractive index is increasing with an extension of alkyl chain length. The refractive index is continual increases with an extension of the alkyl chain length, as shown in Fig. 3.40. The stability

of the refractive index is given in Fig. 3.28 to Fig. 3.39. The C-H atom asymmetric stretching in the alkyl chain is continuously increasing. Which is also responsible for an increment of refractive index. In the 10CB LC, the refractive index abruptly rises. Because the C-H asymmetric stretching corresponds to an IR absorbance is growing instead of decreasing in the benzene ring given in Table 3.10. The refractive index does not express any even-odd effect; it is continual increases. The H atom rocking in both benzene rings corresponding to IR frequency 1532 cm^{-1} increases only in 10CB LC. Which is responsible for abruptly increased refractive index. The IR spectrum of 10CB LC also indicates the absorbance due to the H atom rocking in the both benzene ring.

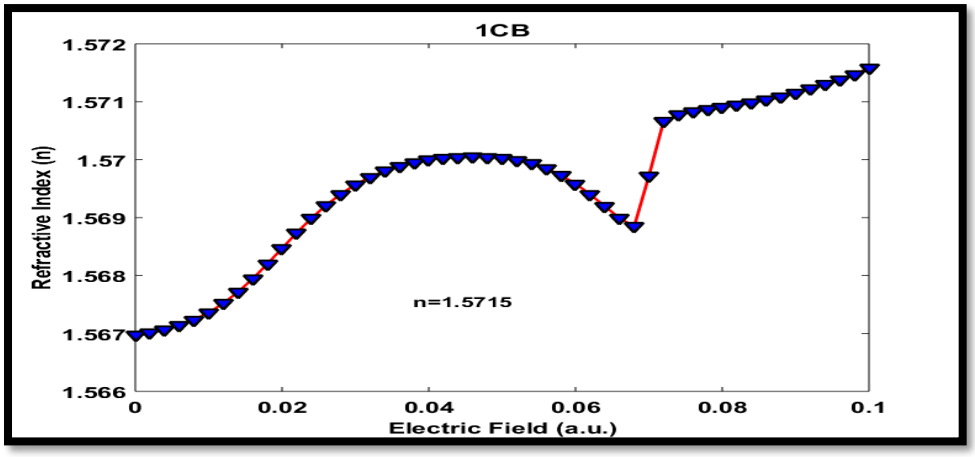

Figure 3.28 Refractive index of 1CB LC under the impact of an electric field

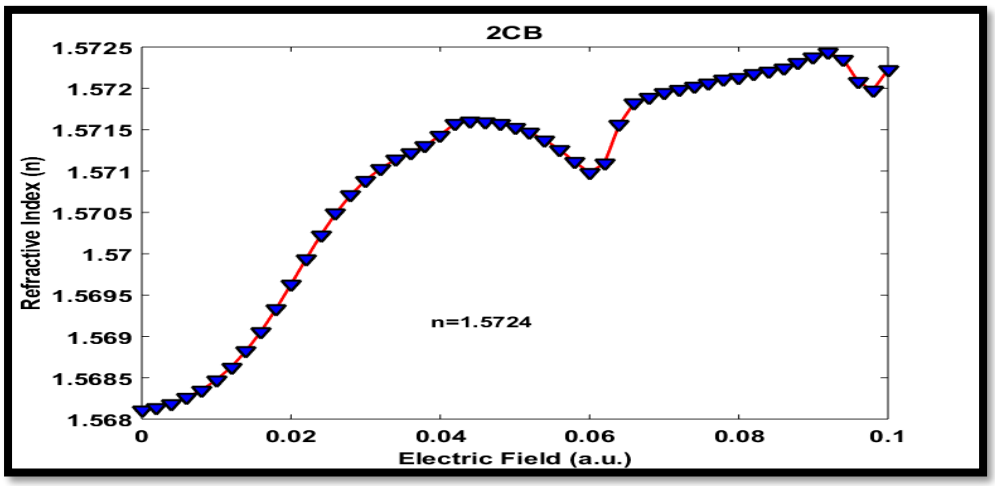

Figure 3.29 Refractive index of 2CB LC under the impact of an electric field

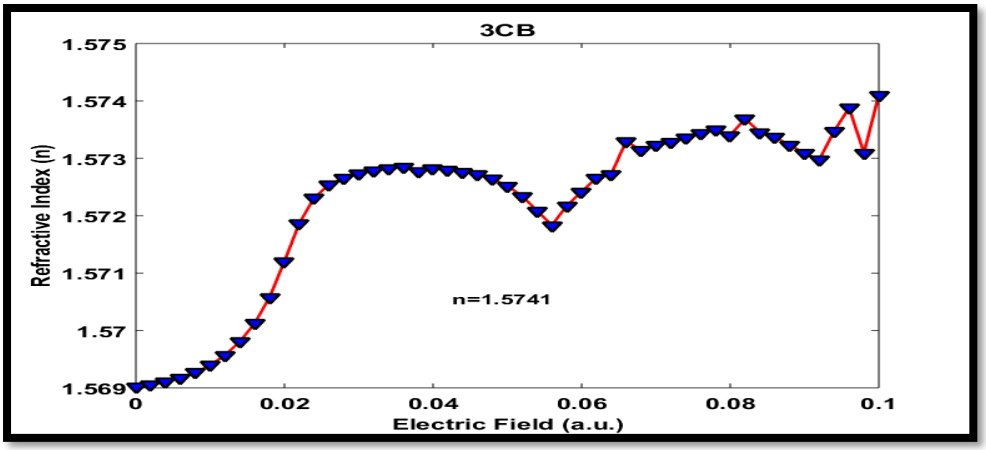

Figure 3.30 Refractive index of 3CB LC under the impact of an electric field

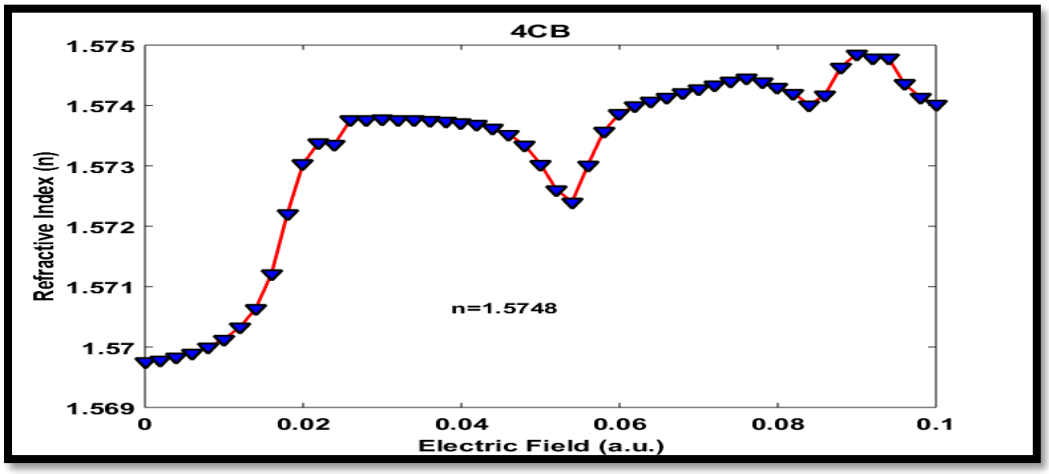

Figure 3.31 Refractive index of 4CB LC under the impact of an electric field

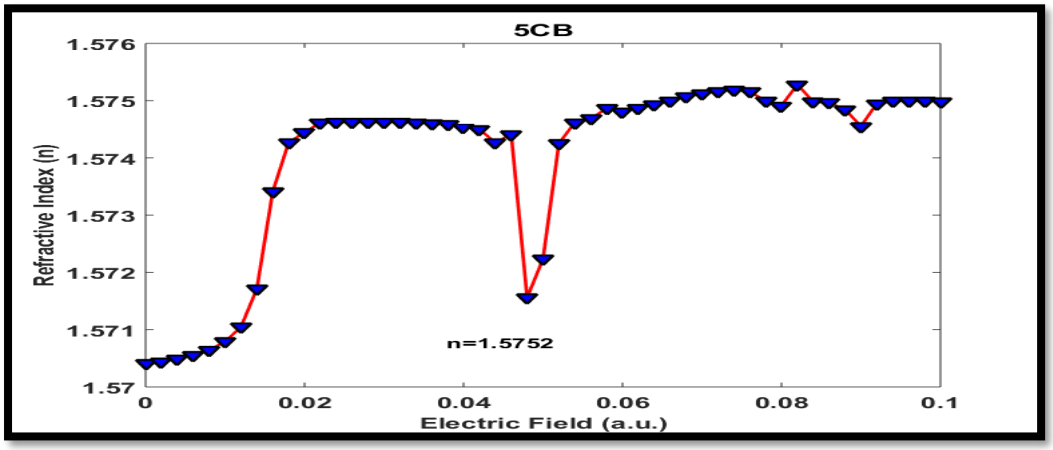

Figure 3.32 Refractive index of 5CB LC under the impact of an electric field

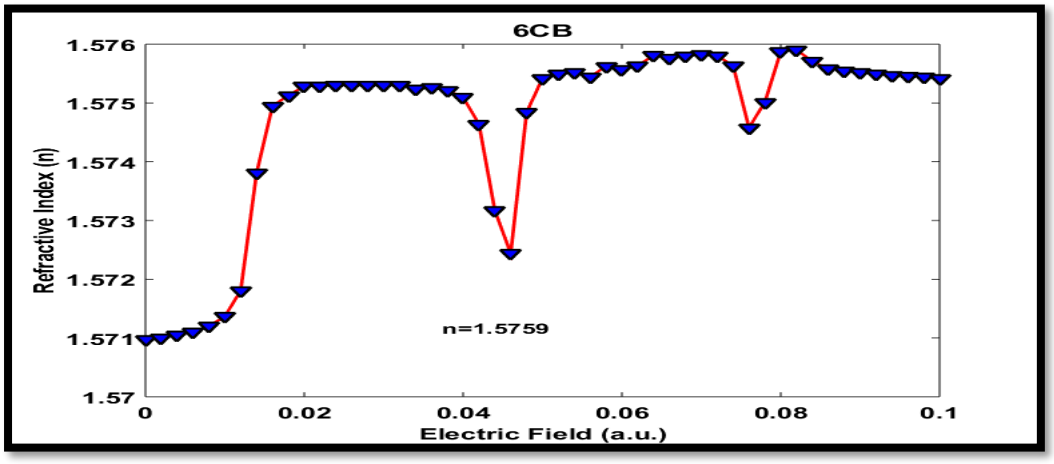

Figure 3.33 Refractive index of 6CB LC under the impact of an electric field

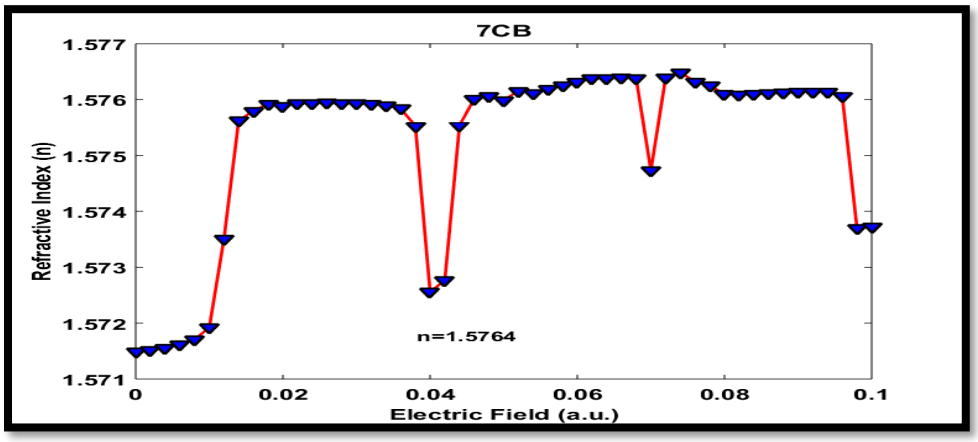

Figure 3.34 Refractive index of 7CB LC under the impact of an electric field

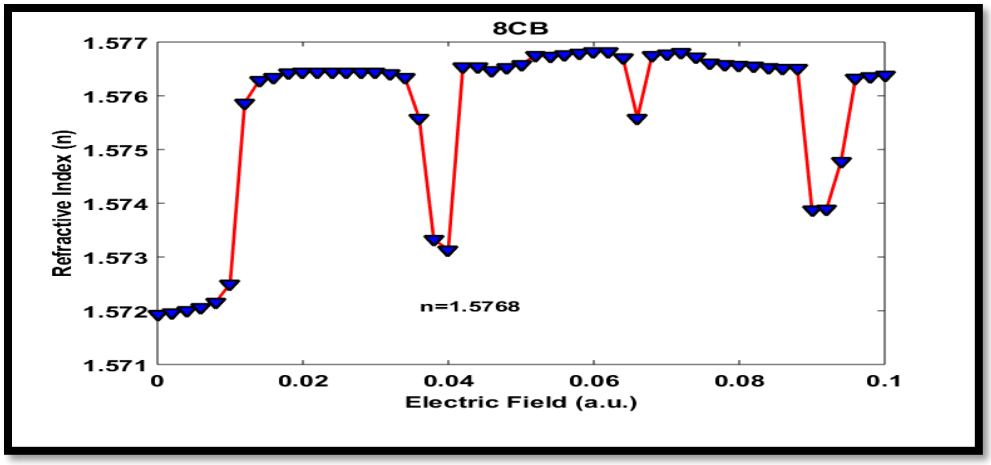

Figure 3.35 Refractive index of 8CB LC under the impact of an electric field

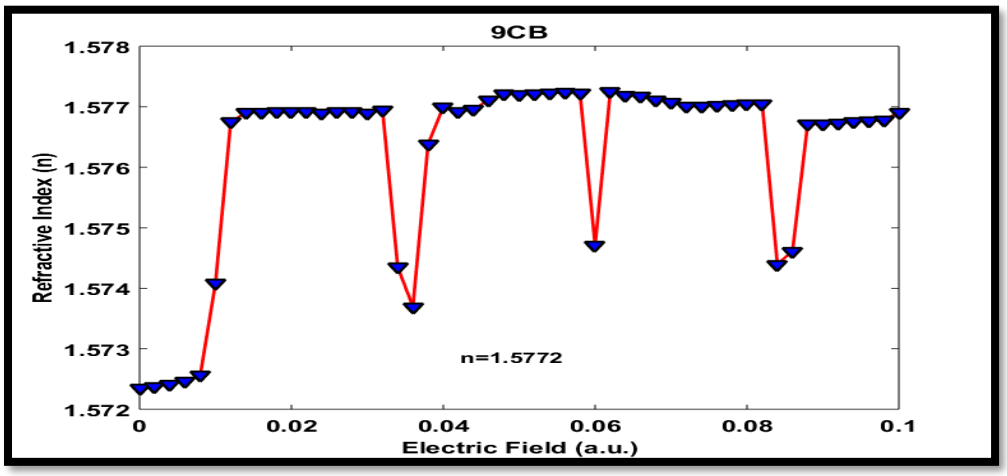

Figure 3.36 Refractive index of 9CB LC under the impact of an electric field

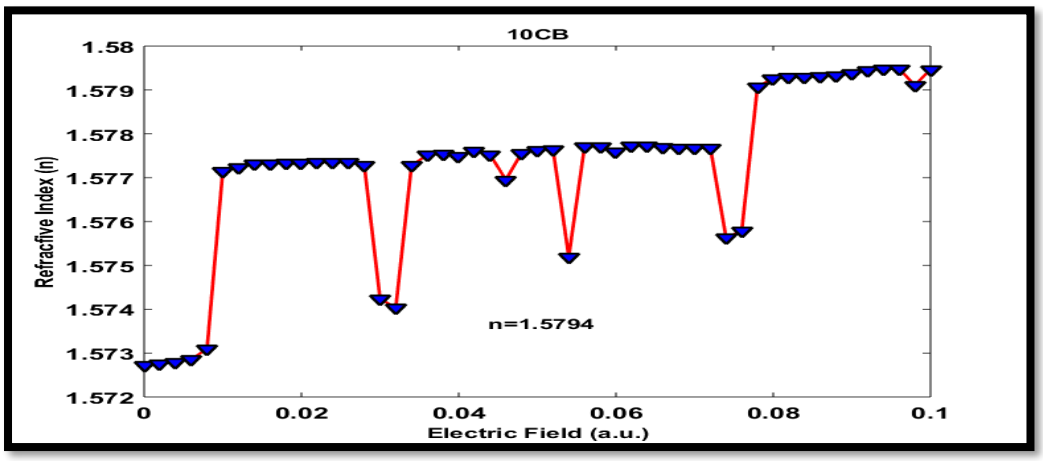

Figure 3.37 Refractive index of 10CB LC under the impact of an electric field

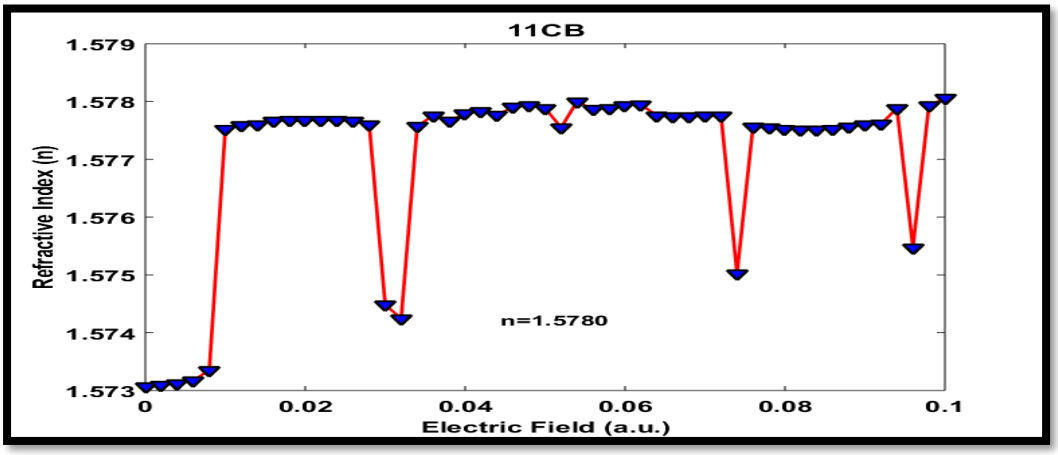

Figure 3.38 Refractive index of 11CB LC under the impact of an electric field

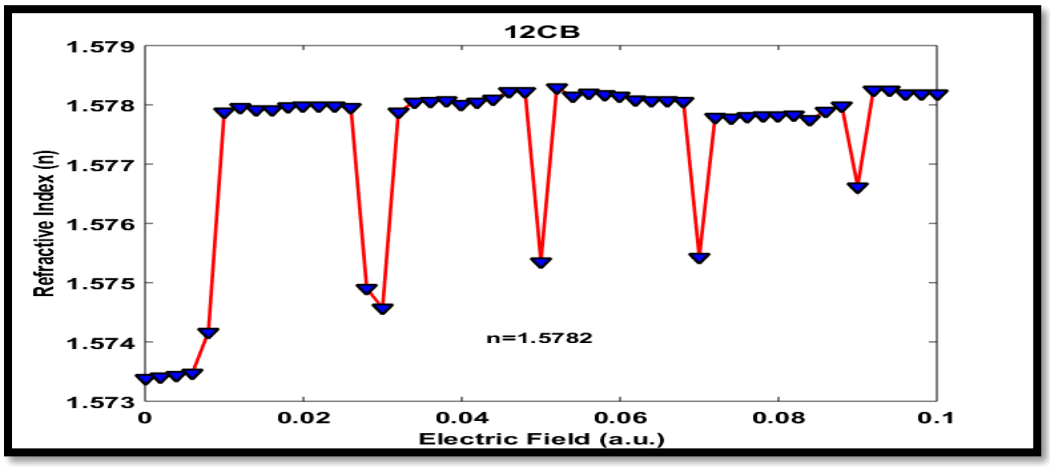

Figure 3.39 Refractive index of 12CB LC under the impact of an electric field

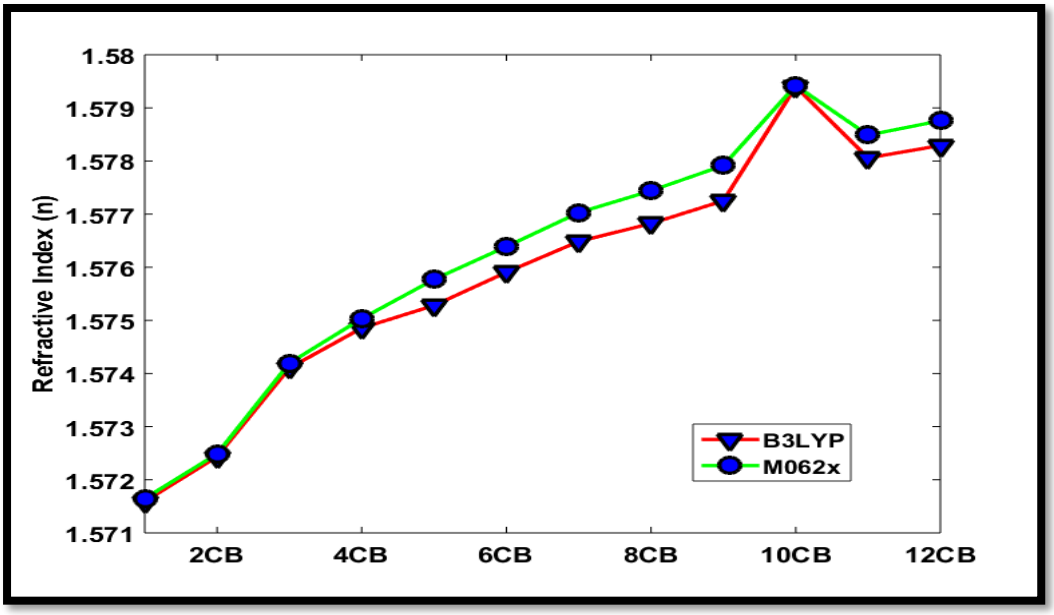

Figure 3.40 The calculated refractive index of nCB series under the external electric field's effect with an extension of the alkyl chain length using B3LYP (red line) and M062X (green line) methods.

3.4 Conclusion

In this chapter, it has been found that the electric field's effect on the nCB LC series. Which is reveals an even-odd effect in optical applications. It has been found that the electric field is another method to find out the optical parameters of the nCB series. The optical parameters are obtaining using derived equations from Vuk's theory. The birefringence of nCB series is decreased continuously and showing an even-odd effect with the extension of the alkyl chain length of the nCB LC molecules. The order parameter of the nCB is steadily increasing with an extension of the alkyl chain length of the nCB series. The stretching of C-C and C-H atom corresponds to higher IR absorbance for odd members and lowers IR absorbance for even members of the nCB series. The C-C and C-H, atom stretching, is contributing to the anisotropy of polarizability. The order parameter and birefringence of the nCB LC molecules are inversely proportional to each other. Under the electric field effect, the birefringence and order parameters are different for different carbon atom numbers. The order parameter, birefringence, and transition

temperature of the nCB series reveal a higher value for odd carbon members, which corresponds to the benzene ring's C-H asymmetric stretching. Our results help to investigate the optical parameters of LC, which can be obtained through electric field and temperature. It is also explaining the correlation between microscopic parameters to mesoscopic parameters of LC, which can be obtained by variation of external electric field and temperature of liquid crystals.

References

[1] J. Ananthaiah, R. Sahoo, M. V. Rasna, S. Dhara, *Phys. Rev. E,* **89**, 022510 (2014).

[2] P. G. De Gennes, *The Physics of Liquid Crystal*, Clarendon Press, Oxford, 1-104 (1974).

[3] S. Chandrasekhar, *Rep. Prog. Phys.* **39**, 613 (1976). R. J. W. Le Fevre, B. P. Rao, *Aust. J. Chem.*, **10**, 1465 (1958).

[4] G. W. Gray, K. I. Harrison, J. A. Nash, *Electron. Lett.*, **9,** 130 (1973).

[5] G. W. Gray, A. Mosley, ***J. Chem. Soc., Perkin Trans., 2***, 97 (1976).

[6] M. I. Caparand, E. Cebe, *J. Comput. Chem.*, **28**, 2140 (2007).

[7] J. R. Lalanne, B. Lemaire, J. Rouch, C. Vaucamps, A. Proutiere, *J. Chem. Phys.*, **73**, 1927(1980).

[8] J. R. Lalanne, J. C. Rayez, B. Duguay, A. Proutiere, R. Viani, *J. Chem. Phys.*, **81**, 344 (1984).

[9] M. J. Aroney, *Angewandte chemie*, **16**, 663 (1970).

[10] T. W. Stinson, J. D. Litster, *Phys. Rev. Lett.*, **25**, 503 (1970).

[11] H. J. Coles, *Mol. Cryst. Liq. Cryst.*, **49**, 67 (1978).

[12] D. A. Dunmur, *Molecular Physics: An International Journal at the Interface Between Chemistry and Physics* **23**, 109 (1972).

[13] P. Sathyanarayana, S. Radhika, B. K. Sadashivab, S. Dhara, *Soft Matter* **8**, 2322 (2012).

[14] A. Eremin, M. Floegel, U. Kornek, S. Stern, R. Stannarius, *Phys. Rev. E,* **86**, 051701 (2012).

[15] E. G. Hanson, Y. R. Shen, G. K. L Wong, *Phys. Rev. A*, **14**, 1281 (1976).

[16] P. Palffy-muhoray, D. A Dunmur, *Mol. Cryst. Liq. Cryst.*, **97**, 337 (1983).

[17] P. Singh, K. B.Thapa, N. Kumar, K. Pal, D. Kumar, *Mater. Res. Express,* **6**, 066209 (2019).

[18] M. J. Aroney, W. P McPherson, R. K. Pierens, *J. Mol. Struct.*, **69**, 289 (1980).

[19] N. Asgharian, Z. A. Schelly, *Biochim. Biophys. Acta*, **1418**, 295 (1999).

[20] D. P. Shelton, *Rev. Sci. Instrum.*, **64**, 917 (1993).

[21] H. Ibrahim, W. Haase, *Mol. Cryst. Liq. Cryst.*, **66**, 189 (1981).

[22] N. Vieweg, C. Jansen, M. K. Shakfa, M. Scheller, N. Krumbholz, R. Wilk, M. Mikulics, M. Koch, *Opt. Exp.*, **18**, 6097(2010).
[23] P. P. Karat, N. V. Madhusudana, *Mol. Cryst. Liq. Cryst.*, **36,** 51 (1976).
[24] Gaussian 09, Revision A.02, M. J. Frisch, G. W. Trucks, H. B. Schlegel, G. E. Scuseria, M. A. Robb, et al. and D. J. Fox, Gaussian, Inc., Wallingford CT, 2010.
[25] A. D. Becke, *J. Chem. Phys.* **98**, 5648 (1993).
[26] C. Lee, W. Yang, R. G Parr, *Phys. Rev. B,* **37**, 785 (1988).
[27] Y. Zhao, D. G. Truhlar, *Theor. Chem. Acc.*, **120**, 215 (2008).
[28] P. J. Hay, W. R. Wadt, *J. Chem. Phys.*, **82**, 299 (1985).
[29] H. D. Cohen, C. C. J. Roothaan, *J. Chem. Phys.*, **43**, S34 (1965).
[30] A. D. Duckingharn, *Adv. Chem. Phys.*, **12**, 107 (1967).
[31] A. Kumar, A. K. Srivastava, S. N. Tiwari, N. Misra, D. Sharma, *Mol. Cryst. Liq. Cryst.*, **681**, 23 (2019).
[32] H. J. Deuling, *Mol. Cryst. Liq. Cryst.*, **19**, 123 (1972).
[33] H. S. Kitzerow, *Mol. Cryst. Liq. Cryst.*, **202**, 51 (1991).
[34] D. Dunmur, A. Fukuda, G. R. Luckhurst, *Physical properties of liquid crystals: nematics*. London, UK: Institute of Electrical Engineers, (2001).
[35] R. G. Horn, *Journal de Physique,* **39,** 105 (1978).
[36] L. G. P. Dalmolen, S. J. Picken, A. F. de Jong, W. H. de Jeu, *Journal de Physique*, **46 (8)**, 1443 (1985).
[37] P. Sherrell, D. Crellin, *J. Phys. Colloq.*, **40 (C3)**, C3-211 (1979).
[38] I. Chirtoc, M. Chirtoc, C. Glorieux, J. Thoen, *Liquid Crystals*, **31**, 229 (2004).
[39] D. A. Dunmur, M. R. Manterfield, W. H. Miller, J. K. Dunleavy, *Mol. Cryst. Liq. Cryst.*, **45**, 127 (1978).
[40] E. Galbiati, G. Zerbi, *J. Chem. Phys.*, **84**, 3509 (1986).
[41] W.-S. Park, *Journal of the Korean Physical Society*, **37**, 331 (2000).
[42] I. Lelidis, M. Nobili, G. Durand, *Phys. Rev. E,* **48**, 3818 (1993).
[43] Miss S. Sen, P. Brahma, S. K. Roy, D. K. Mukherjee, S. B. Roy, *Mol. Cryst. Liq. Cryst.*, **100**, 327 (1983).
[44] S. T. -Wu, *Appl. Opt.*, **26**, 3434 (1987).
[45] Z. Shu-lin, P. Zheng-yu, W. Jin, S. Tie-han, W. Nai-qiang, *Mol. Cryst. Liq. Cryst.*, **91**, 295 (1983).
[46] J. Li, S.-T. Wu, *J. Appl. Phys.*, **96**, 6253 (2004).

CHAPTER 4

Molecular Spectroscopy and Adverse Optical Properties of HBT Liquid Crystal Molecule

4.1 Introduction

The Liquid crystal (LC) phase represents a different state of matter characterized by the molecule's mobility and order. All the particles in the crystalline state possess an orientational and three-dimensional (3D) positional order. Liquid crystal phases possess both orientational order and, in some cases, positional order in one or two dimensions (1D & 2D) [1]. The LC behavior of molecules is responsible for the different types of intermolecular interaction acting between planes, sides, and ends of a pair of the molecule [2]. LC phases are formed by anisotropic molecule, having one molecular axis which is different from the other two [3]. The rod-like molecules are the most common type of LC molecular shape. The nematic phase reveals long-range orientational order but no positional order of the molecule [4]. The effect of the external electric field on LC can be studied and analyzed the polarizability of the molecule [5-6]. In LC's, the molecular polarizability and its anisotropy are important inherent molecular properties because the intermolecular interaction energies depend on them [7]. LC materials may consist of polar and non-polar molecules that depend upon LC's physical structure [8]. The LC molecules can possess permanent dipole along the long molecular axis (x-axis), enhancing LC's dielectric anisotropy. The dipole moment parallels the long molecular axis, then $\Delta\varepsilon>0$, and the molecules tend to orient along the electric field direction because LC possesses more significant dielectric anisotropy along the x-axis (long molecular axis). If the LC molecule carries fewer dipole moments along the molecular

axis, then $\Delta\varepsilon<0$ and fragment tend to orient perpendicular to the electric field direction because the polarity of the molecule is negligible [9]. The orientational order of the LC molecule does not change in the applied external electric field. The applied external electric field to the LC molecule causes the reorientation of the director angle. The LC molecule responds to the applied external electric field E collectively, causing the director angle to fluctuate [10].

Luckhurst et al. [11] reported that the Schiff base compound enhances the molecule's polarity, enhancing the dielectric anisotropy. The dielectric anisotropy is suitable for the electro-optical effect in display applications. Alkyl chain also increased the LC properties, such as the nematic-isotropic (N-Iso) or nematic, to a smectic phase transition temperature [12-13]. According to different theoretical models, the molecular polarizabilities and the anisotropy of LC molecules are considered essential characteristic inherent molecular properties because the intermolecular interaction energies, according to different theoretical models, are dependent on them. The refractive index of HBT LC is 1.58. The birefringence decreases with the increased temperature of the HBT LC molecule. The birefringence in the nematic phase exists between 0.2 to 0.1. The OBT has a smectic B phase. [14-16]. Rao et al. [17] reported that the order parameter increases with an increment of the magnetic field. The nematic to the smectic phase (N-Sm) transition, the order parameter decreases. The HBT LC has an adverse order parameter within the range of 0.45 to 0.58. The α_0 increases, and α_e decreases with increased temperature. The HBT is more stable as a comparison with other molecules. The HBT has a -0.6 order parameter, and OBT has a -0.5 order parameter. The HBT LC has strong intermolecular forces that are responsible for the alignment of molecules. The HBT LC is also having greater translational flexibility, which is dominant in the nematic phase. The HBT LC is an excellent molecule for high-speed optical switching devices, which is the reason for choosing this molecule [18].

4.2 Computational Methodology

HBT LC molecules are optimized by density-functional theory (DFT) method B3LYP [19-20] by 6-31G** [21] basis set using NWChem software package [22]. After the

optimization of all the molecules, we have applied the electric field to the HBT LC along the molecular axis (x-axis) and perpendicular (y-axis) to it from 0.0000 (a.u) to 0.1500 (a.u) at the interval of 0.0020 (a.u). After the applied electric field, we have calculated the molecular polarizability of the HBT LC molecule. X-axis considered as extraordinary molecular polarizability (α_e), and Y-axis considered as ordinary molecular polarizability (α_o) then we have calculated the order parameter, birefringence, refractive index, and magic angle as per the formula is given below [23];

$$\alpha = \frac{1}{3}(\alpha_{xx} + \alpha_{yy} + \alpha_{zz}),$$

$$\beta = \left[(\beta_{xxx} + \beta_{xyy} + \beta_{xzz})^2 + (\beta_{yyy} + \beta_{xxy} + \beta_{yzz})^2 + (\beta_{zzz} + \beta_{xxz} + \beta_{yyz})^2\right]^{1/2},$$

$$\mu = (\mu_x{}^2 + \mu_y{}^2 + \mu_z{}^2)^{1/2},$$

$$\Delta\alpha = 2^{-1/2}\left[(\alpha_{xx} - \alpha_{yy})^2 + (\alpha_{yy} - \alpha_{zz})^2 + (\alpha_{zz} - \alpha_{xx})^2\right]^{1/2},$$

$$\Delta\tilde{\alpha} = \alpha_e - \alpha_o,$$

$$\Delta\tilde{\alpha} = S\Delta\alpha,$$

Where $\tilde{\alpha}$ is mean isotropic polarizability.

Order Parameter (S):-

$$S = \frac{\alpha_e - \alpha_o}{\alpha_e + \alpha_o}, \qquad (1)$$

Birefringence (Δn):-

$$\Delta n = \frac{(\alpha_e - \alpha_o)}{6.3631}\left[R^3 - \left(\frac{2\alpha_o + \alpha_e}{20.244}\right)\right]^{-1}, \qquad (2)$$

Where R is the radius of the liquid crystal molecule.

Magic angle (θ):-

$$\theta = \cos^{-1}\left[\frac{(2S+1)}{3}\right], \tag{3}$$

Refractive index (n):-

$$\alpha = \frac{2\alpha_o + \alpha_e}{3}, \quad \gamma_e = \alpha + \frac{2(\alpha_e - \alpha_o)}{3S}, \quad \gamma_o = \alpha - \frac{(\alpha_e - \alpha_o)}{3S},$$

$$n_e = \frac{7}{2\sqrt{10}} + \frac{\left(2\sqrt{10}/5\right)\pi N\alpha}{1-\frac{4\pi N\alpha}{3}} + \frac{\left(4\sqrt{10}/15\right)\pi N S(\gamma_e - \gamma_o)}{1-\frac{4\pi N\alpha}{3}},$$

$$n_o = \frac{7}{2\sqrt{10}} + \frac{\left(2\sqrt{10}/5\right)\pi N\alpha}{1-\frac{4\pi N\alpha}{3}} - \frac{\left(2\sqrt{10}/15\right)\pi N S(\gamma_e - \gamma_o)}{1-\frac{4\pi N\alpha}{3}}$$

$$n = \frac{7}{2\sqrt{10}} + \frac{\left(2\sqrt{10}/5\right)\pi N\alpha}{1-\frac{4\pi N\alpha}{3}}, \tag{4}$$

Where N is the number of liquid crystal molecules.

4.3 Result and discussion

4.3.1 Order Parameter

The order parameter has been calculated under the influence of an external electric field by the mathematical Eq. no. 1. Rao et al. [17] reported that the order parameter increases with an increment of the magnetic field. The nematic to the smectic phase transition, the

order parameter decreases in the present chapter; the order parameter decreases from nematic to smectic phase transition, as shown in Fig. 4.1. The HBT LC has an adverse order parameter; current work also indicates an adverse order parameter at the electric field 0.0480 (a.u). Sarn et al. [15] reported the α_0 increases and α_e decreases with an increment of temperature in the present work also, the α_0 increases and α_e declines under the influence of an external electric field. Sarn et al. reported the positive order parameter of HBT LC is 0.68 in the present work; the positive order parameter is 0.67. The theoretical prediction is very accurate with the experimental evidence. The maximum order parameter of HBT LC is 0.6788, and the minimum is -0.3865.

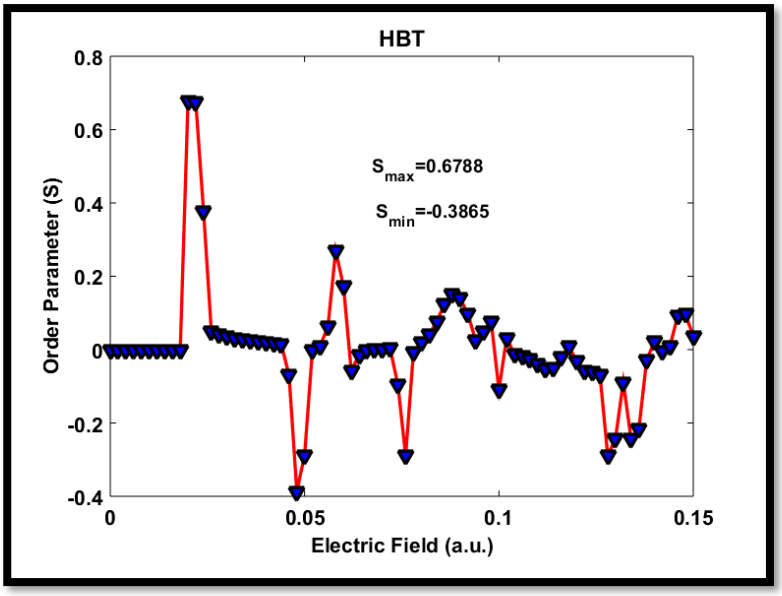

Figure 4.1. Calculated order parameter under the influence of an external electric field by DFT

4.3.2 Birefringence

The birefringence has been calculated under the influence of an external electric field by the mathematical Eq. no. 2. Sarn et al. [15] reported the birefringence decreases with increased temperature of the HBT LC molecule. The birefringence in the nematic phase exists between 0.2 and 0.1; current work also indicates that the nematic phase's

birefringence is 0.1119, as shown in Fig. 4.2. The α_0 increases, and α_e decreases with an extension of temperature; the current work indicates adverse or negative birefringence of HBT LC molecule. The HBT nematic phase is stable at the electric field 0.0220 (a.u) and 0.0240 (a.u) and the smectic phase stable at the electric field 0.0580 (a.u). The maximum birefringence of the HBT LC molecule is 0.1119, and the minimum is -0.0814.

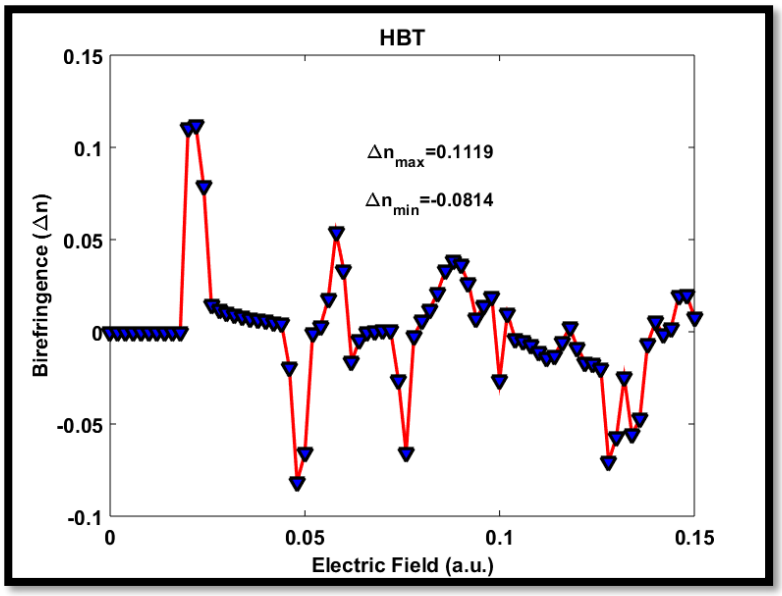

Figure 4.2. Calculated birefringence under the influence of an external electric field by DFT

4.3.3 Refractive Index

The refractive index has been calculated under an external electric field's influence by the mathematical Eq. no. 4. Sarn et al. [15] reported the refractive index of HBT LC is 1.58; the present chapter also indicates the refractive index of HBT LC is 1.58, as shown in Fig. 4.3.

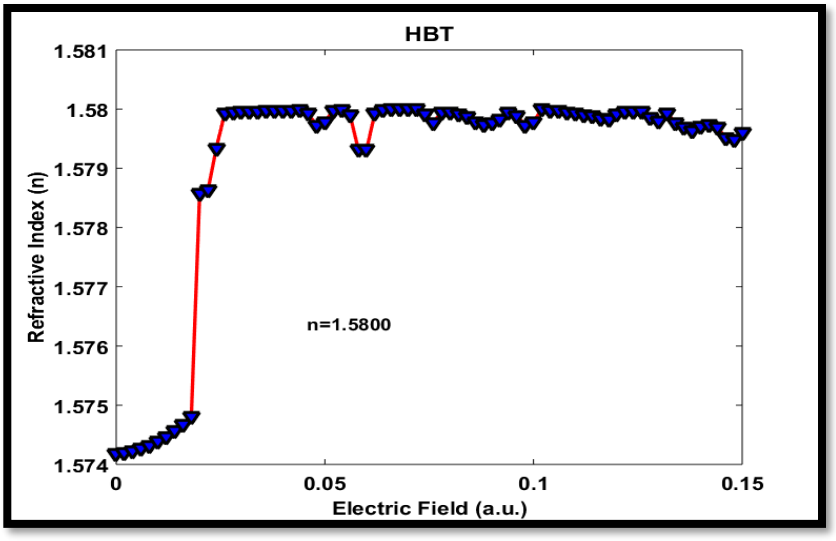

Figure 4.3. Calculated refractive index under the influence of an external electric field by DFT

4.3.4 Director angle or magic Angle

The director angle or magic-angle has been calculated under an external electric field's influence by the mathematical Eq. no. 3. The director angle decreases in the nematic phase and increases in the smectic phase with an expansion of the external electric field as shown in Fig. 4.4. The magic angle of all the liquid crystals is 54.7°; the current chapter also indicates the magic angle of HBT LC is 54.73°. The maximum range of the director angle is 74.03º, and the minimum range is 27.56º. The director angle is stable for the nematic and smectic phase.

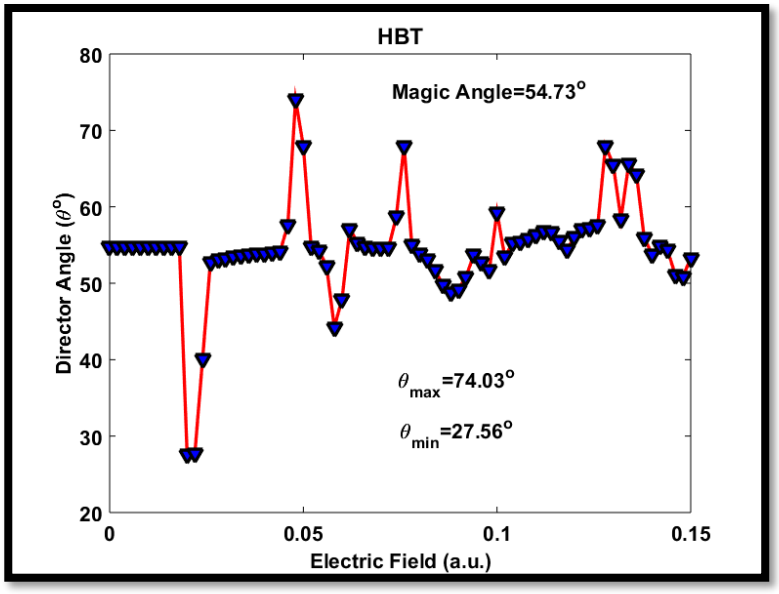

Figure 4.4. Calculated director angle or magic-angle under the influence of an external electric field by DFT

4.3.5 IR spectroscopy of HBT LC

The C-O stretching reveals the maximum absorbance because the oxygen atom transfers the charge to the benzene ring during the intermolecular interaction, as shown in Fig. 4.5 and 4.6, also given in Table 4.1. Zhang et al. reported [24] oxygen atom transfer the proton to the nitrogen atom during an intermolecular interaction, which is responsible for the maximum transmittance of the molecule.

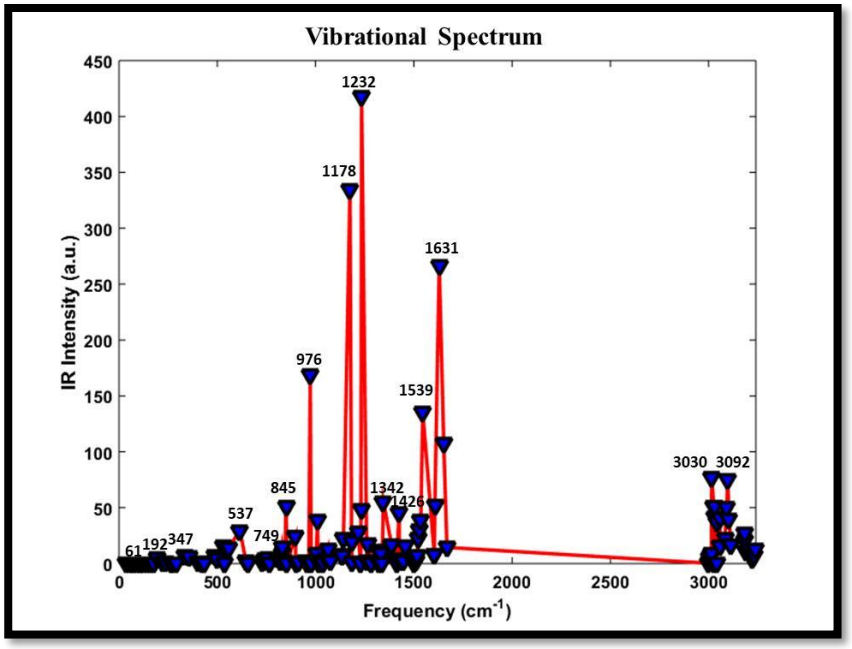

Figure 4.5 Calculated IR spectrum by DFT

Table 4.1 Vibrational mode of HBT LC calculated by DFT methodology

Frequency (cm^{-1})	**Modes of vibration**
565	C-H wagging in benzene
845	Out of plane wagging of the hydrogen atom
976	O-C stretching (carbon atom of alkyl chain)
1178	In-plane scissoring of C-H atom
1232	O-C stretching (carbon atom of benzene ring)
1342	C-C stretching in benzene
1426	C-H Out of plane wagging
1539	C-H In-plane scissoring in benzene
1631	C≡N Stretching and In-plane scissoring of C-H atom
3030	C-H Symmetric stretching in the alkyl chain
3092	C-H Asymmetric stretching in the alkyl chain
3191	C-H Asymmetric stretching in benzene

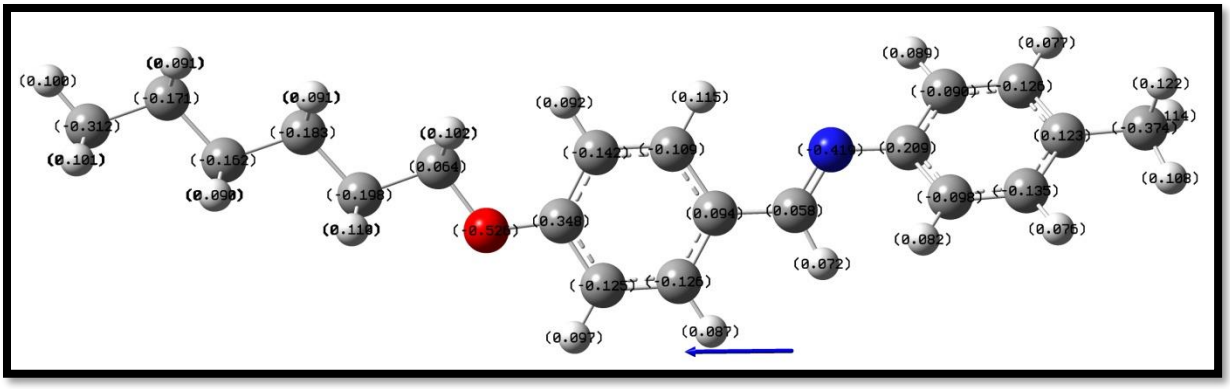

Figure 4.6 Charge distribution of HBT LC molecule

The HBT LC molecule is suitable for sensing and filtering applications because it exhibits a broad range of frequencies given in Table 4.1 and shown in Fig. 4.5. The whole molecule shows Out of plane wagging of Hydrogen atom about the frequency of 845 cm^{-1}. The entire molecule expresses In-plane scissoring of C-H about the frequency of 1178 cm^{-1}. The whole molecule reveals O-C stretching (carbon atom of alkyl chain) about the frequency of 976 cm^{-1}. The entire molecule shows C-C stretching about the frequency of 1342 cm^{-1}. The whole molecule reveals O-C stretching (carbon atom of benzene ring) about the frequency of 1232 cm^{-1}. The entire molecule expresses In-plane scissoring of C-H about the frequency of 1539 cm^{-1}. The whole molecule represents Out of plane wagging of C-H about the frequency of 1426 cm^{-1}. The molecule as a whole shows the Symmetric stretching of C-H atom about the frequency of 3030 cm^{-1}. The entire molecule reveals C-N stretching and C-H In-plane scissoring about the frequency of 1631 cm^{-1}. The whole molecule expresses the Asymmetric stretching of C-H atom about the frequency range from 3092 cm^{-1} to 3191 cm^{-1}.

4.4 Conclusion

In this work, it has been found that the HBT LC molecule has maximum absorbance during the intermolecular interaction because of charge transfer by an oxygen atom to the benzene ring. The birefringence and order parameter have adverse orders with an expansion of the external electric field. The HBT LC molecule is suitable for sensing and filtering applications because HBT LC has a broad range of frequencies. With this

methodology's help, we can predict an unknown organic molecule's optical and sensing properties. B. Bahadur reported HBT LC is diamagnetic, so it is suitable for the diamagnetic material applications. Molecular polarizability is the most crucial parameter in this chapter, which is responsible for the optical properties of the organic molecule. This theoretical model predicts the optical parameters of the unknown organic molecule. The novelty of the current work is modified mathematical equations as a comparison with previously reported results. This theoretical model predicts 97 to 100% accuracy with the experimental evidence.

References

1. P. G. De Gennes and J. Prost, *The Physics of Liquid Crystals second ed.* Oxford University Press (1993).
2. G. W. Gray, *Molecular structure and properties of liquid crystals* Academic Press New York (1962).
3. D. Krishnamurti, H. S. Subramhanyam, *Mol. Cryst. Liq. Cryst.* **31:1-2,** 153 (1975).
4. L. M. Blinov, V. G. Chigrinov, *Electrooptical effects in liquid crystal materials* NewYork (Springer-Verlag) (1994).
5. V. G. Bhide, B. D. Malhotra, V. K. Kondawar, P. C. Jain, *Phys. Lett. A*, **64 (1),** 111 (1977).
6. P. R. Alapati, D. Bhuyan, D. Madhavilatha, P. Pardhasaradhi, V. G. K. M. Pisipati, P. V. Datta Prasad, K. N. Singh, *W. J. Cond. Matt. Phys.* **1(4),** 167 (2011).
7. C. P. Smyth, *Annu. Rev. Phys. Chem.* **17(1),** 433 (1966)
8. R. B. Meyer, *Phys. Rev. Lett.* **22**, 918 (1969)
9. B. Bahadur, R. K. Sarna, V. G. Bhide, *Mol. Cryst. Liq. Cryst.* **88:1-4**, 151 (1982)
10. A. Ferrarini, G. R. Luckhurst, P. L. Nordio, *J. Mole. Phys.* **85(1),** 131 (1995)
11. G. R. Luckhurst, Recent *Adv. Liq. Cryst. Poly.* (L.L. Chapoyed ed.), Elsevier London 105 (1986).
12. S. Marcelja, *J. Chem. Phys.* **60,** 3599 (1974).
13. D. P. Ojha, *J. Phase Transit*. **72(3),** 211 (2000).

14. D. P. Ojha, *J. Z. Naturforsch* **55,** 923 (2000).
15. R. K .Sarna, B. Bahadur, V. G. Bhide, *Mol. Cryst. Liq. Cryst.* **51,** 117 (1979).
16. D. P. Ojha, *J. Z .Naturforsch*. **55** 918 (2000).
17. A. S. N. Rao, P. Narayana Murty, C. R. K. Murty, T. Rs. Reddy, *Z. Naturforsch*. **36a,** 634 (1981).
18. J-J. Zheng, G-L. Zhang, Y-X. Guo, X-P. Li, W-J. Chen, *Chinese Phys.* **16(4),** 1047 (2007).
19. A. D. Becke, *J. Chem. Phys.* **98,** 5648 (1993).
20. C. Lee, W. R. Yang, G. Parr, *Phys. Rev. B* **37,** 785 (1988).
21. P. J. Hay, W. R. Wadt, *J. Chem. Phys.* **82,** 299 (1985).
22. M. Valiev, E. J. Bylaska, N. Govind, K. Kowalski, T. P. Straatsma, Dam H. J. J. van, D. Wang, J. Nieplocha, E. Apra, T. L. Windus, Jong W. A. de, *Comput. Phys. Comm.* **181,** 1477 (2010).
23. A. Kumar, A. K. Srivastava, S. N. Tiwari, N. Misra, D. Sharma, *Mol. Cryst. Liq. Cryst.* **681:1,** 23 (2019).
24. W. Zhang, T. Sakurai, M. Aotani, G. Watanabe, H. Yoshida, V. S. Padalkar, Y. Tsutsui, D. Sakamaki, M. S. S. Ozaki, *Adv. Optical Mater.* **7 (2),** 1801349 (2018).
25. B. Bahadur, *J. Chem. Phys.* **67,** 3272 (1977).

CHAPTER 5

Electro-Optical Odd-Even Effect of the Homologous Series of 7O.m Liquid Crystal

5.1 Introduction

The electronegative oxygen atom plays a crucial role in the compound series of *N(p-n-Heptyloxy-Benzylidene) p-Toluidine* nO.m (n=7, m=1-10); the presence of an oxygen atom in the series of 7O.m is responsible for the nematic phase. On increasing the length of alkoxy or alkyl chain, then the dipole moment increases with the liquid-crystalline range of molecules [1-2]. The nematic to smectic-A (N-A) phase transition has been observed if the alkyl chain length increased. The nO.m compound series shows the odd-even effect under the applied Temperature [3]. The order parameter (S) has been studied by the optical birefringence and molecular polarizability [4]. The removal of an oxygen atom from both sides of the NO.Om compound series is responsible for the reduction of dipole moment and transition temperature. The presence of oxygen atoms on both sides of the compounds NO.Om causes the growth of the clearing temperature and liquid crystalline range [5-8]. The Schiff base compounds are (NO.O.m, nO.m, and n.m) very sensitive to the atmosphere [9]. The nO.m compounds show the orthogonal phase for the $n \leq 6$, and $m \geq 7$, and they exhibit the smectic-F and smectic-G phases. The 7O.1 liquid crystals molecules express the nematic and monotropic-A and smectic-B phase under the effect of temperature. The 7O.1 *N(p-n-heptyloxy-benzy1idene)p-toluidine* (HyBT) liquid crystal compound is a weakly polar compound. It exhibits the nematic phase in heating while cooling of the sample expresses the smectic-A and smectic-B phases. With reduced temperature, the density and ultrasonic velocity in the isotropic phase linearly increases. No hysteresis loop has been observed in the density during heating and cooling cycles

[10-11]. The alkoxy and alkyl-substituted Schiff bases liquid crystal molecules express the liquid crystalline behavior above the room temperature [12-13]. The compound series is denoted by nO.m where *n* and *m* equivalent to the numbers of carbon atoms in the alkyl and alkoxy groups, respectively linked with the benzylidene-aniline frame in the para-positions. The n=7 number is fixed, and m numbers vary from 1 to 5, which is showing the nematic phase, and m=6 indicating only smectic phases (smectic-A, smectic-C, smectic-F, and smectic-G). The n=7 and m≥5 exhibit the nematic and smectic phase while the m≥8 does not express any nematic phase. They exhibit only a series of smectic phases [14-15]. The extended homologous series (m>8) represents the smectic-A phase at a higher temperature and a narrow range of smectic-C or smectic-B and finally smectic-G phase at a lower temperature [16-17]. The 7O.4 compound expresses the ultrasonic velocity in the isotropic phase, which is enhanced linearly with decreasing temperature. The peculiar decrease in the ultrasonic velocity has been observed in the environs of the isotropic-nematic (I-N) phase transition. The ultrasonic velocity firstly reduces in the isotropic phase adjacent to the transition temperature, and further enhanced with decreased temperature in the nematic phase [18-19]. The nematic phase liquid crystal molecules possess long-range orientational order. At the same time, the smectic molecules contain three, two, or one-dimensional periodic order addition with the orientational order. The ultrasonic velocity and molecular volume in a range of temperatures predict the phase transition and also predict molecular packing and molecular interaction [20-25]. In 7O.5, the compound's density decreases linearly, with increases in the smectic-G phase's temperature. The smectic-G to the smectic-B phase transition is the first-order transition in which the structures changed abruptly. The density change at the transition temperature is due to the structural deformation from three dimensional (3D) with smectic-G phase to two dimensional (2D) smectic-B phase [26-31]. The smectic-C to smectic-A phase transition expresses the second-order phase transition because the density changes continuously from smectic-A-smectic-C [32-35]. In the smectic-A phase, the density decreases linearly with the enhancement of temperature continuously. The smectic-A to the nematic phase transition is the first-order phase transition because of the molecules' parallel arrangement [36-40]. The present work theme is searching for the new liquid crystals, which is maybe suitable for the optical

shutters, beam steerers, limiters, and switchable optical filters applications. The current work shows the correlation between the theoretical prediction of the electric field's external effect with the experimental evidence under the impact of temperature.

5.2 Computational Methodology

All the molecules are optimized by the NWChem Software [41] with the help of density functional theory (DFT) method B3LYP [42-43] and M062X [44] by 6-31G** basis set [45-46]. After the simulation of all the molecules, we are applying the electric field (a.u) to the 7O.m liquid crystal compound series along the molecular axis (x-axis) and perpendicular (y-axis). The range of applied electric field is 0.0000 (a.u) to 0.2000 (a.u) at the interval of 0.0020 (a.u) where 1 a.u=5.14 x 10^{11} V/m [53]. We have calculated the molecular polarizability of the 7O.m liquid crystal molecule series after the applied electric field. Along the x-axis, molecular polarizability is considered extraordinary molecular polarizability (αe), and along the y-axis, it is considered ordinary molecular polarizability (α_o). With the help of α_e and α_o, we have calculated the order parameter, magic angle, birefringence and refractive index [48-49] as per the formula given below; The α, β, μ, and molecular anisotropy in polarizability Δα can be revealed as numerical differentiation with an electric field of magnitude 0.002 (a.u). Respectively, equations are given below. Where α, μ, and β are equivalent to the polarizability, dipole moment, and first-order hyperpolarizability components.

$$\alpha = \frac{1}{3}(\alpha_{xx} + \alpha_{yy} + \alpha_{zz})$$

$$\beta = \left[(\beta_{xxx} + \beta_{xyy} + \beta_{xzz})^2 + (\beta_{yyy} + \beta_{xxy} + \beta_{yzz})^2 + (\beta_{zzz} + \beta_{xxz} + \beta_{yyz})^2\right]^{1/2}$$

$$\mu = (\mu_x{}^2 + \mu_y{}^2 + \mu_z{}^2)^{1/2}$$

$$\Delta\alpha = 2^{-1/2}\left[(\alpha_{xx} - \alpha_{yy})^2 + (\alpha_{yy} - \alpha_{zz})^2 + (\alpha_{zz} - \alpha_{xx})^2\right]^{1/2}$$

$$\Delta\tilde{\alpha} = \alpha_e - \alpha_o$$

$$\Delta\tilde{\alpha} = S\Delta\alpha$$

Order Parameter (S):-

$$S = \frac{\alpha_e - \alpha_o}{\alpha_e + \alpha_o} \tag{5.1}$$

Birefringence (Δn):-

$$\Delta n = \frac{(\alpha_e - \alpha_o)}{6.3631}\left[R^3 - \left(\frac{2\alpha_o + \alpha_e}{20.244}\right)\right]^{-1} \tag{5.2}$$

Where, R is the radius of liquid crystal molecule.

Magic angle (θ):-

$$\theta = \cos^{-1}\left[\frac{(2S+1)}{3}\right] \tag{5.3}$$

Refractive index (n):-

$$\alpha = \frac{2\alpha_o + \alpha_e}{3}, \quad (3.1) \qquad \gamma_e = \alpha + \frac{2(\alpha_e - \alpha_o)}{3S}, \quad (3.2) \qquad \gamma_o = \alpha - \frac{(\alpha_e - \alpha_o)}{3S} \tag{3.3}$$

$$n_e = \frac{7}{2\sqrt{10}} + \frac{\left(2\sqrt{10}/5\right)\pi N\alpha}{1 - \frac{4\pi N\alpha}{3}} + \frac{\left(4\sqrt{10}/15\right)\pi NS(\gamma_e - \gamma_o)}{1 - \frac{4\pi N\alpha}{3}} \tag{5.4}$$

$$n_o = \frac{7}{2\sqrt{10}} + \frac{\left(2\sqrt{10}/5\right)\pi N\alpha}{1 - \frac{4\pi N\alpha}{3}} - \frac{\left(2\sqrt{10}/15\right)\pi NS(\gamma_e - \gamma_o)}{1 - \frac{4\pi N\alpha}{3}} \tag{5.5}$$

$$n = \frac{7}{2\sqrt{10}} + \frac{\left(2\sqrt{10}/5\right)\pi N\alpha}{1 - \frac{4\pi N\alpha}{3}} \tag{5.6}$$

Where, N=300 is the number of liquid crystal molecule and γ_e, γ_o is representing the extraordinary and ordinary internal field constant. The difference of γ_e-γ_o is to serve the differential molecular polarizability. The n_e and n_o are representing the extraordinary and ordinary refractive index respectively.

5.3 Results and Discussion

The 7O.m compound series expresses a perfectly odd-even effect by an order parameter, birefringence, and dipole moment under the electric field effect. But the isotropic polarizability, Homo-Lumo gap, and refractive index do not express any odd-even effect. The 7O.m compound series has low birefringence and small order parameter in the presence of an electric field. The Homo-Lumo gap remains constant during the extension of the alkyl chain length of the 7O.m compound. The refractive index and isotropic polarizability are continuously enhanced with the extent of the alkyl chain. The DFT methods reveal the same nature of characteristics for all the parameters but different values. The M062X method expresses the higher values for the refractive index, HOMO-LUMO gap, birefringence, and order parameter compared with the B3LYP method, while isotropic polarizability and dipole moment having higher values for the B3LYP method as compared with the M062X method. The B3LYP and M062X are the most excellent methods for the organic compound; they express good accuracy with the experimental results [50-52]. The 7O.m compound series has a 54.74^o magic angle, and it is calculated by Equation number 3.

5.3.1 Order parameter

The order parameter has been calculated with Eq. no. 1 under an external electric field's influence. The 7O.1 and 7O.2 (m>2) liquid crystal molecules do not exhibit any odd-even effect, and after the 7O.2 molecule, the odd-even effect is observed correctly, as shown in Figure 5.1. The order parameter of the 7O.m series sharply decreases for the 7O.6 liquid crystal molecule expressed by both methods B3LYP and M062X, as shown in Fig. 1. because bond orientational order breaks rotational symmetry and represents the smectic-F phase. Rao et al. [25] have reported that the order parameter of 7O.1 exists between 0.42

and 0.63. The order parameter of 7O.1 is 0.41, shown by the B3LYP method. Gasparoux et al. [35] have reported the order parameter of 7O.4 existing between 0.42 to 0.63, and by the Vuks methods, the order parameter of 7O.4 is 0.41. The order parameter of 7O.4 is 0.40, shown by the B3LYP method, which is approximately equal to the experimental evidence. Rao et al. [26] reported the experimental order parameter of 7O.5 is 0.44. in the current work, the order parameter of 7O.5 is 0.46. The B3LYP method is suitable for m<5, and the M062X method suitable for m>5. Godzwon et al. [19] reported the transition temperature nematic to isotropic (N-Iso) phase transition also reveals the odd-even effect under the impact of temperature. In contrast, the present work also indicates the odd-even effect under the influence of an electric field's external effect. The impact of temperature on the liquid crystals is correlated with the external impact of the electric field.

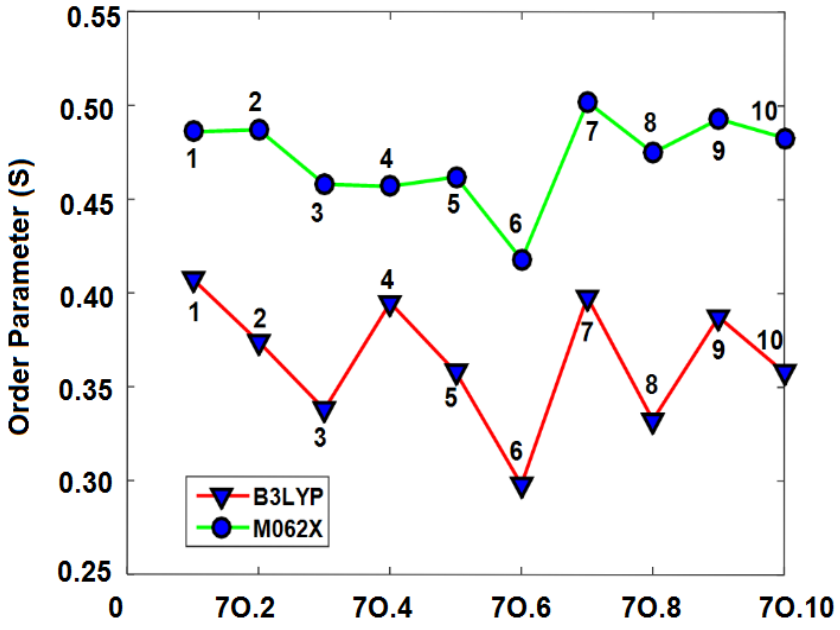

Figure 5.1 Order parameter generated under the applied electric field (a.u) by the B3LYP and M062X methods.

5.3.2 Birefringence

The birefringence has been calculated with Eq. no. 2 under an external electric field's influence. The 7O.m series's birefringence has expressed a perfectly odd-even effect under the applied electric field, as shown in Fig. 5.2. Rao et al. [31] have reported by experimentally calculated birefringence of 7O.2 and 7O.3 is 0.124 and 0.103. In the current work, the birefringence of 7O.2 and 7O.3 is 0.120 and 0.110. Gasparoux et al. [35] have reported the birefringence of 7O.4 an existing between 0.10 to 0.15. In the current work, the birefringence of 7O.4 is 0.10. The theoretical prediction is approximately near to the experimental evidence. The 7O.6 liquid crystal molecule decreases the birefringence because the bond orientational order breaks rotational symmetry and exhibits the smectic-F phase. Smith et al. [28] reported the 7O.6 and 7O.8 LC not having a nematic phase, which is the reason for the sharp decrement of birefringence indicated by the method B3LYP as shown in Fig. 5.2.

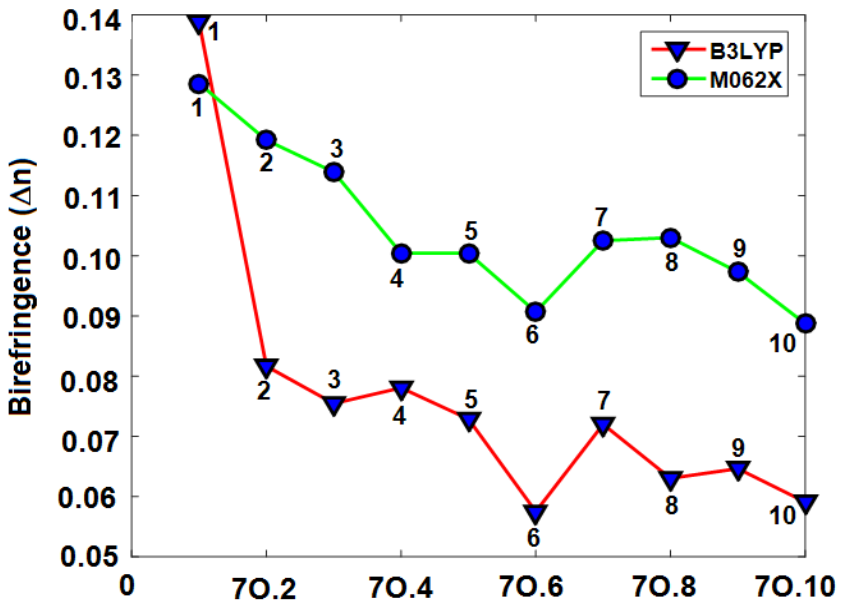

Figure 5.2 Birefringence generated under the applied electric field (a.u) by the B3LYP and M062X methods.

5.3.3 Isotropic polarizability

The isotropic polarizability of the 7O.m series increases continuously, with the extension of the alkyl chain length. Both the methods B3LYP and M062X reveals a perfectly linear graph of isotropic polarizability, as shown in Fig. 5.3. The B3LYP method reveals higher values of isotropic polarizability as a comparison to the M062X method. Fakruddin et al. [4] reported the molecular polarizability is continuously increasing with an extension of the alkyl chain. The liquid crystal's molecular polarizability is continually rising under the impact of temperature; however, the molecular polarizability is continuously increasing under the external electric field's influence in the current work. So we are predicting the impact of temperature on the liquid crystal correlated with the electric field's external effect.

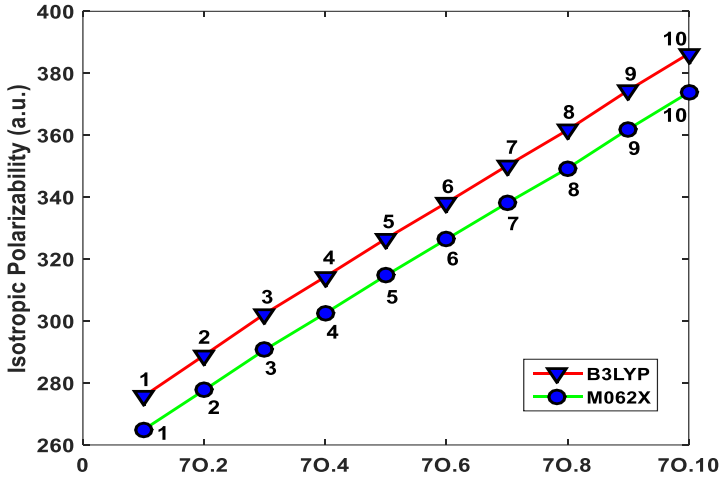

Figure 5.3 Isotropic polarizability generated with an extension of the alkyl chain length

5.3.4 Homo-Lumo energy gap

The **highest occupied molecular orbital** (HOMO) and the **lowest unoccupied molecular orbital (**LUMO) gap of 7O.m series do not express any odd-even effect. In contrast, the Homo-Lumo gap calculated by both B3LYP and M062X methods remains constant for all the 7O.m compound series, as shown in Fig. 5.4. The 7O.10 liquid crystal molecule a little bit increase in the B3LYP method. The HOMO-LUMO energy gap

remains constant with an extension of the alkyl chain length for the whole series of 7O.m liquid crystal compounds. The HOMO-LUMO energy gap is broader for the entire series of 7O.m liquid crystal compounds, which is maybe suitable for the dielectric applications. Most of the dielectric materials have been used for terahertz applications.

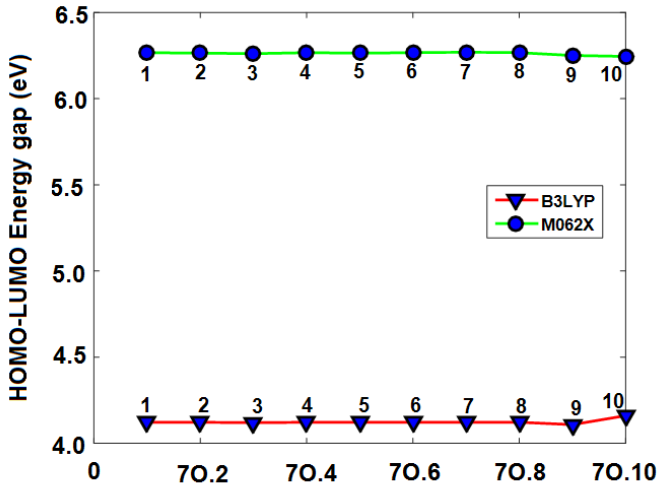

Figure 5.4 Homo-Lumo Energy gaps calculated with an extension of the alkyl chain length

5.3.5 Dipole Moment

The dipole moment perfectly reveals the odd-even effect by increasing the 7O.m compound series' alkyl chain length. The characteristic of the dipole moment of 7O.m series calculated by two DFT methods B3LYP and M062X, is the same but with different values. In the 7O.m compound series, the dipole moment increases for the Odd carbon atom number (3,5,7) of the alkyl chain and express the odd-even effect slightly-slightly the dipole moment decreases with the alkyl chain length increases. Still, after the 7O.7 liquid crystal molecule, the odd-even effect does not observe. Still, the dipole moment decreases continuously as the alkyl chain's length increases, as shown in Fig. 5.5. Latha et al. [15] experimentally reported in the 7O.m series the odd carbon atom number of the alkyl chain increased the transition temp., and even number decreased the transition temperature because the even member of the 7O.m series is making a larger angle with

the long molecular axis; thus, it will reduce the anisotropy of the molecule, and it will reduce the nematic to the isotropic phase transition temperature. However, the odd member of the 7O.m series is making a lower angle with the molecule's long molecular axis; thus, it will enhance the molecule's anisotropy, thereby increasing the transition temperature of 7o.m series. In the current work also express the dipole moment increased for odd members and decreased for even members.

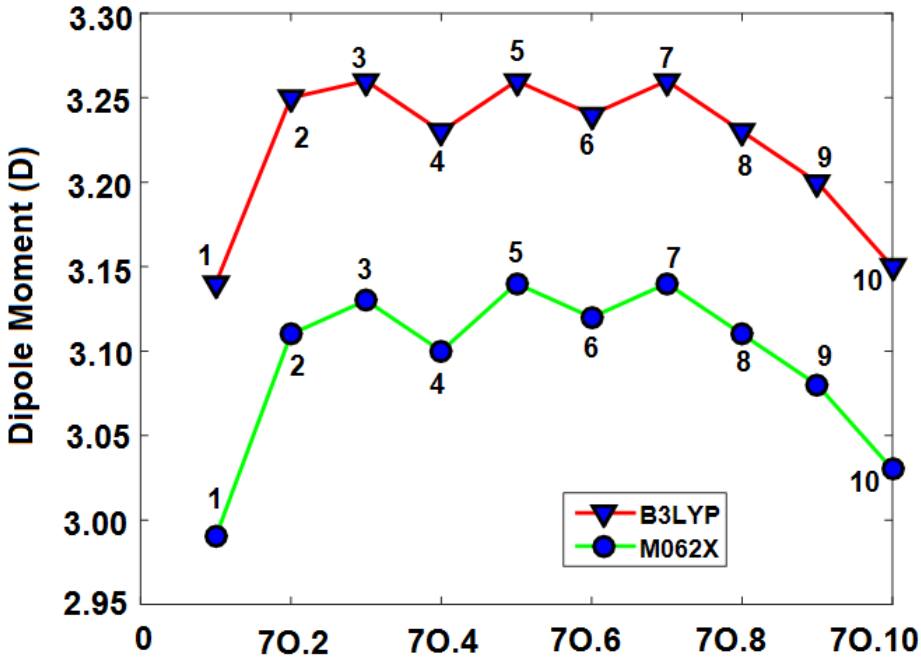

Figure 5.5 Dipole moment calculated with an extension of the alkyl chain length

5.3.6 Refractive index

The odd-even effect does not observe in the refractive index calculated by the B3LYP method. A little bit of odd-even effect is observed in the refractive index calculated by the M062X method, as shown in Fig. 5.6. The refractive index has been calculated by B3LYP and M062X methods under the electric field's impact continuously increase with the alkyl chain's length but with different values. The M062X method reveals a higher amount of refractive index as a comparison to the B3LYP method. Gasparoux et al. [35] have reported the refractive index of 7O.4 is 1.56; however, the theoretical prediction of

7O.4 is 1.57, indicating by the B3LYP method. The theoretical prediction approximately correlates with the experimental evidence.

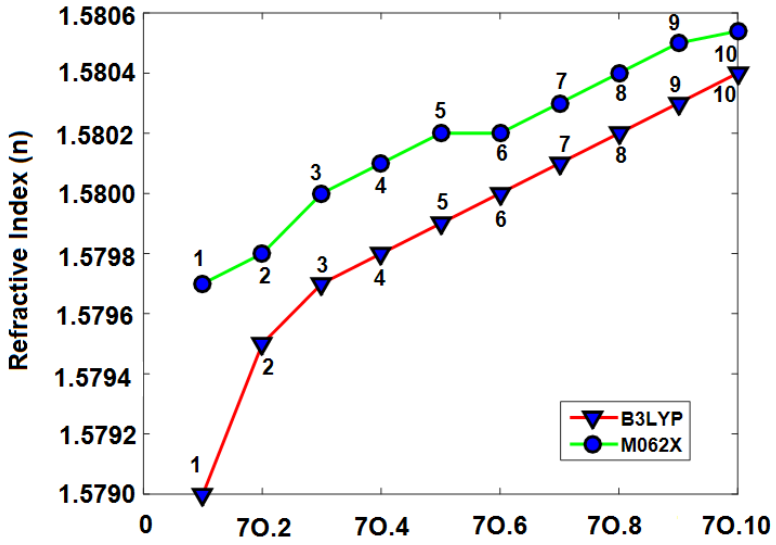

Figure 5.6 Refractive index is calculated under the influence of an external applied electric field (a.u) by the B3LYP and M062X methods.

5.3.7 Birefringence versus order parameter by M062X Method

The M062X method does not have any sharp edge, but the B3LYP method has a sharp edge as shown in Fig. 5.8. The 7O.1, 7O.2, 7O.3, and 7O.4 have the same order parameter; after the 7O.4 molecule, the order parameter fluctuates with the birefringence. The order parameter and birefringence of 7O.6 LC molecule sharply decreases because the bond orientational order breaks rotational symmetry and exhibit the smectic-F phase.

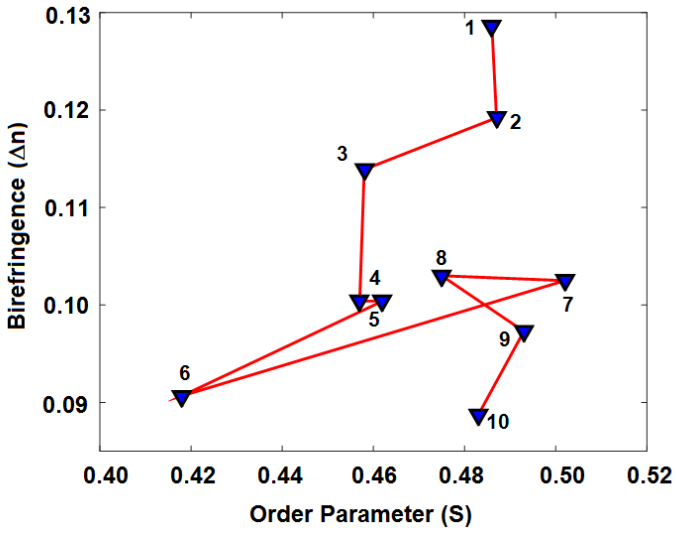

Figure 5.7 Birefringence versus order parameter calculated under the influence of an external applied electric field (a.u) measured by the M062X method.

5.3.8 Birefringence versus order parameter by B3LYP method

The order parameter versus the birefringence graph of the 7O.m series, as shown in Fig. 5.8, is exhibiting the odd-even effect perfectly. The order parameter varies with the birefringence by this method, but this type of character has not been observed in the M062X method shown in Figure 5.7.

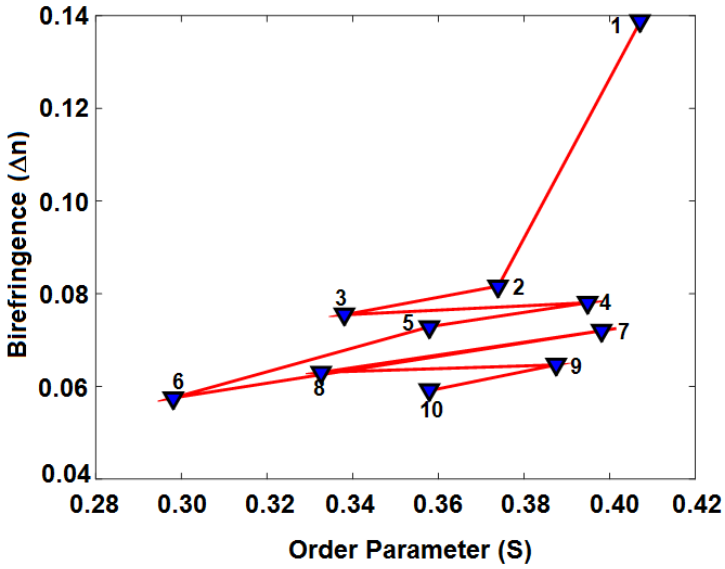

Figure 5.8 Birefringence versus order parameter calculated under the influence of an external applied electric field (a.u) measured by the B3LYP method.

5.4 Conclusion

In this work, it has been found that the 7O.m compound series express a perfectly odd-even effect by order parameter (S), birefringence (Δn), and dipole moment under the impact of the electric field. But the isotropic polarizability, Homo-Lumo gap, and refractive do not express any odd-even effect in the 7O.m series. This compound series has low birefringence and order parameter. The HOMO-LUMO gap remains constant on increasing the length of the alkyl chain. The isotropic polarizability and refractive index continuously improve with an extension of the alkyl chain length. The M062X method produces higher values for the refractive index, HOMO-LUMO gap, order parameter, and birefringence, while dipole moment and isotropic polarizability having higher values which have been calculated by the B3LYP method. The DFT method expresses the perfectly electro-optic and odd-even effect under the applied electric field computed using Eq. 1, 2, 3, and 4. Most probably, it has been found that when the alkyl chain length increased, then the HOMO-LUMO gap some time increased or some time decreased, but in the series of 7O.m compound, the HOMO-LUMO gap remains constant. The homologous series of 7O.m liquid crystal molecules may be suitable for the THz applications. The 7O.m liquid crystals are also ideal for the limiters, optical shutters, beam steerers, and switchable optical filters applications.

References

1. N. Ajeetha, D. M. Potuchi, V. G. K. M. Pisipati, *Phase Transitions*, **78**, 369 (2005).
2. V. G. K. M. Pisipati, A. K. George, Ch. Srinivasu, P. N. Murty, *Z. Naturforsch*, **58a**, 103 (2003).
3. D. M. Latha, V. G. K. M. Pisipati, P. Pardhasaradhi, P. V. D. Prasad, G. P. Rani, *Liq. Cryst.*, **39**, 1113 (2012).

4. K. Fakruddin, R. J. Kumar, P. V. D. Prasad, V. G. K. M. Pisispati, *Mol. Cryst. Liq. Cryst.,* **511**, 146 (2009).
5. F. Heinemann, P. Zugenmaier, *Mol. Cryst. Liq. Cryst.,* **357**, 85 (2001).
6. H. Haga, C. W. Garland, *Liquid Crystals*, **23**, 645 (1997).
7. K. N. Singh, B. Gogoi, R. Dubey, N. M. Singh, H. B. Sharma, P. R. Alapati, *Mol. Cryst. Liq. Cryst.,* **626**, 130 (2016).
8. A. Iwan, *An overview of liquid crystals based on Schiff based compounds, Book Liquid Crystalline Organic Compounds and Polymers as Materials XXI Century:From Synthesis to Applications, 1st edition* (Transworld Research Network Trivandrum, Kerala, 2011).
9. M. Mitra, B. Majumdar, R. Paul, S. Paul, *Mol. Cryst. Liq. Cryst*., **180:2**, 187 (1990).
10. N. V. S. Rao, P. V. D. Prasad, V. G. K. M. Psispati, *Mol. Cryst. Liq. Cryst.,* **126:2-4**, 175 (1985).
11. J. Collett, L. B. Sorensen, P. S. Pershan, J. D. Litster, R. J. Birgeneau, J. Als-Nielsen, *Phys. Rev. Letts.,* **49**, 553 (1982).
12. W. H. D Jeu, J. A. D. Poorter, *Phys. lett. A,* **61A** , 114 (1977).
13. D. E. M. Zambrano, *Temperature dependent surface reconstruction of freely suspended films of 4-n-heptyloxybenzylidene-4-n-heptylaniline*, Lawrence University (2015).
14. V. G. K. M. Pisipati, N. V. S. Rao, *Z. Naturforsch,* **37a**, 1262 (1982).
15. D. M. Lata, P. V. R. Shekar, V. G. K. M. Pisipati, P. Pardhasaradhi, *IJAETMAS*, **04**, 63 (2017).
16. N. Ajeetha, D. P. Ojha, *Z. Naturforsch*, **64a** , 844 (2009).
17. R. Y. Dong, K. R. Sridharan, *J. Chem. Phys.,* **82**, 4838 (1985).
18. V. G. K. M. Pisipati, N. V. S. Rao, *Z. Naturforsch,* **39a**, 696 (1984).
19. J. Godzwon, M. J. Sienkowska, Z. Galewski, *Thermochimica Acta,* **491**, 71 (2009).
20. J. Thoen, G. Seynhaeve, *Mol. Cryst. Liq. Cryst.,* **127**, 229 (1985).
21. K. R. K. Rao, J. V. Rao, P. Venkatacharyulu, V. Baliah, *phys. stat. sol. (a),* **93**, 93 (1986).

22. S. B. Rananavare, V. G. K. M. Pisipati, *An overview of liquid crystals based on Schiff base compounds. Liquid Crystalline Organic Compounds and Polymers as Materials of the XXI Century: From Synthesis to Applications.* 19-52 (2011).
23. P. G. de Gennes, *The Physics of Liquid Crystals, 2nd ed.* (Oxford University Press, Oxford, 1993).
24. P. Bhaskara Rao, D. M. Potukuchi, J. S. R. Murthy, N. V. S. Rao, V. G. K. M. Pisipati, *Cryst. Res. Technol.*, **27**, 839 (1992).
25. N. V. S. Rao, V. G. K. M. Pisipati, P. V. Datta Prasad, P. R. Alapati, D. Saran, *Mol. Cryst. Liq. Cryst.*, **132:1-2**, 1-21(1986).
26. J. V. Rao, K. R. K. Rao, L. V. Choudary, P. Venkatacharyulu, *Cryst. Res. Technol.,* **21**, 1245 (1986).
27. Z. G. Gardlund, R. J. Curtis, G. W. Smith, *J. C. S. Chem. Comm.*, **6**, 202 (1973).
28. G. W. Smith, Z. G. Gardlund, *J. Chem. Phys.*, **59**, 3214 (1973).
29. K. N. Singh, N. M. Singh, H. B. Sharma, P. R. Alapati, *J. Adv.*, **8**, 2176 (2015).
30. B. Bonev, V. G. K. M. Pisiapti, A. G. Petrov, *Liquid Crystals,* **6**, 133 (1989).
31. P. B. Rao, D. M. Potukuchji, J. S. R. Murthyn, N. V. S. Rao, V. G. K. M. Pisipati, *Cryst. Res. Technol.,* **27**, 839 (1992).
32. V. G. K. M. Pisipati, N. V. S. Rao, D. M. Potukuchi, P. R. Alapati, P. B. Rao. *Mol. Cryst. Liq. Cryst.,* **167**, 167 (1989).
33. W. H. de Jeu, Th. W. Lathouwers, *Z. Naturforsch*, **30a**, 79 (1975).
34. H. Haga, C.W. Garland, *Liq. Cryst.*, **22**, 275 (1997).
35. H. Gasparoux, J. R. Lalanne, B. Martin, *Mol. Cryst. Liq. Cryst.,* **51**, 221 (1979).
36. W. Thyen, F. Heinemann, P. Zugenmaier, *Liq. Cryst.,* **16**, 993 (1994).
37. G. P. Rani, D. M. Potukuchi, N. V. S. Rao, V. G. K. M. Pisipati, *Mol. Cryst. Liq. Cryst.*, **289**, 169 (1996).
38. M. Meichle, C. W. Garland, *Phys. Rev. A*, **27**, 2624 (1983).
39. C. R. C. Prabhu, S. Lakshminarayana, V. G. K. M. Pisipati, *Z. Naturforsch*, **59a**, 537 (2004).
40. P. V. D. Prasad, M. R. N. Rao, J. Lalithakumari, V. G. K. M. Pisipati, *Phys. Chem. Liq.*, **47**, 123 (2009).

41. M. Valiev, E. J. Bylaska, N. Govind, K. Kowalski, T. P. Straatsma, H. J. J. van Dam, D. Wang, J. Nieplocha, E. Apra, T. L. Windus, W. A. de Jong, *Comput. Phys. Commun.*, **181**, 1477 (2010).
42. C. Lee, W. Yang, R. G Parr, *Phys. Rev.* B, **37**, 785 (1988).
43. A. D. Becke, *J. Chem. Phys.*, **98**, 5648 (1993).
44. Y. Zhao, D. G. Truhlar, *Theor. Chem. Acc.*, **120**, 215 (2008)
45. P. J. Hay, W. R. Wadt, *J. Chem. Phys.*, **82**, 299 (1985).
46. P. C. Hariharan, J. A. Pople, *Theo. Chim. Acta.*, **28**, 213 (1973).
47. A. R. Johnston, *J. Appl. Phys.*, **44**, 2971 (1973).
48. M. F. Vuks, *Opt. Spect.*, **20**, 361 (1966).
49. A. Kumar, A. K. Srivastava, S. N. Tiwari, N. Misra, D. Sharma, *Mole. Cryst. Liq. Cryst.*, **681:1**, 23-31 (2019).
50. J. Tirado-Rives, W.L. Jorgensen, *J. Chem Theory. Comput.*, **4**, 297 (2008).
51. S-I. Lu, C-C. Chiu, Y-G. Wag, *J. Chem Phys*, **135**, 134104 (2011).
52. B. Kirste, *Chem. Sci. J,* **7:2** (2016).
53. Y. Wang, F. Wang, J. Li, Z. huang, S. Liang, J.Zhou, *Energies, MDPI*, **10(4)**, 1 (2017).

CHAPTER 6

Even-Odd Effect of the Homologous Series of nCHBT Liquid Crystal Molecules

6.1 Introduction

The general structure of nCHBT consists of one phenyl ring attached by the cyclohexane ring with the chair conformation and the isothiocyanate (–NCS) group linked with the phenyl ring and the alkyl chain (C_nH_{2n+1}) attached to the cyclohexane ring. Based on technological applications, it has been found that the nematic liquid crystals (LC) possess orientational order due to which they have been used for the extensive applications in LC display (LCD) devices [1-2]. The birefringence and refractive index depend upon the temperature, wavelength, and structure of the particular material. But for the use of LC in the form of a display device, the temperature factor is essential [3]. A simulation using computational techniques have used to know the transport properties of a particular LC. The transfer of momentum gives rise to shear viscosity. In CHBT LC, viscosity is independent of the velocity gradient, whether it is nematic or isotropic phase [4]. The strength of the odd-even effect has undetermined with the increase in the alkyl chain of the compound. The clearing temperature also depends on the alkyl chain length. On increasing the temperature, the value of the extraordinary refractive index decreases while the ordinary refractive index's value increases [5]. With the introduction of the NCS group, the value of polarizability increases in the case of CHBT, as phenyl ring combines with π electron. In the nematic phase of CHBT, the antiparallel association of the molecule is not present. The antiparallel conformation has generated the dipole between the cyanobiphenyl (CN) group; however, the NCS group does not create any

dipole [6]. The infrared spectrum of the isotropic LC is similar to the IR spectra of the nematic phase. The nematic LC's are capable of scattering light to a greater extent; its special appearance makes it more visible, among others [7]. The NCS group exposed to UV radiation, it has found that it resist exposure. Their color, conductivity, and phase transition temperature remains the same. These contain a smectic layer spacing, which is similar to the length of one molecule. Its mixture with the CN group yields a high value of dielectric anisotropy [8]. The increased melting point observed when the number of carbon atoms in the alkyl chain is odd. The small changes in the rigid core structure lead to the change in attractive and repulsive forces [9]. The transfer of momentum in liquids is different from the transport phenomenon in solids. The rigid core in CHBT is known as the mesogenic core. The ratio of apparent molecular length and calculated the molecular distance indicates that some biomolecule associates with CHBT. Short-range associations are highly dependent on the structure of the molecule. Quantitatively, founded by a Kirkwood correlation factor, and this reveals that correlation is less in the isotropic phase [10-11]. When two LC have a resemblance in structure and length, but their polarity is different, then dielectric relaxation spectroscopy is required to study their orientational order. For the comparison between two LC compounds, the relative temperature is generally used [12]. Buchecker et al. [13] have revealed that the isothiocyanates group and the side chain could help form a homologous series in which a rigid core is free from double bonds. The compounds having an odd number of alkyl groups, the range of mesogenic state temperature is broad compared to the compounds having an even number of alkyl groups. The mechanical properties of an LC-like elasticity depend upon the dipolar interaction. Schulz et al. [14] have reported that the LC is thermally stable or not; it relies on its terminal group's nature. The nCHBT compounds are having –NCS as the terminal group, which is more fluctuates in the high-temperature range. The objective of this chapter is to find out an unknown LC molecule for electro-optical applications. The present work's motivation is to search for a new unknown LC molecule suitable in the terahertz (THz) applications because we are applying a very high electric field of 0.001 a.u, which is equal to 6.5 THz.

6.2 Computational Methodology

All the nCHBT molecules are optimized by the NWChem Software [15] with the help of density functional theory (DFT) method B3LYP [16-17] and M062X [18] by 6-31G** basis set [19-21]. After the optimization of all the molecules, we have applied the electric field to the nCHBT LC compound series along the molecular axis (x-axis) and perpendicular (y-axis). The applied electric field range is 0.000 a.u to 0.100 a.u at the interval of 0.0020 a.u [22] where 1 a.u. = 5.14×10^{11} V/m. We have calculated the molecular polarizability of the nCHBT LC molecule series after an applied electric field. The molecular polarizability along the x-axis is considered extraordinary molecular polarizability (αe), and along the y-axis is considered ordinary molecular polarizability (α_o). With the help of α_e and α_o, we have calculated the order parameter, refractive index, magic angle, and birefringence [23-30]. The finite-field approach framework predicts the total molecular energy under the impact of the electric field is given below [31];

$$E = E_o - \mu_i F_i - \frac{1}{2}\alpha_{ij}F_iF_j - \frac{1}{6}\beta_{ijk}F_iF_jF_k$$

Where E_o is the total energy in the absence of the electric field, and F_i, μ_i, α_{ij} and β_{ijk} equivalent to the components of the electric field, dipole moment, and polarizability and first-order hyperpolarizability and respectively directions specified along with the subscripts i, j and k=x, y and z. The molecular anisotropy in polarizability (Δα) can be revealed as numerical differentiation with an electric field of magnitude 0.002 a.u. Respectively, equations are given below [32];

$$\Delta\alpha = 2^{-1/2}\left[(\alpha_{xx} - \alpha_{yy})^2 + (\alpha_{yy} - \alpha_{zz})^2 + (\alpha_{zz} - \alpha_{xx})^2\right]^{1/2}$$

$$\Delta\tilde{\alpha} = \alpha_e - \alpha_o$$

$$\Delta\tilde{\alpha} = S\Delta\alpha$$

Where α̃ is the mean isotropic polarizability.

Order Parameter (S):-

$$S = \frac{\alpha_e - \alpha_o}{\alpha_e + \alpha_o} \tag{1}$$

Birefringence (Δn):-

$$\Delta n = \frac{(\alpha_e - \alpha_o)}{6.3631}\left[R^3 - \left(\frac{2\alpha_o + \alpha_e}{20.244}\right)\right]^{-1} \tag{2}$$

Where R is the radius of the liquid crystal molecule.

Magic angle (θ):-

$$\theta = \cos^{-1}\left[\frac{(2S+1)}{3}\right] \tag{3}$$

Refractive index (n):-

$$\alpha = \frac{2\alpha_o + \alpha_e}{3}, \quad \gamma_e = \alpha + \frac{2(\alpha_e - \alpha_o)}{3S}, \quad \gamma_o = \alpha - \frac{(\alpha_e - \alpha_o)}{3S}$$

$$n_e = \frac{7}{2\sqrt{10}} + \frac{\left(2\sqrt{10}/5\right)\pi N\alpha}{1 - \frac{4\pi N\alpha}{3}} + \frac{\left(4\sqrt{10}/15\right)\pi NS(\gamma_e - \gamma_o)}{1 - \frac{4\pi N\alpha}{3}}$$

$$n_o = \frac{7}{2\sqrt{10}} + \frac{\left(2\sqrt{10}/5\right)\pi N\alpha}{1 - \frac{4\pi N\alpha}{3}} - \frac{\left(2\sqrt{10}/15\right)\pi NS(\gamma_e - \gamma_o)}{1 - \frac{4\pi N\alpha}{3}}$$

$$n = \frac{7}{2\sqrt{10}} + \frac{\left(2\sqrt{10}/5\right)\pi N\alpha}{1 - \frac{4\pi N\alpha}{3}} \tag{4}$$

Where, N=300 is the number of liquid crystal molecules and γ_e, γ_o is representing the extraordinary and ordinary internal field constant. The difference of γ_e-γ_o is to serve the

differential molecular polarizability. The n_e and n_o is representing the extraordinary and ordinary refractive index.

6.3 Results and Discussion

The birefringence, transition temperature, and dipole moment reveal an even-odd effect due to the increment of the alkyl chain of CHBT LC; however, the HOMO-LUMO gap is not affected. The present chapter is indicating birefringence is inversely related to the order parameter. However, the refractive index, order parameter, range of director angle ($\Delta\theta^o$), and refractive index continuously increase with an increment of alkyl chain length while birefringence steadily decreases. Rozga et al. [36] have reported an unusually high electric field used for ion separation, which increases the propagation rate of streamers to be at least 10^9 V/m; the present chapter used 10^{10} V/m electric field for the charge separation of the molecules. Baran et al. [6] have reported that the nematogen nCHBT series displayed a very high electrical resistance 10^9 Ω cm, which is why applied an unusually high electric field 10^{10} V/m in the present chapter.

6.3.1 Transition Temperature

The transition temperature from the nematic to isotropic (N-Iso) phase reveals the even-odd effect as shown in Fig. 6.1. Dabrowski et al. [8-9] have reported the increased amount of the melting point observed when the number of carbon atoms in the alkyl chain is odd, and the small changes in the rigid core structure lead to the change in attractive and repulsive forces. Buchecker et al. [13] reported the nCHBT compounds having an odd number of alkyl groups; the range of mesogenic state temperature is broad compared to the compounds having an even number of alkyl groups. The transition temperature reveals the even-odd effect under the extension of the alkyl chain length of nCHBT LC. The odd carbon atom number has a higher prospective; however, even the carbon atom number has a lower prospective. The odd carbon atom number of the alkyl

chain length increases the transition temperature, and even number decreases the transition temperature because the even member of the nCHBT series is making a larger angle with the long molecular axis; thus, it will reduce the anisotropy of the molecule, and it will also reduce the nematic to the isotropic phase (N-Iso) transition temperature. However, the odd member of the nCHBT series is making a lower angle with the long molecular axis; thus, it will enhance the molecule's anisotropy, thereby increasing the transition temperature.

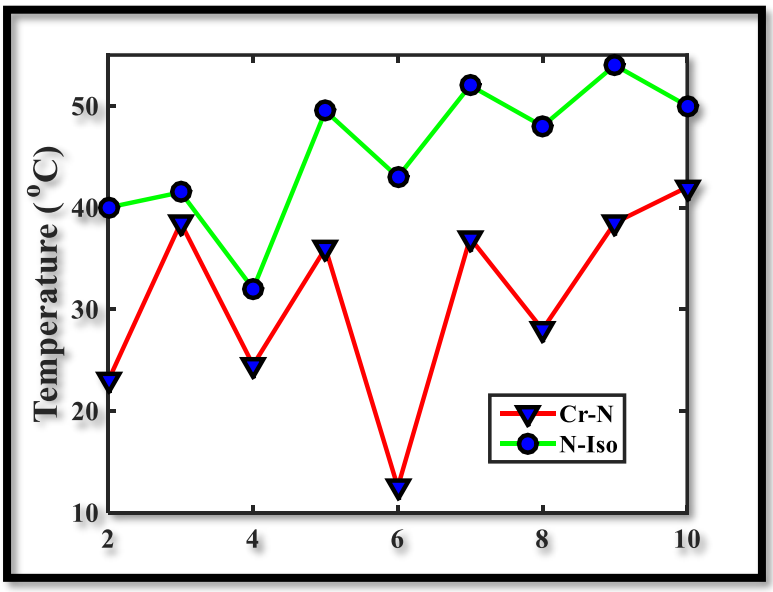

Figure 6.1 Transition temperature of nCHBT LC under the extension of alkyl chain (Crystalline to Nematic phase transition (Cr-N) and Nematic to Isotropic phase transition (N-Iso) expresses the odd carbon atom number has a higher melting point; however, even the carbon atom number has a lower melting point [8])

6.3.2 Dipole Moment

Wang at el. [22] have reported the dipole moment of the molecule opposite the applied electric field; the present chapter also expresses the dipole moment increases for the even carbon atom number of the alkyl chain. However, under the electric field effect, the birefringence increases for the odd carbon atom number, as shown in Fig. 6.5; the experimental evidence also increases for the odd carbon atom number as shown in Fig.

6.1. The dipole moment reveals the even-odd effect with the increased alkyl chain length, as shown in Fig. 6.2. The even carbon atom number of the alkyl chain reveals the higher value of dipole moment while the odd carbon atom number shows a lower value because the C-H atom wagging and C-C twisting frequency increases for the even carbon atom number of the benzene ring but twisting frequency decreases for odd carbon atom number. The C-S stretching frequency is also responsible for the even carbon atom in the upward direction and odd carbon atom number in the downward direction. The dipole moment variance indicates that the CHBT LC molecules are changing shape and size due to the alkyl chain length's increment.

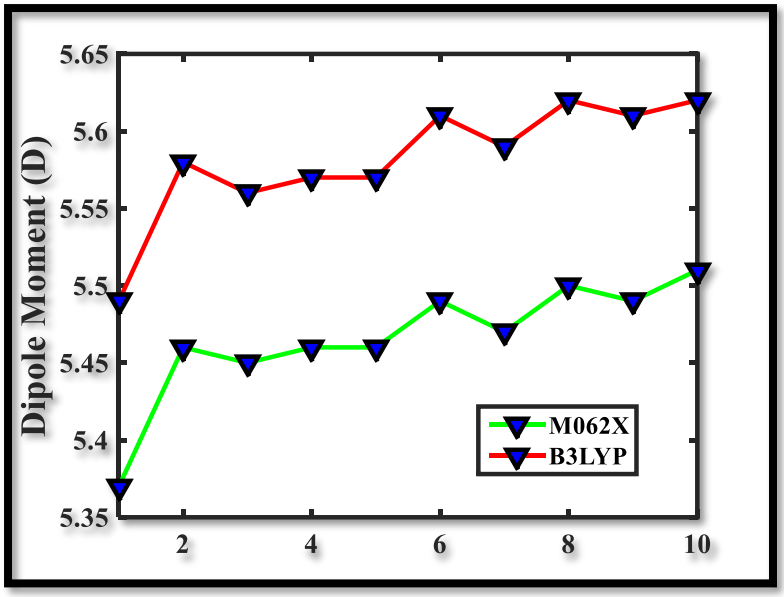

Figure 6.2. Dipole moment has been calculated under the extension of the alkyl chain (The dipole moment expresses an even-odd effect under the expansion of the alkyl chain length of CHBT LC. The dipole moment studied by DFT methodology (B3LYP & M062X) and the nature of both the methods is similar. B3LYP and M062X methods are suitable for the organic molecules that are the reason for selecting these methods.)

6.3.3 HOMO-LUMO gap

The HOMO-LUMO energy gap does not affect the increment of alkyl chain length, as shown in Fig. 6.3. The DFT methodology B3LYP and M062X express the same nature of

characteristics. The HOMO-LUMO energy gap remains constant for 6.25 eV in the B3LYP method, and by the M062X method, the energy gap remains constant for 8.20 eV. All kinds of molecular stretching do not deflect the HOMO-LUMO energy gap, and it does not exhibit any odd-even effect; it remains constant for all the series because of the nCHBT LC is an insulating material. Baran et al. [6] have reported the nematogen nCHBT series displayed a very high electrical resistance of 10^9 Ω cm. The number of monomers of the nCHBT series does not affect the insulating behavior, which is the reason for the constant bandgap.

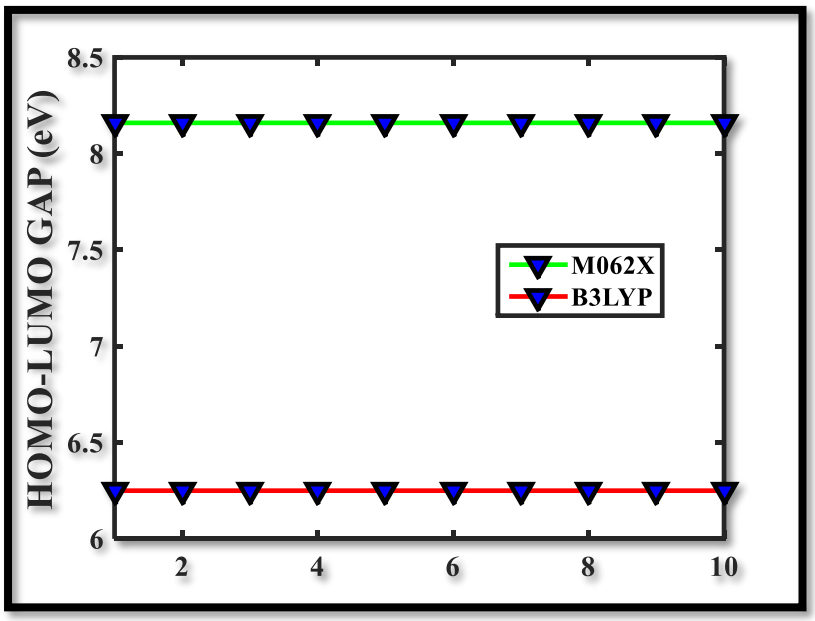

Figure 6.3. HOMO-LUMO gap has been calculated under the extension of the alkyl chain (The HOMO-LUMO gap studied by DFT methodology (B3LYP & M062X) under the extension of alkyl chain length of CHBT liquid crystal. HOMO-LUMO gap is not considered under the effect of an electric field; it is considered only under the extension of alkyl chain length. The nature of both methods is similar.)

6.3.4 Refractive Index

The refractive index was calculated with the help of Eq. no. 4. The refractive index continuously increases with the alkyl chain length, as shown in Fig. 6.4. Devi et al. [3] reported the birefringence and refractive index to depend upon the particular material's

temperature, wavelength, and structure. Still, the refractive index also depends upon the electric field (current chapter). Baran et al. [6] have reported the refractive index increases under the impact of temperature; the current chapter also expresses refractive index increases under the electric field's impact, as shown in Fig. 6.4. The 9CHBT reveals the refractive index sharply increased because the IR absorbance was very high in the 9CHBT LC because of the benzene ring's C-H wagging frequency. The rocking frequency corresponds to IR absorbance is very high in the tail of 9-CHBT. The C-N stretching corresponds to the IR absorbance is continual increases for the nCHBT series, but C-N stretching decreases in the 9CHBT LC that is the reason for the enhanced refractive index. The 5CHBT and 6CHBT have the same refractive index predicted by M062X methodology because they have one transition state (i.e, ready to react to any material). Still, the refractive index continuously increases in B3LYP methodology. The 9CHBT does not have any transition state, although the 5CHBT and 8CHBT, and 10CHBT LC also have one transition state. The refractive index is an optical parameter used for the measurement of an electro-optical effect of LC.

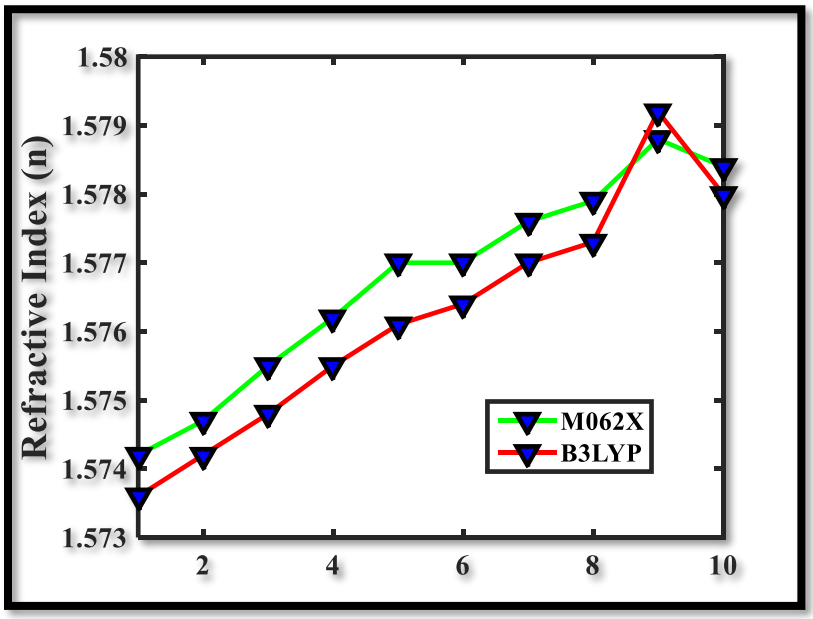

Figure 6.4 Refractive index has been calculated under the extension of the alkyl chain (The refractive index studied by DFT methodology (B3LYP & M062X) under the extension of the alkyl chain length of CHBT liquid crystal. The refractive index was

calculated by Eq. 4 under the effect of the electric field. The nature of both methods is similar.)

6.3.5 Birefringence

The birefringence was calculated with the help of Eq. no. 2. Dabrowski et al. [35] reported the birefringence of 5CHBT, and 6CHBT LC is 0.19 and 0.15 under the impact of temperature in the present chapter the birefringence of 5CHBT, and 6CHBT LC is 0.21 and 0.18 which is very close to the experimental evidence [6] as shown in Fig. 6.5. Sielezin et al. [2] have reported the birefringence decreases with an extension of the alkyl chain length. In the present chapter, birefringence decreases and reveals an even-odd effect due to alkyl chain length increment. The C-C symmetric and asymmetric stretching correspond to IR absorbance increases for the odd carbon atom number and decreases for even carbon atom number of benzene and cyclohexane ring. Buchecker et al. [13] have reported the dielectric anisotropy, birefringence, and elastic constant increases for the odd number and decreases for the even number of carbon atoms the alkyl chain length; the present chapter also predicts the same evidence as shown in Fig. 5. The M062X method shows a more even-odd effect as compared with the B3LYP method because of the M062X method predominant the nonbonded molecular interactions; however, the B3LYP method predominant the Vanderwall forces and hydrogen bond interaction. The birefringence continuously reduces with the extension of the alkyl chain length. According to the M062X method, the 2CHBT & 3CHBT, 6CHBT & 7CHBT, and 8CHBT & 9CHBT having the same birefringence because of the dispersion interaction contribute by the molecules, but according to the B3LYP method, 4CHBT & 5CHBT having the approximately same value of birefringence because of an equal amount of intermolecular forces. The birefringence is an optical parameter used for the measurement of an electro-optical effect of liquid crystal.

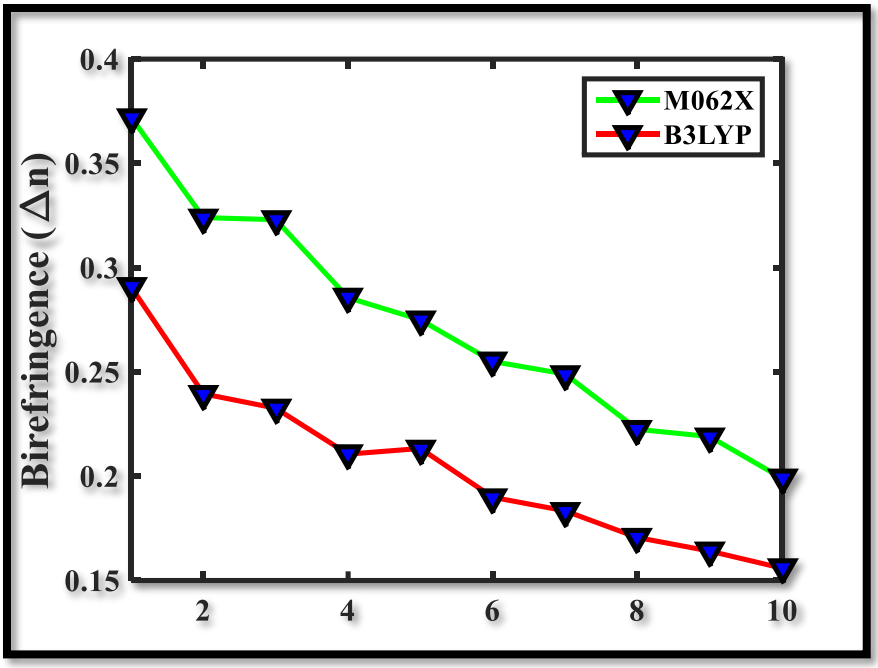

Figure 6.5 Birefringence has been calculated under the extension of the alkyl chain (The birefringence studied by DFT methodology (B3LYP & M062X) under the extension of the alkyl chain length of CHBT liquid crystal. The birefringence calculated by Eq. 2 under the effect of the electric field. The nature of both methods is similar.)

6.3.6 Order Parameter:

The order parameter of LC exists in the range of 0.3 to 0.8; below the range of 0.3 it is entirely liquid, and above the range of 0.8, it is perfectly crystal. The order parameter was calculated with Eq. no. 1 under an external electric field's impact. Bauman et al. [33] have reported the order parameter of 7CHBT LC 0.61 under the effect of temperature; the present chapter also shows the order parameter of 7CHBT LC is 0.64, which is close to the experimental value [34] as shown in Fig. 6.6. (a) Raszewski et al. [37] have reported the order parameter of 6CHBT LC is 0.68; the present chapter also reveals the order parameter of 6CHBT is 0.68, which is supports the experimental evidence as shown in Fig. 6.6. (a) The DFT method M062X represents the nematic phase stability due to the contribution of molecular anisotropic. Sarkar et al. [11] have reported the order parameter increases with the extension of alkyl chain length under the impact of temperature in the present chapter; also, the order parameter continuously increases with alkyl's extension

chain length under the impact of an electric field. The order parameter continuously increases with the increment of alkyl chain length because C-N and C-C atom stretching correspond to the IR absorbance continually increases for the nCHBT series. The order parameter has expressed the even-odd effect with minor deviation. The order parameter is an essential parameter for calculating the physical state of liquid crystal; with this methodology's help, we can predict unknown molecules' state. The extension of alkyl chain length under the electric field's impact reduces the range of nematic phase stability, as shown in 3D Fig. 6.6.(b)

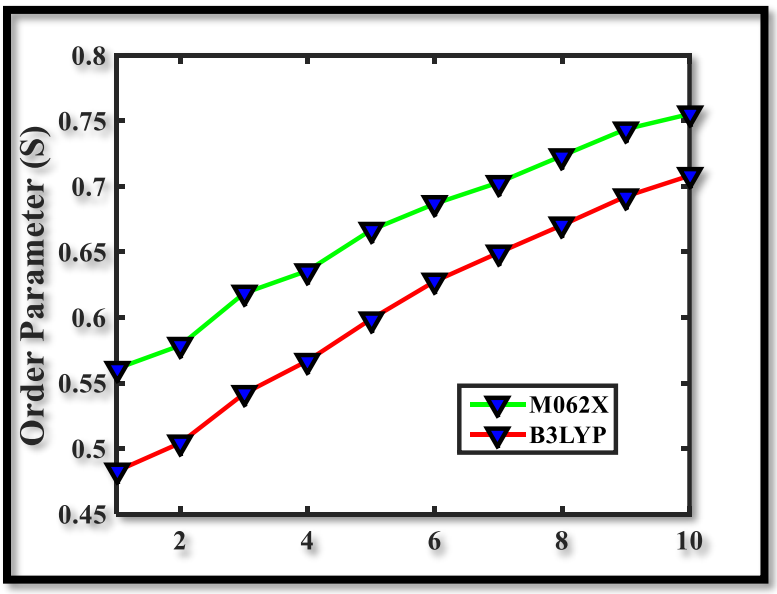

Figure 6.6 (a) Order parameter has been calculated under the extension of the alkyl chain (The Order parameter studied by DFT methodology (B3LYP & M062X) under the extension of the alkyl chain length of CHBT liquid crystal. The Order parameter was calculated by Eq. 1 under the effect of the electric field. The nature of both methods is similar.)

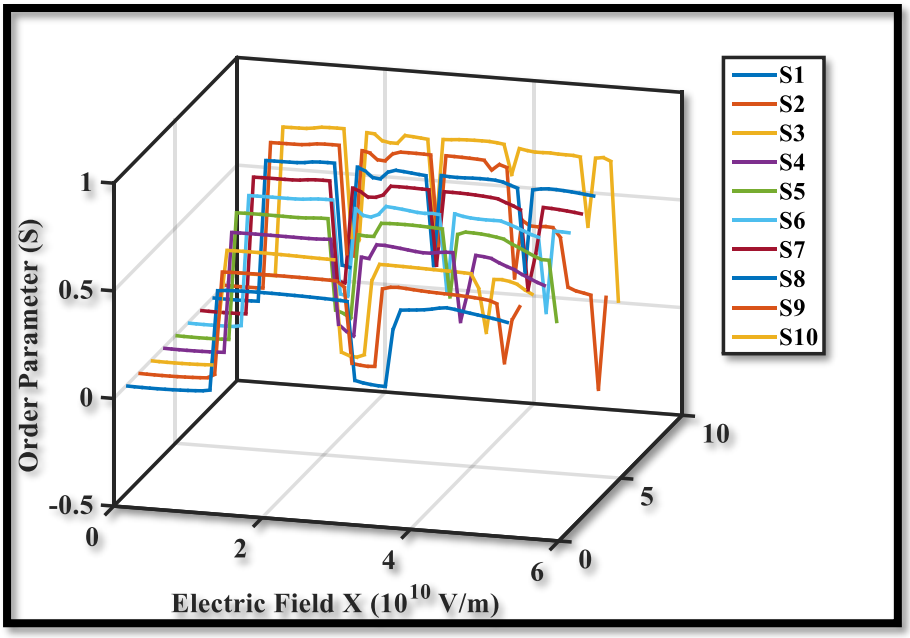

Figure 6.6(b) The order parameter has been calculated under the extension of the alkyl chain length (The order parameter studied by DFT methodology (B3LYP) of nCHBT liquid crystal. The order parameter is calculated by equation no. 1 under the effect of the electric field.)

6.3.7 Magic Angle

Dabrowski et al. [9] have reported 1CHBT not having the LC's property; however, 2CHBT to 10CHBT has the property of the LC because the present chapter expresses the magic angle of 1CHBT LC is higher and very close to 54.80º as shown in Fig. 6.7. The magic angle was calculated with the help of Eq. no. 3. The standard value of the magic angle is 54.7° for all LC molecules. The magic angle of LC depends upon the order parameter. The 1-CHBT LC molecule expresses an approximate 54.8° magic-angle, but the series represents a 54.7° magic angle AS shown in Fig. 6.7. The magic angle decreased continually with the increased alkyl chain, but the magic angle increased again in 10CHBT; however, the nCHBT maintains a 54.7 magic-angle for all the series. The magic angle of the LC molecule depends upon the molecular anisotropic. The molecular anisotropic continuously decreases with an extension of alkyl chain length, which is why the magic angel's decrement. The nCHBT LC series are uniaxial; however, 9CHBT is

biaxial. The magic angle of the 9CHBT decreases, and 10CHBT increases due to the LC's biaxial and uniaxial behavior.

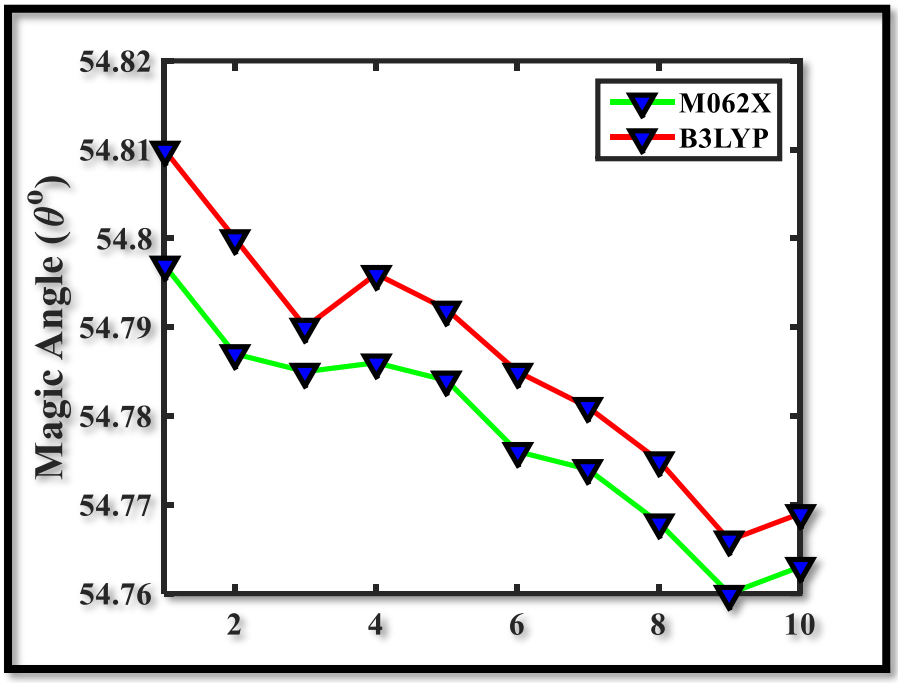

Figure 6.7 The magic angle has been calculated under the extension of an alkyl chain (The Magic angle was studied by DFT methodology (B3LYP & M062X) under the extension of the CHBT liquid crystal length. The Magic angle is calculated under the effect of the electric field by Eq. 3. The nature of both methods is approximately similar.)

6.3.8 Range of Director Angle

Eq. no. 3 calculates the range of director angle ($\Delta\theta^o$) under the electric field's influence. The range of director angle ($\Delta\theta^o$) considers from the magic angle, as shown in Fig. 6.8. The range of director angle ($\Delta\theta^o$) continuously increases with an extension of the alkyl chain length. The C-N and C-C atom stretching contribute to enhancing frequency due to the range of director angle ($\Delta\theta^o$) increases continually. The minimum director angle (θ^o_{min}) continuously decreases with the extension of alkyl chain length; however, the maximum director angle (θ^o_{max}) remains constant with alkyl chain length. The maximum director angle remains constant for 55° because the C-H atom stretching of the benzene ring remains constant for all the series; however, the minimum director angle decreases

from 35º to 25º. The difference of director angle (Δθº) is continually increased from 19º to 29º and reveals the broad range of director angle due to the alkyl chain's extension.

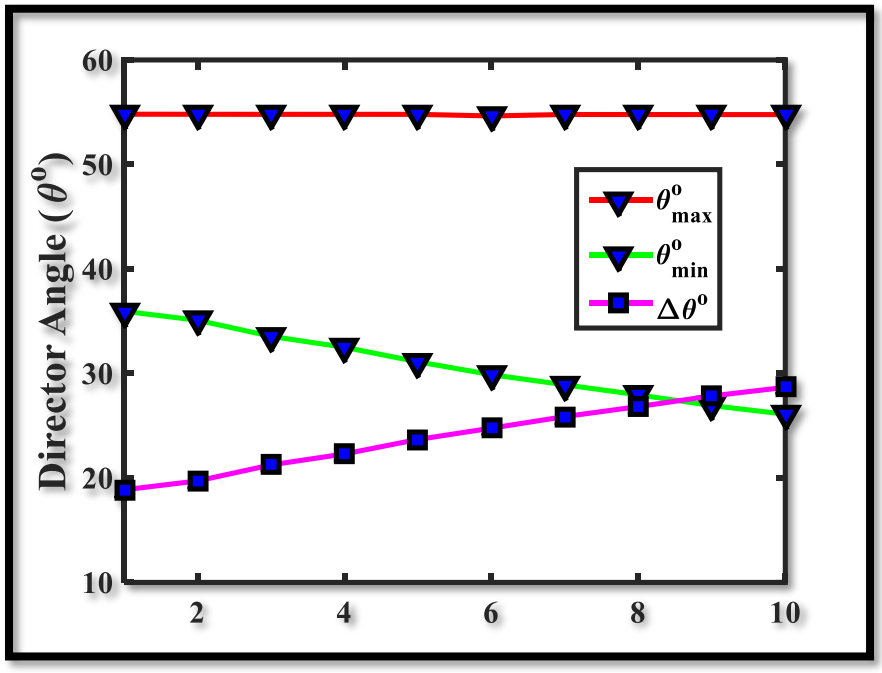

Figure 6.8 Range of director angle has been calculated under the extension of alkyl chain (The range of director angle (magic angle) studied by DFT methodology (B3LYP) under the extension of the alkyl chain length of nCHBT liquid crystal. The range of director angle calculated by Eq. 3 under the impact of the electric field. The difference of director angle (Δθº) continually increases, but the minimum director angle (θ^o_{min}) continuously decreases; however, the maximum director angle (θ^o_{max}) remains constant.)

6.3.9 Isotropic Polarizability

Baran et al. [6] have reported that the π-electron conjugation of the phenyl ring with terminal -NCS group gives stronger polarizability than the -CN group. Jadzyn et al. [34] have reported the external electric field to align the nematogen molecules in the applied axis with maximum polarizability, and the parallel molecular axis (x-axis) gives a minimum moment of inertia of the molecule. The 6CHBT LC shows three absorption bands with a 0.61 order parameter for the nematic phase; the present chapter also supports the experimental evidence. The isotropic polarizability increased continuously

with alkyl chain length because C-N atom stretching corresponds to IR absorbance continuously increases. The C-C twisting frequency of benzene continuously increases, so the isotropic polarizability increased continuously with alkyl chain length. Both the DFT methodology expresses the same prediction with minor deviation shown in Fig. 6.9. Baran et al. [6] have reported that isotropic polarizability continually increases with the alkyl chain length because the alkyl chain contributes to the molecular polarizability with the phenyl ring's help NCS terminal group; that is the reason for the continues enhancement of isotropic polarizability.

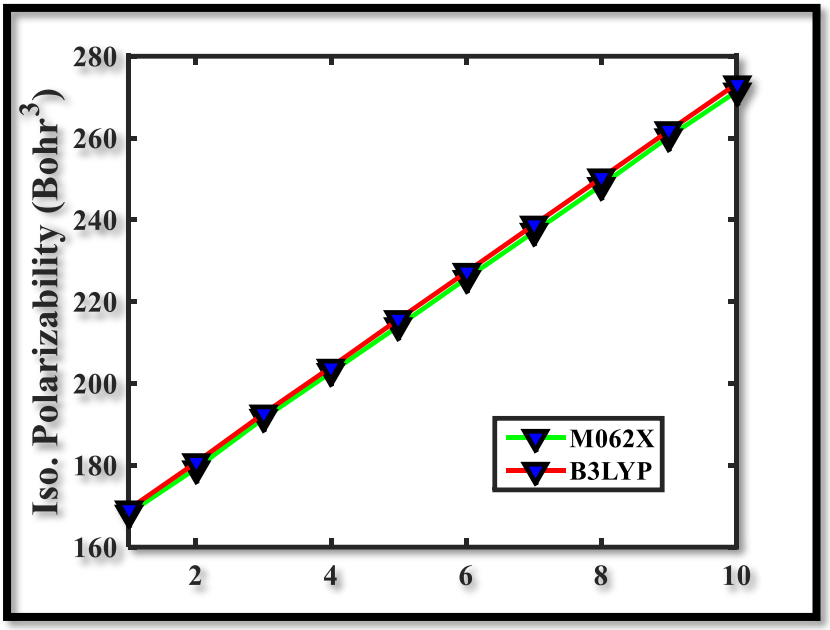

Figure 6.9 Isotropic polarizability has been calculated under the extension of the alkyl chain (The Isotropic Polarizability was studied by DFT methodology (B3LYP & M062X) under the extension of alkyl chain length of CHBT liquid crystal. The Isotropic Polarizability is not calculated under the electric field; it is estimated only under the extension of alkyl chain length. The nature of both methods is similar.)

6.4 Conclusion

In the present work, it has been found that under the extension of alkyl chain length, the transition temperature, dipole moment, and birefringence exhibits the even-odd effect. At the same time, the HOMO-LUMO energy gap remains stable due to insulating behavior.

The range of director angle, order parameter, refractive index, and isotropic polarizability of the CHBT molecule increases gradually with an extension of alkyl chain length because C-N atom stretching corresponds to IR absorbance continuously increases. The order parameters and birefringence are inversely related to each other. Hence the birefringence decreases and the order parameter increases of the CHBT series due to the continuous extension of alkyl chain length under an electric field. The birefringence and magic angle continually decrease with the increment of alkyl chain length. The influence of an electric field is an alternative to the temperature for optical applications. The present chapter strategy can predict all the optical parameters of the unknown molecules. The current chapter strategy can predict the physical parameters isotropic polarizability, dipole moment, state density, and Intermolecular interactions of the unknown molecules. This work's motivation is to search for new liquid crystal molecules that are suitable under the terahertz (THz) applications.

Reference

1. H. K. Bisoyi, S. Kumar, *Chem. Soc. Rev.,* **39,** 264 (2010).
2. K. Sielezin, R. Kowerdziej and J. Parka, *Liq Crys.*, **46(9),** 1367 (2019).
3. T. K. Devi, B. Choudhury, A. Bhattacharjee, R. Dabrowski*, Opto−Electronics Rev.,* **22(1),** 24 (2014).
4. J. Jadzyn, R. Dabrowski, K. Glumiak, G. Czechowski. *Z. Naturforsch,* **55a,** 637 (2000).
5. J. Jadyn, G. Czechowski, N. T. Shonova, *Liq. Cryst.*, **3:12,** 1637 (1988).
6. J. W. Baran, Z. Raszewski, R. Dabrowski, J. Kedzierski, J. Rutkowska, *Mol. Cryst. Liq. Cryst.,* **123,** 237 (1985.)
7. G. H. Brown, J. W. Doane, V. D. Neff, *crit. rev. solid state,* **303,** 124 (2006).
8. R. Dabrowski, J. Dziaduszek, T. Szczucinski. *Mol. Cryst. Liq. Cryst.,* **102,** 155 (1984).
9. R. Dabrowski, J. Dziaduszek, T. Szczucinski, *Mol. Cryst. Liq. Cryst.*, **124,** 241 (1985).
10. J. Jadzyn, R. Dabrowski, K. Glumai, G. Czechowski, *J. Chem. Eng. Data.,* **45,** 1027 (2000).
11. P. Sarkar, P. Mandal, S. Paul, R. Paul, R. Dabrowski, K. Czuprynski, *Liq. Cryst.,* **30,** 507 (2003).
12. J. Jadzyn, G. Czechowski, J. L. Dejardin, M. Ginovska, *J. Phys. Chem. A.,* **111,** 8325 (2007).

13. R. Buchecker, M. Schadt, *Mol. Cryst. Liq. Cryst.,* **149,** 359 (1987).
14. J. Szulc, Z. Stolarz, *Mol. Cryst. Liq. Cryst.,* **263,** 623 (1995).
15. M. Valiev, E. J. Bylaska, N. Govind, K. Kowalski, T. P. Straatsma, H. J. J. van Dam, D. Wang, J. Nieplocha, E. Apra, T. L .Windus, W. A. de Jong, *Comput. Phy Comm.,* **181,** 1477 (2010).
16. A. D. Becke, *J. Chem. Phys.,* **98,** 5648 (1993).
17. C. Lee, W. Yang, R. G. Parr, *J. Phy. Rev. B.,* **37,** 785 (1988).
18. Y. Zhao, D. G. Truhlar, *Chem. Acc.,* **120,** 215 (2008).
19. P. J. Hay, W. R. Wadt , *J. Chem. Phys.,* **82,** 299 (1985).
20. P. C. Hariharan, J. A. Pople, *Theo. Chim. Acta.,* 28, 213 (1973).
21. R. Ditchfield, W. J. Hehre, J. A. Pople, *J. Chem. Phys.,* **54(2),** 724 (1971).
22. Y. Wang, F. Wang, J. Li, Z. Huang, S. Liang, J. Zhou. *Energie*s, **10(4),** 510 (2017).
23. P. Upadhyay, *Qunatum mechanical study of optical properties of liquid crystal molecules.* Ph.D *Thesis,* (BBAU, Lucknow, INDIA (2016).
24. J. H. Robson, *The temperature Dependence of the Electro-optic Kerr effect in solutions,* Ph.D *Thesis* (Aston University U.K. 1993).
25. N. V. Madhusudana, S .Chandrasekhar, *Pramana–J. Phys.,* **1,** 12 (1973).
26. M. S. Beevers, G. Williams, *Mol. Chem. Phys.,* **72,** 2171 (1976).
27. B. R. Sangala, A. Nagarajan, P. Deshmukh, H. Surdi, G. Rana, V. G. Achanta, S. S. Prabhu, *Pramana–J. Phys.,* **94(2),** 1 (2020).
28. M. F. Vuks, *Opt. Spect.,* **20,** 361 (1966).
29. S. Chandrasekhar, *Rep. Prog. Phys.,* **39,** 613 (1976).
30. P. Singh, K. B. Thapa, N. Kumar, D. Singh, D. Kumar, *Pramana–J. Phys.,* **93(50),** 1 (2019).
31. H. D. Cohen, C. C. J. Roothaan, *J. Chem. Phys.,* **43,** S34 (1965).
32. A. D. Duckingharn, *Adv. Chem. Phys.,* **12**,107 (1967).
33. D. Bauman, J. Jadzyn and G. Czechowski, *IEEE.,* 8, 381 (2001).
34. J. Jadzyn, G. Czechowski, C. Legrand, R. Douali, *Dielectric properties of 6-CHBT in isotropic and nematic phases, Proc. SPIE 4147, Liquid Crystals: Chemistry, Physics, and Applications* (2000).
35. R. Dabrowski, P. Kula, J. Herman. *Cryst.,* **3,** 443 (2013).
36. P. Rozga, *IEEE Trans. Dielectr. Electr. Insul.,* **22:1,** 754 (2015).
37. Z. Razewski, R. Dabrowski, Z. Stolarzowa, J. Zmija**,** *Crys. Res. Technol.,* **22(60),** 835 **(**1987**).**

CHAPTER 7

Conclusion and Future Prospects

The work's motivation has studied the reason behind the even-odd effects obtained by temperature and electric field variation. The temperature and electric field both parameters are shown the odd-even effect in the LC series. Hence, the study's interesting part is the correlation between the electric field and temperature to cause the even-odd effect in the LC series. This strategy is useful for the electro-optical effect of future molecules. The present theoretical model predicts the optical parameters of the unknown organic molecule. The novelty of the current work is modified mathematical equations as a comparison with previously reported results. This theoretical model predicts 97 to 100% accuracy with the experimental evidence.

Chapter 3: In this chapter, it has been found that the electric field's effect on the nCB LC series. Which is reveals an even-odd effect in optical applications. It has been found that the electric field is another method to find out the optical parameters of the nCB series. The optical parameters are obtaining using derived equations from Vuk's theory. The birefringence of nCB series is decreased continuously and showing an even-odd effect with the extension of the alkyl chain length of the nCB LC molecules. The order parameter of the nCB is steadily increasing with an extension of the alkyl chain length of the nCB series. The stretching of C-C and C-H atom corresponds to higher IR absorbance for odd members and lowers IR absorbance for even members of the nCB series. The C-C and C-H, atom stretching, is contributing to the anisotropy of polarizability. The order parameter and birefringence of the nCB LC molecules are inversely proportional to each other. Under the electric field effect, the birefringence and order parameters are different for different carbon atom numbers. The order parameter, birefringence, and transition temperature of the nCB series reveal a higher value for odd carbon members, which corresponds to the benzene ring's C-H asymmetric stretching. Our results help to

investigate the optical parameters of LC, which can be obtained through electric field and temperature. It is also explaining the correlation between microscopic parameters to mesoscopic parameters of LC, which can be obtained by variation of external electric field and temperature of liquid crystals.

Chapter 4: In this chapter, it has been found that the HBT LC molecule has maximum absorbance during the intermolecular interaction because of charge transfer by an oxygen atom to the benzene ring. The birefringence and order parameter have adverse orders with an expansion of the external electric field. The HBT LC molecule is suitable for sensing and filtering applications because HBT LC has a broad range of frequencies. With this methodology's help, we can predict an unknown organic molecule's optical and sensing properties. B. Bahadur reported HBT LC is diamagnetic, so it is suitable for the diamagnetic material applications. Molecular polarizability is the most crucial parameter in this chapter, which is responsible for the optical properties of the organic molecule. This theoretical model predicts the optical parameters of the unknown organic molecule. The novelty of the current work is modified mathematical equations as a comparison with previously reported results. This theoretical model predicts 97 to 100% accuracy with the experimental evidence.

Chapter 5: In this chapter, it has been found that the 7O.m compound series express a perfectly odd-even effect by order parameter (S), birefringence (Δn), and dipole moment under the impact of the electric field. But the isotropic polarizability, Homo-Lumo gap, and refractive do not express any odd-even effect in the 7O.m series. This compound series has low birefringence and order parameter. The HOMO-LUMO gap remains constant on increasing the length of the alkyl chain. The isotropic polarizability and refractive index continuously improve with an extension of the alkyl chain length. The M062X method produces higher values for the refractive index, HOMO-LUMO gap, order parameter, and birefringence, while dipole moment and isotropic polarizability having higher values which have been calculated by the B3LYP method. The DFT method expresses the perfectly electro-optic and odd-even effect under the applied electric field computed using Eq. 1, 2, 3, and 4. Most probably, it has been found that when the alkyl chain length increased, then the HOMO-LUMO gap some time increased

or some time decreased, but in the series of 7O.m compound, the HOMO-LUMO gap remains constant. The homologous series of 7O.m liquid crystal molecules may be suitable for the THz applications. The 7O.m liquid crystals are also ideal for the limiters, optical shutters, beam steerers, and switchable optical filters applications.

Chapter 6: In the present chapter, it has been found that under the extension of alkyl chain length, the transition temperature, dipole moment, and birefringence exhibits the even-odd effect. At the same time, the HOMO-LUMO energy gap remains stable due to insulating behavior. The range of director angle, order parameter, refractive index, and isotropic polarizability of the CHBT molecule increases gradually with an extension of alkyl chain length because C-N atom stretching corresponds to IR absorbance continuously increases. The order parameters and birefringence are inversely related to each other. Hence the birefringence decreases and the order parameter increases of the CHBT series due to the continuous extension of alkyl chain length under an electric field. The birefringence and magic angle continually decrease with the increment of alkyl chain length. The influence of an electric field is an alternative to the temperature for optical applications. The present chapter strategy can predict all the optical parameters of the unknown molecules. The current chapter strategy can predict the physical parameters isotropic polarizability, dipole moment, state density, and Intermolecular interactions of the unknown molecules. This work's motivation is to search for new liquid crystal molecules that are suitable under the terahertz (THz) applications.